

Report No. FHWA-RD-78-203

PB292-645



THE DEVELOPMENT OF A MICROWAVE RADIOMETER FOR USE AS A HIGHWAY ICE DETECTOR



September 1978
Final Report

Document is available to the public through
the National Technical Information Service,
Springfield, Virginia 22161

Prepared for
FEDERAL HIGHWAY ADMINISTRATION
Offices of Research & Development
Washington, D. C. 20590

REPRODUCED BY:
U.S. Department of Commerce
National Technical Information Service
Springfield, Virginia 22161

NTIS

FOREWORD

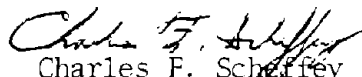
This report represents in considerable detail the theoretical background and highlights in the development and preliminary testing of a highway ice detector based on microwave radiometry. This 10 GHz radiometer and its accompanying signal processor are capable of passively determining the surface conditions of areas of **cement and asphaltic concrete pavements**. The radiometer located in a position overlooking the pavement, in conjunction with a simple surface temperature sensor in the pavement, determines whether the surface is dry, wet, or contains frozen precipitation extensive enough to present a hazard to motor vehicles.

A prototype of this area ice detection system has been delivered to FHWA and is scheduled to be evaluated during the winter of 1978-79 on a low traffic volume road at the Fairbank Highway Research Station. Parameters to be investigated include stability of adjustments, mean-time-between-failures, false and missed alarm rate, and susceptibility to interference by vehicles and gas discharge lamps.

Research in highway ice detection is included in the Federally Coordinated Program of Highway Research and Development as Task 5 of Project 1L, "Improved Traffic Operations During Adverse Environmental Conditions."

Mr. Richard N. Schwab is the Project Manager and Mr. Philip Brinkman is the Task Manager. Mr. Joseph C. Leifer was the Contract Manager for this study.

Two copies of this report are being distributed to each FHWA regional office.


Charles F. Schreffey
Director, Office of Research
Federal Highway Administration

This document is disseminated under the sponsorship of the Department of Transportation in the interest of information exchange. The United States Government assumes no liability for its contents or use thereof. The contents of this report reflect the views of the contractor, who is responsible for the accuracy of the data presented herein. The contents do not necessarily reflect the official views or policy of the Department of Transportation. This report does not constitute a standard, specification, or regulation.

The United States Government does not endorse products or manufacturers. Trade or manufacturers' names appear herein only because they are considered essential to the object of this document.

1. Report No. FHWA-RD-78-203		2. Government Accession No.		3. Report Category No. PB-292645	
4. Title and Subtitle The Development of a Microwave Radiometer for Use as a Highway Ice Detector				5. Report Date September 1978	
				6. Performing Organization Code	
7. Author(s) S. Berinsky, H.K. Hong, T.H. Lee, and W.T. Schrader				8. Performing Organization Report No.	
9. Performing Organization Name and Address Lockheed Missiles & Space Company, Inc. P.O. Box 504 Sunnyvale, California 94086				10. Work Unit No. (TRAIS)	
				11. Contract or Grant No. DOT-FH-11-9328	
12. Sponsoring Agency Name and Address Offices of Research and Development Federal Highway Administration U.S. Department of Transportation Washington, D.C. 20590				13. Type of Report and Period Covered Final Report (September 1977 to August 1978)	
				14. Sponsoring Agency Code E0373	
15. Supplementary Notes FHWA contract manager: J. C. Leifer (HDV-11)					
16. Abstract The program objective was to develop a system capable of detecting snow, ice, frost, or slush over a highway bridge deck area greater than 4 x 2 feet (1.2 x 0.6 m) and generate a valid alarm signal to warn motorists of a hazard. The detection system selected was a microwave radiometer operating at 10 GHz which continuously samples a reference noise source and internal amplifier noise to provide measurement corrections of radiated power received from the road surface being observed. Principal radiometer components are: rectangular horn antenna; sensitive receiver; and signal processor/alarm unit. The successive program phases were: (1) design optimization and system tradeoffs; (2) breadboard model laboratory and field tests; and (3) prototype model design, fabrication and test. Test results on asphalt and concrete roadway simulators, as well as actual asphalt roads, correlated with previously published radiometric temperatures for similar surfaces. The following road conditions were detectable: dry/warm; dry/cold; wet; slush; ice layer (0.1 cm. minimum); and snow layer (1 cm. minimum). All road hazard detection objectives were met except for frost detection. Descriptions of recommended additional effort are presented, including detailed evaluation of the prototype model; advanced alarm logic; self-test techniques; and a scanning antenna to cover increased road areas.					
17. Key Words Bridge Deck Hazards; Snow, Ice, Frost & Slush Detection; Microwave Radiometer; Motorist Warning System			18. Distribution Statement This document is available to the public through the National Technical Information Service, Springfield, Virginia 22161.		
19. Security Classif. (of this report) Unclassified		20. Security Classif. (of this page) Unclassified		21. No. of Pages 152	22. Price Aφ8-Aφ1

TABLE OF CONTENTS

<u>Section</u>	<u>Page</u>
1.0 INTRODUCTION, PROBLEM STATEMENT AND BACKGROUND	1
1.1 Introduction	1
1.2 Statement of the Problem	1
1.3 Background	1
1.3.1 Previous Approaches to the Problem	1
1.3.2 Selected Approach: The Microwave Radiometer	2
1.3.3 General Principles of Radiometer Operation	3
2.0 SUMMARY OF REQUIREMENTS AND WORK PERFORMED	12
2.1 Contract Requirements	12
2.2 Highlights of Work Phases	12
3.0 DESCRIPTION OF PHASE I EFFORT	16
3.1 Design Optimization	16
3.1.1 Radiometer Configuration	16
3.1.2 Detection Performance	20
3.2 System Tradeoffs	23
3.2.1 False Alarm/Missed Alarm Probabilities	24
3.2.2 Tradeoff of Detection Threshold, T_D	28
3.2.3 Tradeoff of Measurement Errors, ϵ_D	28
3.2.4 Example of Use of System Tradeoffs	31
3.2.5 Reliability Analysis	35
3.3 Theoretical Analyses	35
3.3.1 General	35
3.3.2 Description of Analytical Reports	35
3.4 Test Plan	37
3.4.1 Objective	37
3.4.2 Laboratory Test Plan	37
3.4.3 Field Test Plan	42
4.0 DESCRIPTION OF PHASE II EFFORT	43
4.1 Breadboard Laboratory Tests	43
4.1.1 Bench Tests	43
4.1.2 Calibration	44
4.1.3 Stability Tests	47
4.1.4 Simulator Tests	51
4.2 Breadboard Field Tests	75
4.2.1 Site Survey	75
4.2.2 Test Results	79

TABLE OF CONTENTS (Continued)

<u>Section</u>	<u>Page</u>
4.3 Alarm Logic and Circuit Development	88
4.3.1 Logic Rationale	88
4.3.2 Development of Breadboard Alarm Unit	94
4.3.3 Test Results	96
4.4 Recommended Modifications	98
4.4.1 Antenna and Receiver	99
4.4.2 Processor and Alarm Circuit	99
4.4.3 Interconnection Cables and Connectors	100
5.0 DESCRIPTION OF PHASE III EFFORT	101
5.1 Prototype Design and Test Details	101
5.1.1 Receiver Functional Modifications	101
5.1.2 Receiver and Processor Repackaging	104
5.1.3 Alarm Circuit Addition	104
5.1.4 Test Results	106
5.2 Prototype Design Documentation	106
5.2.1 Requirements	106
5.2.2 Drawings	107
6.0 EQUIPMENT DESCRIPTION	115
6.1 Performance Specifications	115
6.1.1 Radiometer Specifications	115
6.1.2 Measurement Error Discussion	115
6.2 Size, Weight, Power and Environmental Restrictions	116
6.2.1 Receiver and Horn Antenna	120
6.2.2 Processor Electronics	120
6.2.3 Surface Temperature Sensing Unit	121
6.3 Operating Instructions	121
6.3.1 System Turn-On	121
6.3.2 System Calibration	122
6.3.3 Alarm Circuit Adjustments	123
6.4 Suggestions for Location and Test/Evaluation Procedures	124
6.4.1 Location	124
6.4.2 Test/Evaluation Procedures	125
7.0 CONCLUSIONS	127
7.1 Evaluation of Equipment Performance	127
7.1.1 Breadboard Radiometer Performance	127
7.1.2 Prototype Radiometer Performance	127
7.2 Comparison with Development Objectives	128

TABLE OF CONTENTS (Continued)

<u>Section</u>		<u>Page</u>
8.0	RECOMMENDATIONS	129
8.1	Evaluation of Prototype Radiometer System	129
	8.1.1 Objectives	129
	8.1.2 Approach	130
8.2	Single Axis and 2-Axis Scanning Antennas	130
	8.2.1 General Comments	130
	8.2.2 Proposed Tasks	132
8.3	Advanced Surface Simulator	132
	8.3.1 Capability	132
	8.3.2 Approach	134
8.4	Self-Test Techniques	135
	8.4.1 Proposed Self-Test Modifications	135
	8.4.2 Alternate Self-Test Methods	136
8.5	Advanced Alarm Logic	137
	8.5.1 Microprocessor Implementation	137
	8.5.2 Frost Alarm Circuit	139
8.6	"Map-Matching" Techniques for Detection/ Discrimination of Hazards	139
	8.6.1 Background	139
	8.6.2 Approach	139
8.7	Analysis of Multilayer Rough Surfaces	142
	8.7.1 General Comments	142
	8.7.2 Proposed Study	142
8.8	Design Study for Low Cost 10 GHz Radiometer	142
	8.8.1 General Comments	142
	8.8.2 Proposed Study	143

LIST OF FIGURES

<u>Figure</u>		<u>Page</u>
1	Program Tasks and Schedule	13
2	10 GHz Radiometer Block Diagram (with Microwave Switch)	17
3	10 GHz Radiometer Block Diagram (No Microwave Switch)	18
4	94 GHz Radiometer Block Diagram (Dual-Polarization Sensing)	19
5	Probability of False Alarm	25
6	Probability of Missed Alarm	26
7	False Alarm Time with Various Response Times	27
8	Antenna Size vs. Beamwidth and Frequency	29
9	Radiometric Temperature vs. Antenna Beamfill	30
10	Radiometer Accuracy vs. Production Cost	32
11	RF Beamwidth vs. Resolution and Cost	33
12	Receiver Noise Figure vs. Resolution and Cost	34
13	Roadway Surface Simulator	39
14	Roadway Surface Simulator Tests	41
15	Revised Radiometer Configuration	44
16	Breadboard Processor (Top View, Cover Removed)	45
17	Strip Chart Recording of Radiometer Calibration	46
18	Data Recording System	48
19	Input Voltage Stability Tests (Tests 1 and 2)	49
20	Lockheed Radiometer Block Diagram	50
21	Scale Factor Drift vs. Receiver Temperature	52
22	Radiometer Receiver and Horn Antenna (Photo)	54
23	Processor and Data Recording System (Photo)	55
24	Completed Asphalt Roadway Surface Simulator (Photo)	56
25	Simulator Test Set-Up (Photo)	58
26	Simulator Test Set-Up and Geometry	59
27	Test 1 - Dry, Warm Surface	61
28	Test 2 - Dry, Cold Surface	66

LIST OF FIGURES (Continued)

<u>Figure</u>		<u>Page</u>
29	Wet Surfaces	67
30	Frost on Asphalt Simulator (Photo)	68
31	Frosty Surface - Stripchart Data	70
32	Ice on Concrete	72
33	Ice Layer Buildup vs. Time	73
34	Ice Test Data (Not Normalized)	74
35	Ice Surface Incidence Angle Effects	76
36	Temperature Profile for Various Conditions	77
37	Field Test Area Map	82
38	Field Test Configuration Verification Test	84
39	Field Test 1 - Test Set-Up Photographs	85
40	Field Test 2 - Ice Layers on Asphalt Surface	87
41	Field Test 2 - Ice and Snow on Asphalt	89
42	Breadboard Alarm Circuit - Block Diagram	95
43	Breadboard Alarm Unit (Photo)	97
44	Phase III Prototype Receiver Block Diagram	102
45	Prototype Alarm Circuit - Block Diagram (Hazard Inhibit Added)	105
46	Receiver, Top Assembly	109
47	Processor, Top Assembly	111
48	Receiver Unit, Oblique View (Photo)	117
49	Processor Unit, Top View (Photo)	118
50	Processor Unit, Oblique View (Photo)	119
51	Test Data Collection Block Diagram	126
52	Prototype Evaluation Continuous Monitor Approach	131
53	Sample Scan Coverage Pattern	133
54	Advanced Alarm Logic Block Diagram	138
55	Dewpoint Alarm Block Diagram	140

LIST OF TABLES

<u>Table</u>		<u>Page</u>
1	Performance Assessment	21
2	Test Plan Test Sequence	60
3	Emissivities of Simulator Test Surfaces	62
4	Dry, Cold Temperature Tests	64
5	Frosty Surface T_R Values	69
6	Simulator Temperatures and Emissivities	75
7	Summary of Conditions	78
8	Test Site Survey Summary	80
9	Field Test 1 - Data	86
10	Physical Parameters Affecting Surface Condition	90
11	Hazard Logic Table	94
12	Phase III Prototype Receiver Parts List	103
13	Prototype Radiometer Drawing List	108



Section 1.0

INTRODUCTION, PROBLEM STATEMENT AND BACKGROUND

1.1 INTRODUCTION

This report describes the study, test and design tasks performed under Contract No. DOT-FH-11-9328, entitled "Area Detectors for Snow and Ice". This contract is sponsored by the Federal Highway Administration, Office of Research, Environmental Design and Control Division. Mr. Joseph C. Leifer is the Contract Manager for this program

Section 2.0 provides a summary of contract requirements, a review of the work performed, and highlights of results obtained and conclusions reached. Sections 3.0, 4.0, and 5.0 provide detail descriptions of the successive work phases: I, II and III. Section 6.0 contains a description of the prototype radiometer system in terms of performance specifications, environmental restrictions, operating instructions, and typical evaluation procedures. Performance evaluation and development objectives discussions are included in Section 7.0, Conclusions. Finally, brief descriptions of recommended additional development and study tasks are given in Section 8.0.

1.2 STATEMENT OF THE PROBLEM

The specific problem addressed by this contract is the development of a system capable of detecting snow, ice, frost, or slush over an extensive area of a highway bridge deck as contrasted with conventional systems which are sensitive over only a few square inches.

As a design objective, a valid alarm signal is to be generated to provide a hazard warning to motorists when a frozen area appears having a length of about 4 feet (1.2 m) or more, and a width of 2 feet (0.6 m) or more. Additionally, if more than one frozen area exists, then this alarm signal is to be generated for smaller dimension frozen patches.

Alarm signals shall occur during or after the precipitation of dry or wet snow, hail, frost, freezing rain, snow over a wet bridge deck, or various combinations of these conditions. This includes the freezing of water on the deck or the refreezing of melted ice, with or without the presence of anti-icing or de-icing chemicals.

1.3 BACKGROUND

1.3.1 Previous Approaches to the Problem

Previous approaches to the specific problem of area detection of ice and snow include the use of detectors on the roadway, embedded in the roadway, or located nearby but off the roadway. The latter approach

has been unsatisfactory to date since roadway conditions may be markedly different from conditions nearby, but off-road. Where the roadway has been plowed or where anti-icing or de-icing chemicals have been used on the roadway, measurement elsewhere where such chemicals are not present is likely to result in error.

Detectors which protrude above the roadway surface are short-lived because of direct exposure to snowplows, tire chains, and general traffic. Embedding the detectors below the surface reduces but does not eliminate the problem of detector failure. Area coverage by means of point detectors requires many detectors with the attendant decrease in reliability of the overall sensor system.

Detection schemes which have been used with some success include: (a) a combination of heated probe and unheated probe with a conductive imbalance between them; (b) use of temperature sensors and humidity sensors to indicate when ice can be expected to form; and (c) use of detector plates on which ice may form and cause a change on a frosted plate to which a thermal pulse has been applied.

Probes and plates embedded in a roadway are exposed to severe environments which include chemicals for de-icing and anti-icing. This type of detection system has provided reliable performance but is generally effective only for spot rather than area hazards. Additionally, these probe or plate systems may be adversely affected by de-icing/anti-icing chemicals. The approach described below is free of road chemical effects and provides an effective area detection scheme.

1.3.2 Selected Approach: The Microwave Radiometer

Lockheed applied a microwave radiometer to solve the problem of detecting snow, ice, and other hazardous conditions on a designated area of roadway. The radiometer consists of an antenna, a sensitive microwave receiver, and signal processing circuitry. Thermal noise power radiated and/or reflected in the microwave spectrum by the roadway and by snow and ice is measured by this radiometer whose output voltage is proportional to average radiometric temperature of the composite of materials on the roadway area within the antenna beam. In actual field use, the radiometer is to be installed above the roadway on a luminaire or on a structural tower so as not to interfere with traffic, and high enough to obtain the required area coverage. The radiometer is provided with a protective cover which will not interfere with the measurement function.

An existing design, which was developed in 1974 and field tested in 1975, was utilized as a solution to the area detection of ice and snow. The Lockheed breadboard radiometer used on this program is a solid-state design and operates at 10 GHz. A radiometer may be designed to operate at a higher frequency (e.g., 35 GHz) for this

application but only at a penalty of increased cost which was not justified.

The passive radiometer offers the advantage of presenting no hazard to motorists or to pedestrians since this system does not radiate microwave energy. An auxiliary temperature sensor, embedded in the roadway, was added to minimize false alarms.

1.3.3 General Principles of Radiometer Operation

All materials not at absolute zero temperature will radiate electromagnetic energy with a spectral distribution described by thermal radiation laws. Microwave radiometry is concerned with measuring that portion of radiated energy in a given microwave spectral region. The measuring device is known as a microwave radiometer, a sensitive microwave receiver with special design features and an energy collecting aperture (antenna). The amount of energy collected by the aperture depends on the emitting material characteristics, its absolute temperature, the characteristics of the intervening medium (atmospheric conditions) or devices (radomes), the surrounding radiation sources, and on observed material-antenna geometrical relationships. The sensitivity of the radiometer, a measure of its internal noise generation, depends on equipment design parameters and dynamic operating conditions (time-on-target).

Thus, there are four areas of interest in understanding microwave radiometry. These are:

- a) The energy radiating from the material in a given spectral range λ to $\lambda+d\lambda$, where λ is the wavelength of the radiation.
- b) The amount of this radiated energy collected by the radiometer aperture due to geometrical considerations (field-of-view, material size, etc.).
- c) The effect of the intervening medium or devices on the energy collected by the antenna.
- d) The sensitivity of the radiometer which enters into signal-to-noise ratio considerations.

Each of these four areas are discussed in the following subsections.

1.3.3.1 Energy Radiated From Material

In microwave radiometry, the radiometric temperature (expressed in degrees Kelvin) of a material is used as a measure of the energy radiated from a material. The concept of radiometric temperature is discussed here and its relationship to radiated energy is shown. The thermal radiation laws describe the energy emitted by a body; the differences and applicability of the several radiation laws are explained

in order to prevent misunderstanding on their use. The concepts of black bodies and nonblack bodies are also introduced and discussed.

o Radiation Laws

The radiation laws of interest to microwave radiometry are the Rayleigh-Jean's distributional law and Kirchoff's law. The Rayleigh-Jean's law is a simplified approximation of Planck's distributional law that very accurately describes the energy emitted by a black body in the long wavelength spectral region (microwave spectrum). This emitted energy is shown to be proportional to the absolute temperature of the black body. Kirchoff's law leads to the equality of emittance and absorptance, total or spectral, under thermal equilibrium conditions. This equality is important in determining the energy radiated from nonblack bodies and will be discussed in more detail later.

Other thermal radiation laws, although not of direct interest to microwave radiometry, are of general interest to the reader. Planck's distribution law correctly describes the complete spectral energy distribution emitted by a black body as a function of its absolute temperature. As mentioned above, the Rayleigh-Jean's law is an approximation of Planck's law applicable only to the long wavelength region of the spectrum. Similarly, Wein's distributional law is an approximation of Planck's law applicable only to the short wavelength region of the spectrum. If Planck's law is integrated over all wavelengths, it will yield the Stefan-Boltzmann law which states that the total power radiated by a black body is proportional to the fourth power of its absolute temperature. Wein's displacement law describes the wavelength at which maximum energy radiation per unit wavelength interval occurs as a function of the black body temperature. Planck's law was formulated and published a number of years after the laws of Rayleigh-Jean, Stefan-Boltzmann, and Wein.

The Rayleigh-Jean law is given as:

$$R_{\lambda} = \frac{2 \pi c K T}{\lambda^4} \text{ watts/cm}^2$$

where

- R_{λ} is defined as the spectral radiant emittance, the radiant power emitted per unit area per unit wavelength interval centered at wavelength λ .
- c is the velocity of light, 3×10^{10} cm/sec.
- K is Boltzmann's constant, 1.38×10^{-23} joules/ $^{\circ}$ K
- λ is the wavelength of interest in cm.
- T is the absolute temperature of the black body in $^{\circ}$ K.

This equation shows that the energy radiated by a black body is proportional to its absolute temperature.

o Black Body and Nonblack Body Concepts

A black body is a body that absorbs all radiation incident upon it. It is also a perfect radiator and thus radiates energy at the maximum rate per unit area at each wavelength for any given temperature. Although black bodies do not exist in nature, they serve as a standard of reference since their emitted energy can be described in Planck's law, and also by Rayleigh-Jean's law for the microwave region.

Since a nonblack body does not absorb all radiant energy incident upon it, part of the incident energy is reflected at the surface for an opaque body and part will be transmitted through for a transparent or translucent body. Applying the law of conservation of energy, the incident radiation upon a body can be expressed as:

$$E_i = E_\alpha + E_\rho + E_\tau$$

where E_i is the incident radiant energy, E_α is the absorbed energy, E_ρ is the reflected energy and E_τ is the transmitted energy. Dividing both sides of this equation by E_i yields:

$$1 = \alpha + \rho + \tau$$

where

$$\alpha = \frac{E_\alpha}{E_i} = \text{absorptance}$$

$$\rho = \frac{E_\rho}{E_i} = \text{reflectance}$$

$$\tau = \frac{E_\tau}{E_i} = \text{transmittance}$$

The parameters α , ρ , and τ are used in determining the radiation energy from a body. Their values can range from 0 to 1. For a black body, $\alpha = 1$ and therefore $\rho = \tau = 0$. For an opaque nonblack body, $\tau = 0$ and $\alpha + \rho = 1$.

For nonblack bodies, a term known as emittance is introduced which is a measure of the nonblack body emitted energy relative to that energy that would be emitted by a black body at the same thermodynamic temperature. Thus, emittance is defined as:

$$\epsilon = \frac{E}{E_{bb}}$$

Kirchoff's radiation law states that under thermal equilibrium conditions, the emittance of a body is equal to its absorptance or:

$$\alpha = \epsilon$$

Thus we can write:

$$1 = \epsilon + \rho + \tau$$

The total radiated energy for a nonblack body is therefore the sum of emitted, reflected, and transmitted energies. Thus:

$$E_R = E_\epsilon + E_\rho + E_\tau$$

or

$$E_R = \epsilon E_{bb} + \rho E_i + \tau E_{Background}$$

o Concept of Radiometric Temperature

Consider the energy radiated by a black body as described by Rayleigh-Jean's law. What is of interest is the amount of this energy collected by an antenna of effective aperature A_e located at a distance D from the black body. The antenna as viewed from the black body subtends a solid angle A_e/D^2 . Each differential surface area of the source then radiates an amount of energy into this solid angle in a wavelength interval given by:

$$dP_\lambda = \left(\frac{R_\lambda}{\pi}\right) (\Delta\lambda) (ds) \left(\frac{A_e}{D^2}\right) \text{ watts}$$

For the case where the solid angle subtended by the black body is much larger than the antenna beamwidth and significant sidelobes, the total power received can be shown to be:

$$P_{\lambda,p} = KT \Delta f \quad (\text{subscript p refers to plane polarized antenna case})$$

$$P_{\lambda,p} = KTB_n$$

where

B_n is the predetection noise bandwidth of the radiometer.

T is the absolute temperature of the black body.

K is Boltzmann's constant.

This indicates that the power received by a radiometer is very dependent on its bandwidth and that two radiometers of different bandwidth will measure different power levels received from the same

source. This problem can be circumvented by calibrating radiometers to indicate the noise temperature received since this is independent of the radiometer bandwidth.

Thus, the noise temperature received or radiometric temperature will be:

$$T_R = \frac{P}{KB_n} \lambda, P$$

where T_R is the radiometric temperature seen by the antenna for the special case of extended material and no intervening loss.

For the black body, the radiometric temperature will be its absolute thermodynamic temperature. For a nonblack body, if each of the energy contributors are thermal radiation sources, then the radiometric temperature of a nonblack body can be written as:

$$T_R = \epsilon T_{bb} + \rho T_i + \tau T_{Background}$$

For terrain viewing applications from an airborne position, T_{bb} is the ground or ambient absolute temperature and T_i is generally the radiometric temperature of the incident portionⁱ of the sky designated as T_{sky} . Since most objects on the ground can be considered as opaque (no signal transmission through the body), then the simplified form used for a terrain viewing application becomes:

$$T_R = \epsilon T_G + \rho T_{sky}$$

This equation is generally used to determine the radiometric temperature of a material. It is seen that this temperature is dependent on ϵ (emittance) and ρ (reflectance), material properties that vary with surface roughness, surface conditions, incidence angle, and polarization. It is also dependent on T_{sky} which varies considerably with weather losses and atmospheric path length. The dependency on T_G is minimal since the absolute temperature of the ground varies only by a relatively small percentage. Highly emissive material such as vegetation and soil have radiometric temperatures of about 250°K, slightly less than the ground temperature. Highly reflective materials such as metal and water have radiometric temperatures in the order of 60 to 150°K, and are referred to as "cold" materials as compared to "warm" vegetation and soil. Asphalt and concrete fall between "cold" and "warm" materials.

1.3.3.2 Geometrical Considerations

Thus far, only radiation from extended materials has been considered. Generally, however, in observing a scene composed of several different nonextended materials, the energy contributions of the several materials located within the radiometer antenna pattern must be considered. Since thermal radiation energy is random in nature, the energy contribution of each material can be considered singly and the collective contribution is then the sum of the individual contributions.

The received radiometric temperature for a nonextended material (neglecting intervening losses) can be written as:

$$T_A = T_R \left[\frac{1}{4\pi} \int_{\Omega} G(\theta, \phi) d\Omega \right]$$

where

T_A is the radiometric temperature of a nonextended material seen by the antenna

T_R is the radiometric temperature of an extended material seen by the antenna

The collective temperature will then be:

$$T_{A_{\text{scene}}} = T_{A_1} + T_{A_2} + T_{A_3} + \dots$$

where

T_{A_1} corresponds to the antenna temperature for material #1 as determined by the T_A equation, etc.

For a nonextended material, the integral above will be less than 4π and therefore $T_A < T_R$. For multiple nonextended materials, viewed simultaneously, the collective radiometric temperature received by the antenna will be less than the radiometric temperature of the warmest material observed and greater than the radiometric temperature of the coldest material observed. For example, if extended soil measures at 250°K, extended asphalt at 220°K, and extended water at 100°K, then an observed area consisting of water, asphalt and soil subareas will have a collective temperature between 250°K and 100°K.

There is no simple formula to determine accurately the antenna temperature for a mixed scene. An approximate formula yielding ballpark numbers can be used if the assumption is made that the antenna gain function, $G(\theta, \phi)$, is constant everywhere within the solid angle $\Omega_{-3\text{db}}$ defined by its half-power or -3 db points and zero everywhere outside.

A question often arises as to whether the power measured decreases proportionally with the inverse square of the range between source and antenna as is the case for radar and communication links. Consider the surface of the source as composed of many elemental areas Δs each radiating a power ΔP per unit solid angle. As the emitter-antenna range is increased, from R_1 to R_2 , the power density at the antenna, and hence the collected power, decreases by the ratio $(R_1/R_2)^2$. However, more elemental areas are now included within the directive collecting pattern of the antenna. For an extended material, the increase in elemental areas is proportional to $(R_2/R_1)^2$, and hence the change in received power from an extended surface varies as $(R_1/R_2)^2 (R_2/R_1)^2 = 1$, or no change. For a nonextended target, changes do occur.

1.3.3.3 Effects of Intervening Medium or Devices

An intervening medium or device affects the amount of energy collected by the antenna in two ways. First, if the medium or device transmittance is not unity, only part of the energy entering the body will be transmitted through. If this energy loss is due to absorption within the material, it is generally termed as attenuation. Second, a device or medium that exhibits attenuation will itself be a source of thermal radiation. This additional emission is directly additive to the attenuated emergent energy transmitted through the body.

It was noted that $\epsilon + \rho + \tau = 1$ is a necessary condition under thermal equilibrium. If $\tau \ll 1$, then $\epsilon + \rho \cong 1$. For a diffuse medium, it is generally assumed that $\rho = 0$ and therefore $\epsilon + \tau = 1$.

If the input energy to a device or medium is T_{in} , then the total output energy will be:

$$T_{out} = \tau T_{in} + \epsilon T_M$$

where

T_M is the absolute temperature (black body temperature) of the medium or device

Since it is assumed that $\epsilon + \tau = 1$, then

$$T_{out} = \tau T_{in} + (1 - \tau) T_M$$

In microwave measurements, the transmittance is given in terms of attenuation, L , where $\frac{1}{L} = \tau$. Thus,

$$T_{out} = \frac{T_{in}}{L} + \left(\frac{L-1}{L} \right) T_M$$

The convenience of this form is that if the attenuation is known, 3 db for instance, then $L = 2$ corresponding to 3 db can be easily substituted. Attenuation values are generally available for weather losses.

1.3.3.4 Radiometer Sensitivity Considerations

The function of the radiometer is to facilitate measurement of the noise power collected by the antenna. This is accomplished by amplifying and rectifying the signal, and then filtering the resultant dc voltage. The use of a square law detector results in a linear relationship between the rectified voltage and the input power to the detector.

Two parameters are used to assess the quality of the radiometer design. The first is its temperature-voltage conversion factor and the second is its inherent temperature resolution. The temperature-voltage conversion factor is determined by calibration tests and permits calculation of the radiometric temperature seen by the antenna based on measurements of the radiometer output voltage. Assuming that one is able to measure this output voltage very accurately, then the accuracy in determining the antenna temperature is dependent solely on the constancy of the conversion factor. Major causes for changes in this factor are the gain instabilities and drifts in the pre-detection amplifier.

The temperature resolution of a radiometer is a measure of the fluctuations in the detected output voltage that prevent the observer from concluding whether an incremental change in voltage was due to random fluctuation or from an incremental change in antenna noise temperature. The actual temperature resolution will be poorer than the inherent temperature resolution; the latter is a function of nominal design parameters, whereas the former includes additional degradation due to instabilities in the nominal design parameters. By proper design, the inherent temperature resolution can be approached through reduction of instability effects and this is generally the parameter that is given as minimum detectable temperature change or ΔT_{\min} .

The inherent temperature resolution can be expressed as:

$$\Delta T_{\min} = K \frac{(F-1)T_o + T_A}{\sqrt{B\tau}}$$

where

- T_{\min} is the equivalent rms input noise temperature that will produce the output fluctuations.
- K is a constant depending on the design configuration of the radiometer
- F is the receiver noise figure

T_o is 290°K by definition of noise figure.

T_A is the antenna noise temperature.

B is the equivalent predetection noise bandwidth.

τ is the equivalent integrating time of the post-detection smoothing circuit and is inversely related to the post-detection bandwidth.

For terrain viewing applications, where $T_A \leq T_o$, this can be simplified to

$$\Delta T_{\min} \approx K \frac{FT_o}{\sqrt{B\tau}} = (K) \left\{ \frac{F}{\sqrt{B}} \right\} (T_o) \left(\frac{1}{\sqrt{\tau}} \right)$$

The factor K will be equal or greater than 1; it is equal to one for a total power radiometer, equal to 2 for a Dicke radiometer with square wave modulation and demodulation, equal to 2.22 for square wave modulation and sine-wave demodulation, etc. The factor F/\sqrt{B} is a function of the components used in the receiver and a figure of merit, $M = \sqrt{B}/F$, can therefore be defined to be used in assessing the performance of various front-end components; the higher the value of M , the lower will be the radiometer ΔT_{\min} .

The parameter τ is not determined by design but is a constraint placed by the operating conditions. In observing a given unchanging scene, there will be no change in the received temperature (assuming constancy in sky and weather conditions) and a lengthy observation time, and hence a long integrating time can be used. This results in an almost negligible value for ΔT_{\min} . For operations where the received temperature is rapidly changing, such as when scanning the beam across a scene or changing the range between antenna and scene, the information or postdetection bandwidth must be increased to accommodate the increased received information rate, resulting in the use of a shorter integrating time and hence a larger ΔT_{\min} .

Section 2.0

SUMMARY OF REQUIREMENTS AND WORK PERFORMED

2.1 CONTRACT REQUIREMENTS

The period of performance of this contract was from September 21, 1977 through August 31, 1978. Figure 1 indicates the work phases, tasks, and a summary schedule of program milestone items.

The deliverable prototype radiometer system has specific requirements invoked. The system shall not be harmed by de-icing chemicals, snowplowing operations, chains, or heavy trucks. It must operate in the presence of both light and heavy vehicular and pedestrian traffic without presenting any danger to this traffic. It must be capable of operating before, during, and after the application of de-icing chemicals such as salt or urea. The physical principle employed by the detector must not create any significant hazard to drivers or pedestrians through radiation (ionizing or non-ionizing) or through distraction by bright visible light beams. The equipment must be capable of operating continuously 24 hours per day for at least the 9 coldest months of the year without being seriously affected by seasonal or diurnal sun position.

2.2 HIGHLIGHTS OF WORK PHASES

Phase I, a 3-month effort, concerned optimization of the Lockheed breadboard radiometer for the purpose of obtaining a measurements data base on hazardous road conditions. Another effort during this phase was on system tradeoffs, e.g., false alarm rate vs. sensitivity (temperature error) and receiver cost vs. system bandwidth and noise figure. Various theoretical analyses were also made involving design and performance factors for the intended application. The final effort on Phase I was generation of a test plan detailing the overall objective, laboratory tests using fabricated roadway simulators, and field tests to be run at suitable sites in the Northern Sierras region.

The 4-month, Phase II effort involved modifications and checkout of Lockheed's breadboard radiometer; conduct of laboratory tests using fabricated roadway simulators; field testing at several sites in the Northern Sierras region; and submittal of a Test and Interim Recommendations Report (LMSC/D472217, dated May 1, 1978).

In conducting Phase II tests, emphasis was placed on the most important aspects of testing, namely:

- o Determine radiometer stability characteristics.
- o Verify that radiometric temperature measurements are equivalent

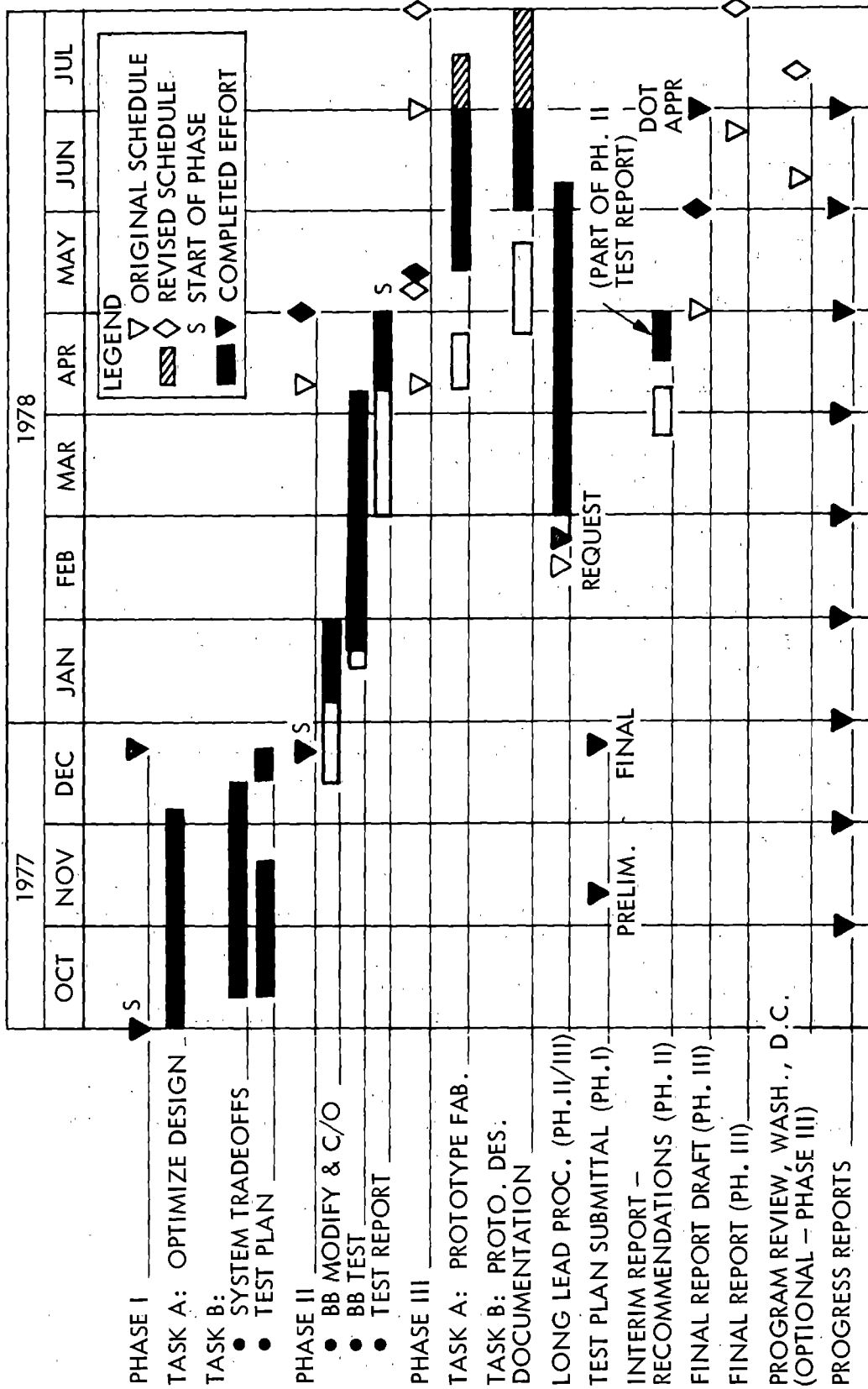


FIGURE 1. PROGRAM TASKS AND SCHEDULE

to other previously published results since feasibility for detecting ice is based on theoretical derivations taken from such reports.

- o Prove or disprove feasibility of detecting actual hazards using roadway surface simulators.
- o Determine radiometric temperature effects of the most widely used anti-icing methods: salt and sand.
- o Perform limited testing under actual field conditions in a cold weather environment.
- o Develop rationale for development of a hazard warning alarm circuit and fabricate and test such a unit.

The overall test program proved very successful. Stability characteristics were defined and a temperature instability problem was discovered. Provisions have been made to correct this problem in the Phase III prototype unit.

Radiometer performance matched that of previous tests and was in agreement with theoretical predictions. In addition, a theoretical analysis of effects of ice on a concrete surface was developed and the test data supported this theory.

A radiometric approach to detecting hazards of ice, snow and wet surfaces is shown to be feasible using today's technology. However, detection of a frost hazard was shown to be not feasible, although another approach to this problem is available by simply adding a dew point sensor input to the alarm circuit.

Effects of sand and salt on an existing ice surface were determined. Sand does not make any appreciable difference to radiometric temperatures, but salt makes a profound effect to both dry surfaces and icy surfaces. No study has been made of the effect of calcium chloride. Further study of these effects will be necessary to negate any false alarms or missed alarms which might be caused by these and other anti-icing methods.

Field testing was accomplished during a storm of Artic origin in the Sierra Nevada mountains. Further substantiation of radiometric sensor feasibility was gained from these tests.

The rationale for an alarm circuit was developed and a breadboard alarm fabricated. Limited testing was performed with this unit and the results are encouraging.

The final effort, the 4-month duration Phase III, concerned design, fabrication, and test of a deliverable prototype detector system; preparation of schematic, layout and assembly drawings; and preparation of the subject Final Report.

This prototype detector system incorporated two modifications to achieve the required receiver unit temperature stability: (1) addition of a controlled heater to a mixer-1st IF amplifier subassembly; and (2) on-off control of the local oscillator (L.O.) output signal by use of a microwave switch (pin diode). In the breadboard radiometer the L.O. was switched by a gating waveform. The processor unit includes two circuit cards for the alarm circuitry which was breadboarded and tested in Phase II. The processor also houses a 28 VAC transformer for the receiver heater element. Appropriate test points have been added and the readout display was changed from LED (light-emitting diode) to LCD (liquid crystal diode) type for better visibility in daylight.

From a repackaging standpoint, the receiver unit was designed to be weatherproof through the use of environmentally resistant connectors and cables, a protective receiver housing, and a sealed horn antenna. The processor unit, although not intended to be exposed to the same environment as the receiver unit, was housed in a weather resistant aluminum carrying case and is a more rugged package than the breadboard unit. An antenna calibrator unit, three 100 foot (30 m) interconnect cables, and a power line cord complete the prototype Hazard Detector System, Serial No. 1.

The prototype system was calibrated and adjusted (per the procedures of 6.3.2 and 6.3.3). Functional tests were performed at subsystem and system levels; test results met all anticipated performance requirements. Snow and ice detection tests were not performed during Phase III; however, simulated inputs were provided as needed to verify alarm circuit operation.

Reproducible drawings were prepared and delivered under separate cover. These drawings included schematics; wiring diagrams; printed wiring board and circuit card layouts; and unit and interconnect cable assembly drawings.

Section 3.0

DESCRIPTION OF PHASE I EFFORT

3.1 DESIGN OPTIMIZATION

The breadboard radiometer system optimization was performed with the following objectives in mind:

- 1) Provide a sensor to obtain measurements and provide a data base on snow, ice, slush and frost on a variety of roadway surfaces. This data base is to be used to determine the design of an appropriate hazard alarm circuit.
- 2) Provide design-proofing data for the design and fabrication of a deliverable prototype sensor under Phase III of this contract dedicated to effective detection of road surface hazardous conditions.

3.1.1 Radiometer Configuration

LMSC ID radiometers were used in three distinct configurations:

- a) X-Band radiometer with microwave switch (Figure 2).
- b) X-Band radiometer without microwave switch. (Hong Radiometer) (Figure 3).
- c) 94 GHz dual-polarization sensing radiometer (Hong Radiometer implementation) (Figure 4).

To accomplish the objectives noted above, a radiometer sensor was implemented from a combination of the Hong X-Band radiometric receiver (configuration b), and the 94 GHz processor (configuration c). This combination was arrived at, in part, by cost and scheduling considerations for producing the Phase III prototype and a sensor suitable for Phase II testing. An X-Band radiometer is desirable due to the availability and lower cost of X-Band components. Additionally, the processor of the 94 GHz system was documented and fabricated on printed circuit cards, whereas configurations a) and b) were breadboarded on handwired boards. Also, there was no documentation available on parts layout on the a) and b) processors making reproduction and modifications of the circuits difficult.

The parameters of the radiometer considered for optimization were: (1) frequency; (2) RF bandwidth; (3) video output bandwidth; (4) antenna beamwidth; and (5) packaging. Since the test planning was in its early stages, the optimization of frequency, RF bandwidth, and antenna beamwidth were performed during the test planning to minimize the hardware schedule impact. The frequency and antenna beamwidth

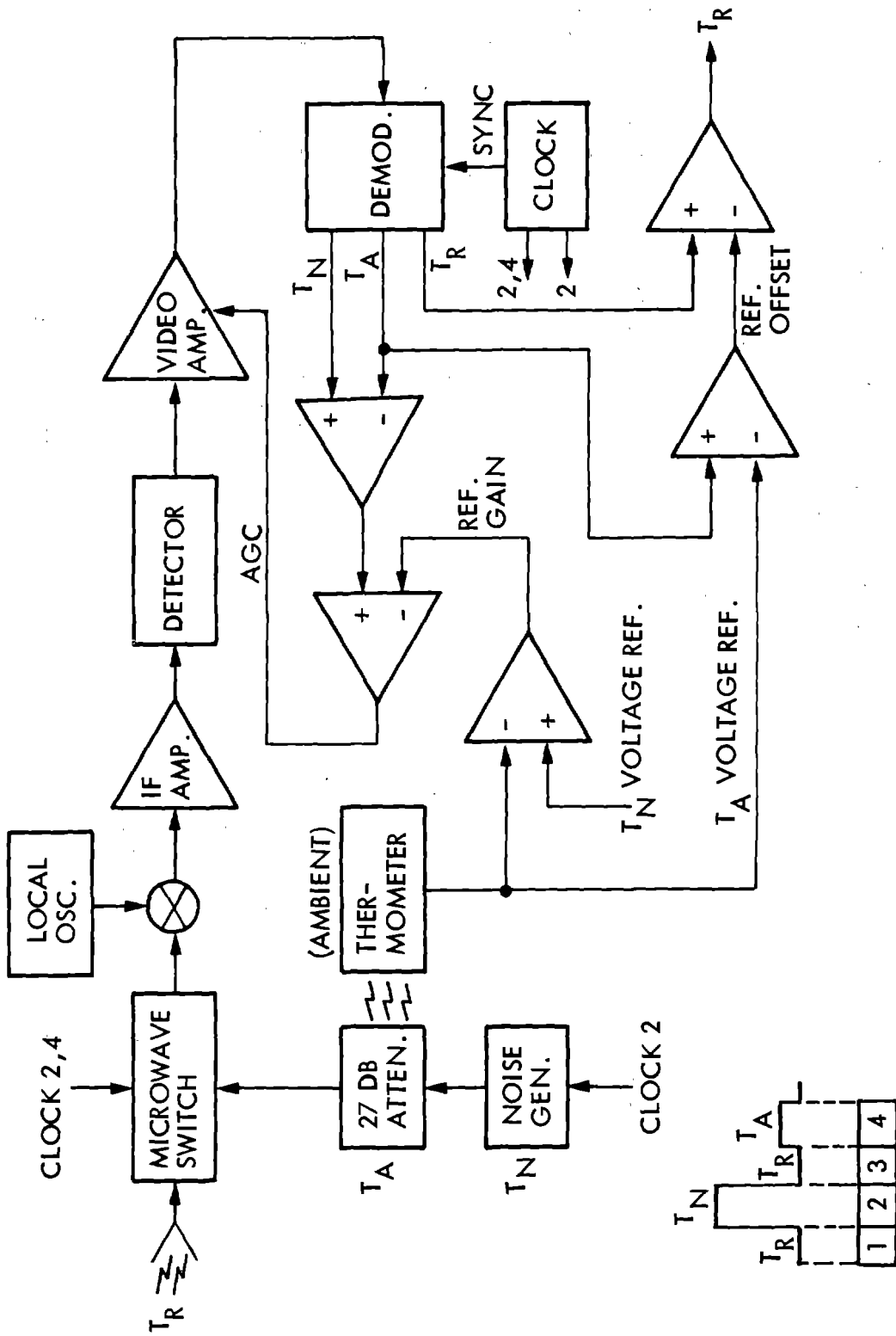


FIGURE 2. 10 GHZ RADIOMETER BLOCK DIAGRAM (WITH MICROWAVE SWITCH)

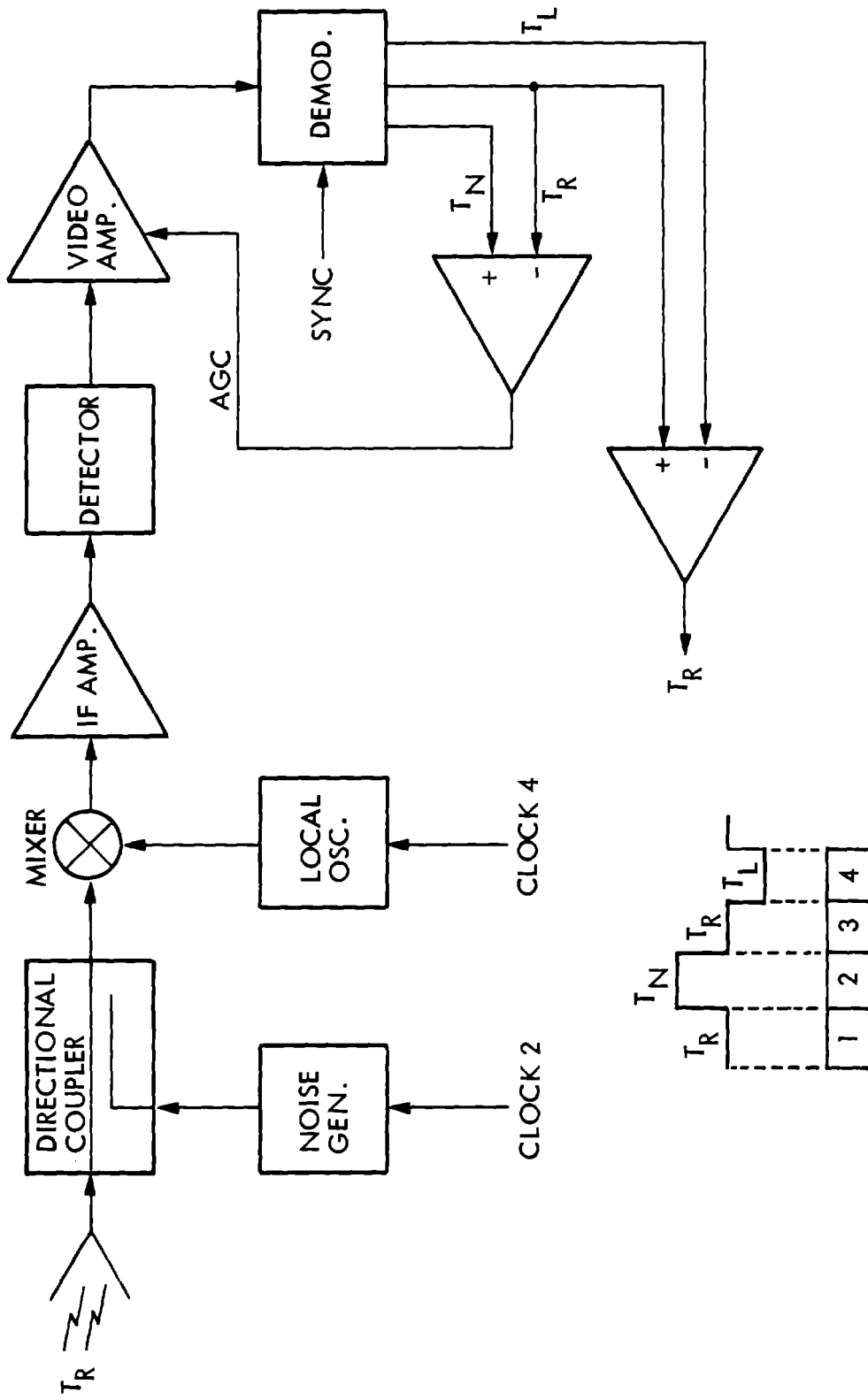


FIGURE 3. 10 GHZ RADIOMETER BLOCK DIAGRAM (NO MICROWAVE SWITCH)

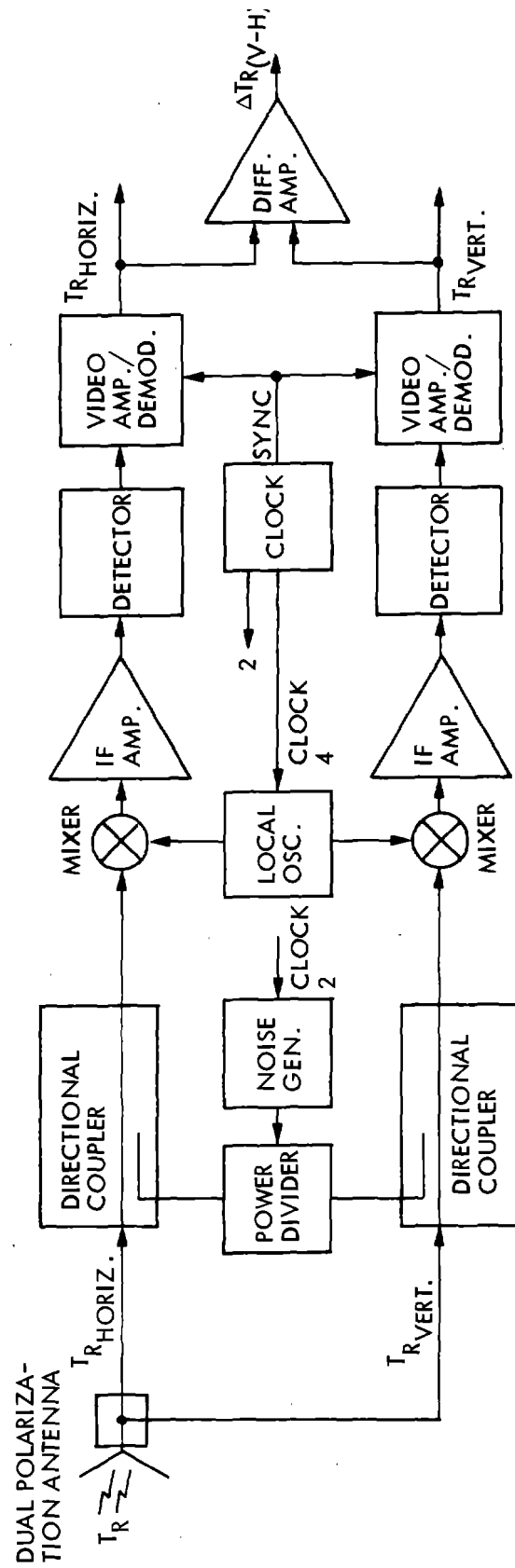


FIGURE 4. 94 GHZ RADIOMETER BLOCK DIAGRAM (DUAL-POLARIZATION SENSING)

combination determines the area coverage as a function of the height of the radiometric antenna above the test specimen. The RF bandwidth has a minor effect on the performance of the radiometer under controlled test conditions. The video bandwidth of 300 Hz was originally mechanized to resolve ground targets from a moving airborne test bed. For the snow and ice detector application, where the targets of interest are essentially stationary, the video bandwidth could be reduced to below 1 Hz. However, for minimal change to the output circuits, the video bandwidth was reduced to 10 Hz. The packaging considerations were to facilitate the simulator testing and field testing with no modifications. This required repackaging of the configuration b) X-Band receiver to accommodate a mounting fixture to provide for horizontal polarization, vertical polarization, and off-normal look angles to the test targets. The additional interface power supply and L.O. drive circuit were incorporated into the receiver during this repackaging. Detailed analyses on the interaction of radiometer parameters vs. performance is included in System Tradeoffs, Section 3.2.

3.1.2 Detection Performance

The snow and ice detector performance analysis based on an initially limited data base is summarized in Table 1. This analysis was prepared prior to Phase II testing. One unknown in this analysis is the quantitative definition of hazardous conditions. Static measurement and analysis has been performed on snow, ice, and slush. Measurable temperature differences were noted between ice, slush, and dry roads. Therefore, if the definition of a hazardous condition is between an icy and a slush condition, the breadboard snow and ice detector system will have a high success rate only affected by the percent of hazardous road within the antenna beam. No data was available on the effects of de-icing chemicals; therefore, these effects were to be determined during Phase II of the study.

Summaries of other special conditions relating to detection performance are noted below.

- o Effects of Pedestrian Traffic - Pedestrian traffic does not pose a problem due to the small beamfill a pedestrian would provide to the snow and ice detector; under heavy foot traffic, the detector might give a false alarm. However, since the detector would be positioned to monitor the roadway, it is unlikely that heavy foot traffic would be encountered within the area of interest.
- o Vehicle Traffic - Vehicle traffic introduces errors into the radiometric sensor. The vehicles are metallic, presenting a cold radiometric source (approximately 70°K) and, depending on the size and number of vehicles, the beam filling by the vehicles will be a variable. Thus, a wide range of radiometric temperatures would result, some of which could be in

TABLE 1. PERFORMANCE ASSESSMENT

<u>Parameter</u>	<u>Probability of Success</u>	<u>Remarks</u>
1. 24 Hour Operation	Excellent	All solid state design.
2. 9 Coldest Months	Good	Unit tested to -20°C; heating of critical elements will be considered.
3. All Weather	Good	Protective housing will be provided.
4. Sun Position	Excellent	Negligible effect on measurements.
5. Vehicle Traffic Heavy Light	TBD TBD	Vehicles affect the radiometer temperature measurement; method TBD to best isolate the errors introduced.
6. Pedestrian Traffic	Very Good	Minor perturbation into measurement.
7. De-icing Chemicals Salts Urea	TBD TBD	Inadequate data available to estimate radiometric measurements.
8. Snowplow	Excellent	No effects on equipment.
9. RFI External Roadway Lighting	Very Good TBD	10 GHz antenna highly directional. Interference is unlikely. Frequency band is assigned to radar and inter-satellite communications. Vapor lamps emit noise, possibly altering the sky temperature.
10. Hazards to: Vehicle Pedestrian	Excellent Excellent	Passive system. No radiation hazard.

TABLE 1. PERFORMANCE ASSESSMENT (Continued)

<u>Parameter</u>	<u>Probability of Success</u>	<u>Remarks</u>	
11. Alarm			
Wet Snow	Excellent	Results from previous measurements indicate that if the scene is 90% uniform within the effective beamwidth, the sensor can discriminate a hazardous ice condition from all the other condition parameters listed here. For the case of partial beamfill, more data will be required.	
Dry Snow	Excellent		
Wet	Excellent		
Hail	Excellent		
Frost	Excellent		
Rain, Freezing	Excellent		
Snow over Wet Deck	Excellent		
Freezing w/wo Chemicals	TBD		
12. Maintainability	Excellent		All solid state design; modules are replaceable. Installation cost will be minimal.
13. Cost	Good		Based on initial production estimate.

the simple alarm band proposed for the breadboard system. Therefore, unless a more sophisticated alarm criteria is used, a high missed alarm rate is predicted for vehicle traffic. Analysis of a typical vehicle situation is discussed in Section 3.3 (Theoretical Analyses).

- o Sun Position - The sun position does not introduce appreciable error into the radiometric sensor. Although the sun is a very hot radiometric source, the beamfill presented to the radiometer is very small. Analysis of this effect is treated in Section 3.3 (Theoretical Analyses).
- o Radio Interference - Initial analysis of Radio Frequency Interference (RFI) indicates that some potential problems exist. The 10 GHz frequency band is allocated for radar and intersatellite communications. At these high frequencies, the radiating antennas are highly directive providing some immunity to the radiometer. Pulse radars introduce no problems to the radiometer due to the low pass filter of the radiometer. However, CW radar, such as the speed detection radars utilized at 10.5 GHz by law enforcement agencies could possibly introduce errors.

Another source of RFI is the roadway lighting. A majority of the lamps are of the gas discharge type which is a good source of radiometric noise. The effect of the noise, if present, would change the sky temperature term, introducing a change in radiometric temperature. These errors would cause a missed alarm using the simple breadboard alarm technique. This does not make the radiometric sensor ineffective, since this effect is a predictable error which can be calibrated out.

3.2 SYSTEM TRADEOFFS

The system tradeoffs for the snow and ice detector are for the most part dependent on the criteria chosen for the detection of defined hazardous conditions in radiometric parameters. The tradeoffs discussed here will be related to the snow and ice detector performance in terms of false alarm rate and the probability of missed alarm.

In order to make this preliminary tradeoff study meaningful, and also provide some insight on how the various radiometer parameters interact on the snow and ice detector performance, the following simplifying assumptions are made:

- 1) The hazardous/nonhazardous condition can be defined by a change in radiometric temperature which is unique and the alarm mechanism is a simple detection of this change.
- 2) All external influences such as cars, changes in the ambient radiometric scene, and radio frequency interference will be considered non-existent.

3.2.1 False Alarm/Missed Alarm Probabilities

With these two simplifying conditions, the false alarm probability and missed alarm rate can be traded off against the errors, ϵ , in the radiometer measurement and the detection criteria of radiometer temperature change from nonhazardous to hazardous condition, defined by the term T_D (detection threshold, as illustrated in Figure 9).

The probability of false alarm, P_{FA} , is defined by:

$$P_{FA} = \exp \left[- \left(\frac{3 T_D}{2 \epsilon} \right)^2 \right]$$

P_{FA} is plotted in Figure 5. The probability of missed alarm, P_{MA} , is defined by:

$$P_{MA} = 1 - \frac{1}{2} \left[1 - \operatorname{erf} \left(\frac{3}{2} \frac{(T_D - T_I)}{\epsilon} \right) \right]$$

where

T_D = detection threshold

T_I = actual radiometric temperature

ϵ = radiometer measurement error

$$x = \frac{3(T_D - T_I)}{2 \epsilon}$$

and $\operatorname{erf}(x) = \frac{2}{\sqrt{\pi}} \int_0^x \exp(-u^2) du$ (the standard Error Function)

P_{MA} is plotted in Figure 6. These probability curves are for a single measurement event. The length of each such measurement is determined by the response time, τ , required for the detector system to determine a hazardous condition.

The false alarm time, T_{FA} , (inverse of false alarm rate) is defined by:

$$T_{FA} = \tau \exp \left[\left(\frac{3 T_D}{2 \epsilon} \right)^2 \right]$$

T_{FA} is plotted in Figure 7 as a function of the detection threshold to measurement error ratio, T_D/ϵ , for various response times, τ . This T_D/ϵ term is being used here in a fashion analogous to the signal-to-noise ratio, S/N , in conventional radar detection analysis.

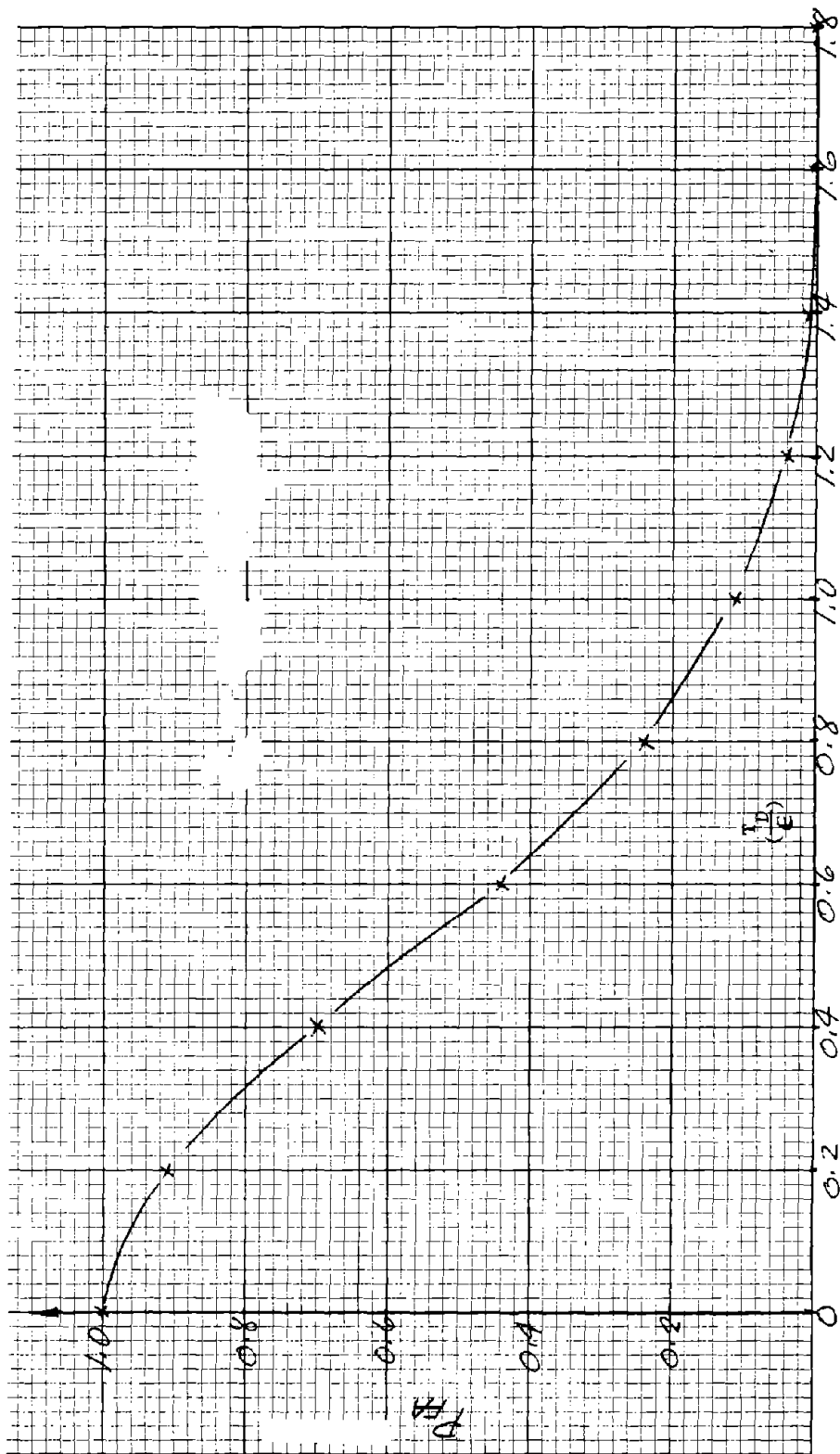


FIGURE 5. PROBABILITY OF FALSE ALARM

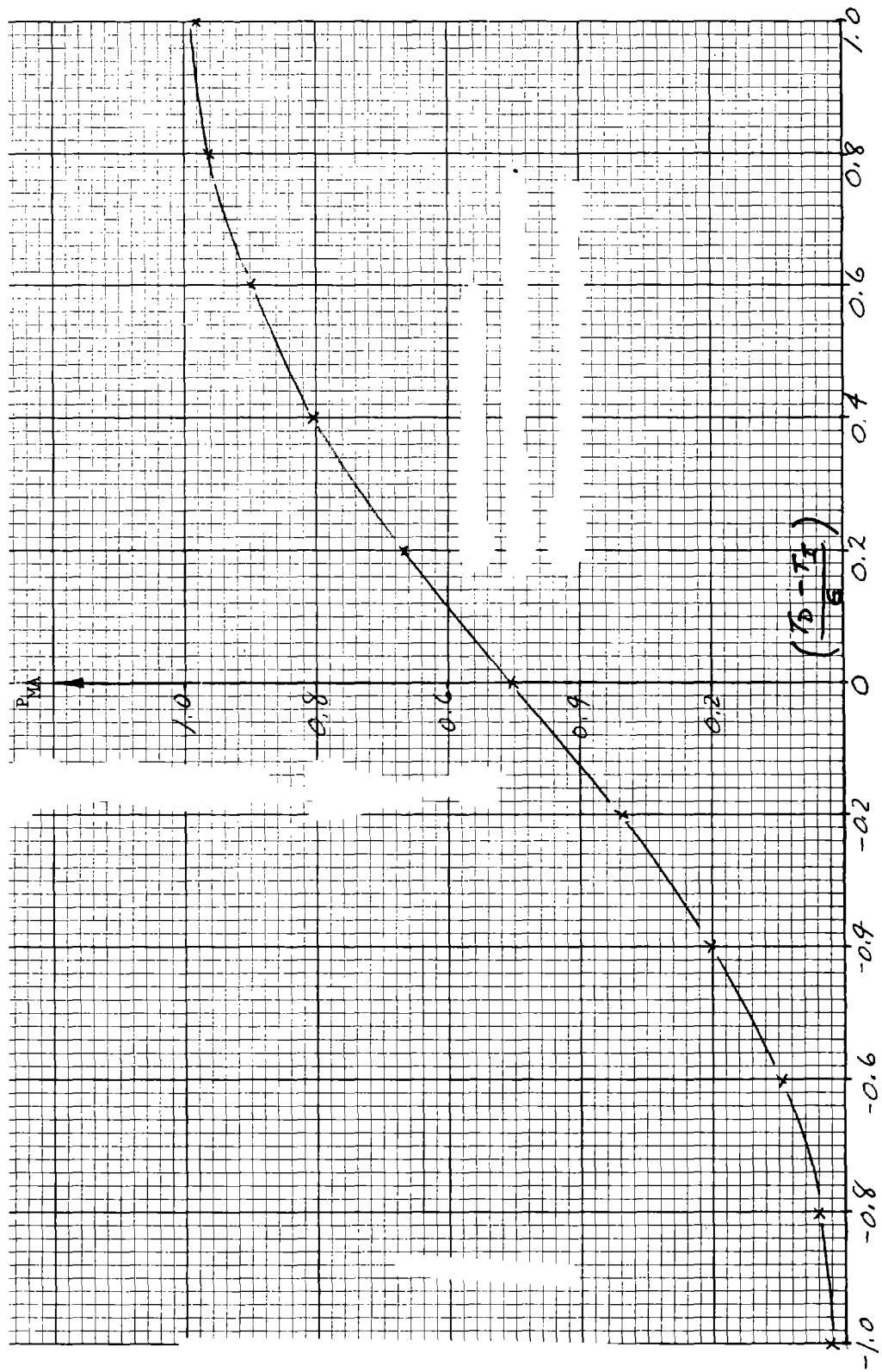


FIGURE 6. PROBABILITY OF MISSED ALARM

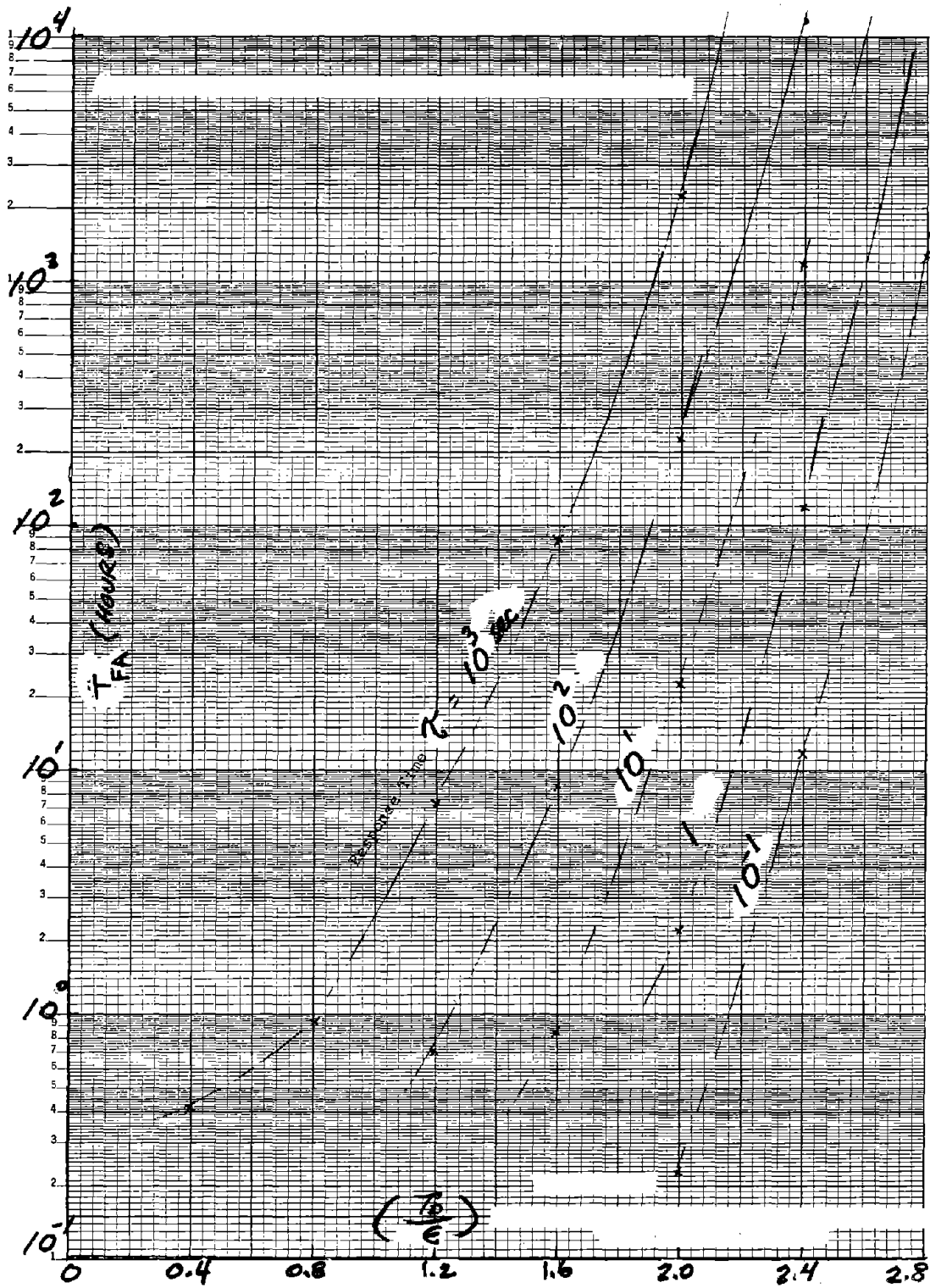


FIGURE 7. FALSE ALARM TIME WITH VARIOUS RESPONSE TIMES

3.2.2 Tradeoff of Detection Threshold, T_D

The relationship of the radiometric parameters to the false alarm and missed alarm factors includes the radiometric sensor errors, ϵ , and the temperature difference to be measured, T_D . T_D is related to the choice of frequency, antenna aperture size, and other factors. The antenna size/frequency/beamwidth relation is illustrated in Figure 8. The breadboard radiometer is noted in the figure. Also related to T_D is the smallest hazardous area to be detected and the antenna beamfill projected by this area. In essence, the optimum case would be to have a small size antenna which provides a large area of roadway coverage, yet is able to detect very small patches of icy areas within the antenna beam. This optimum case would then provide a small T_D , which requires ϵ to approach zero in order for the false alarm rate and missed alarm rate to approach zero. As in any ideal case, the parameter requirements are contradictory. Shown in Figure 9 is the effect of a normalized beamfill factor and radiometric temperature, but as the beam narrows to provide a large T_D , the area of surveillance is reduced. This therefore leads to the desirability of having a scanning antenna which will provide large areas of coverage along with high resolution. The added cost and complexity of such a system would be in the order of \$1.5 K (per system in production) to provide for the mechanical scan mechanism, drive and control circuit, and microprocessor computer to determine the alarm threshold for the various scan angles.

3.2.3 Tradeoff of Measurement Errors, ϵ

The radiometric temperature measurement error comprises two components: (1) the residual accuracy T_ϵ ; and (2) the minimum resolution of the radiometer (ΔT_{\min}). The error in the radiometric measurement is simply the arithmetic sum, $\epsilon = T_\epsilon + \Delta T_{\min}$. The residual accuracy (T_ϵ) of the radiometric sensor is constrained by the mechanization, the interval between precision calibrations, and the accuracy of the calibration source. The resolution (ΔT_{\min}) is defined as follows:

$$\Delta T_{\min} = \frac{K T_o F L_S}{\sqrt{2 B \tau}}$$

where

K = constant (modulation technique, etc.)

T_o = temperature of radiometer and source filling beam

F = noise figure

L_S = system loss factor (radome, antenna, etc.)

B = RF (predetection) bandwidth

τ = integration time

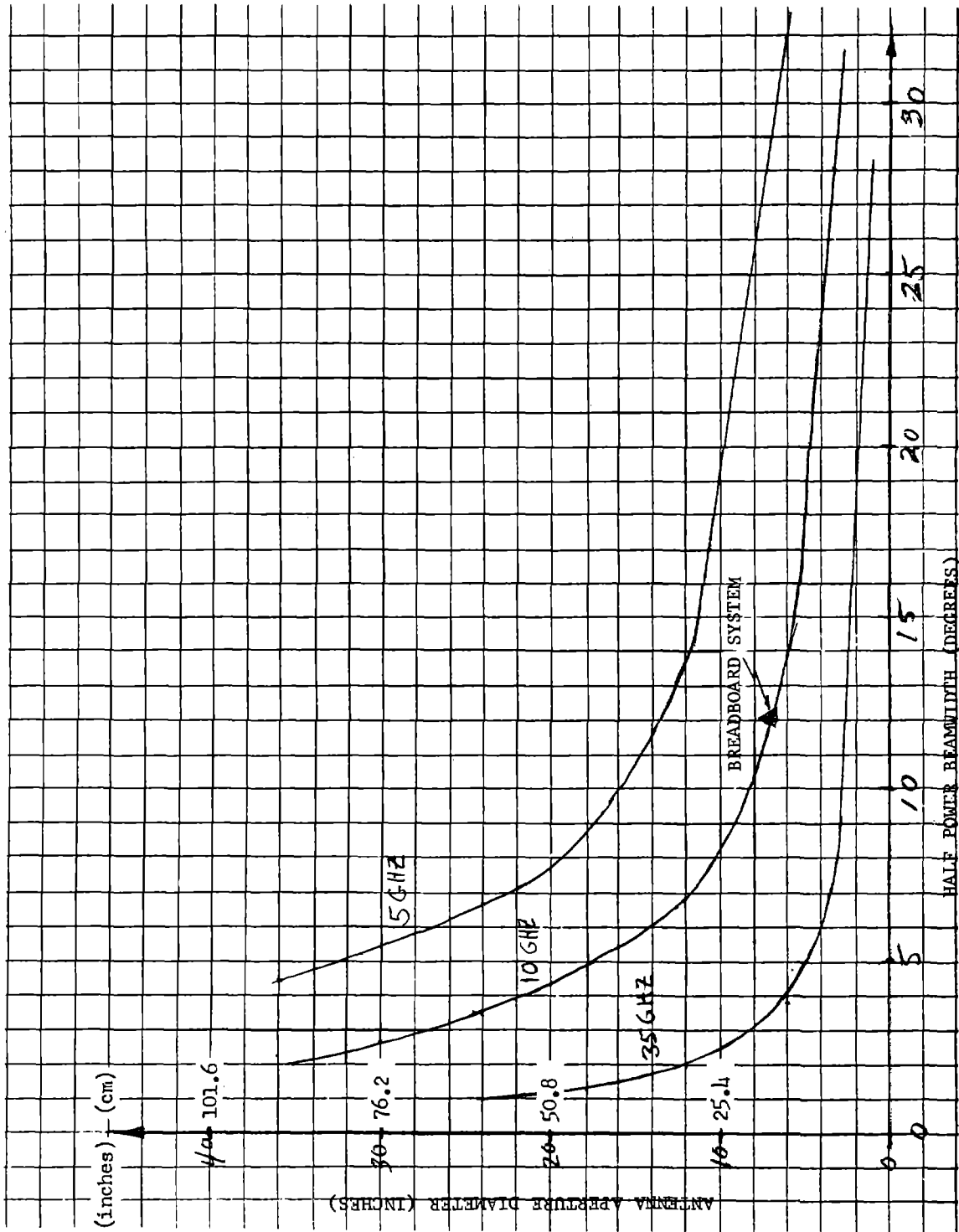


FIGURE 8. ANTENNA SIZE VS. BEAMWIDTH AND FREQUENCY

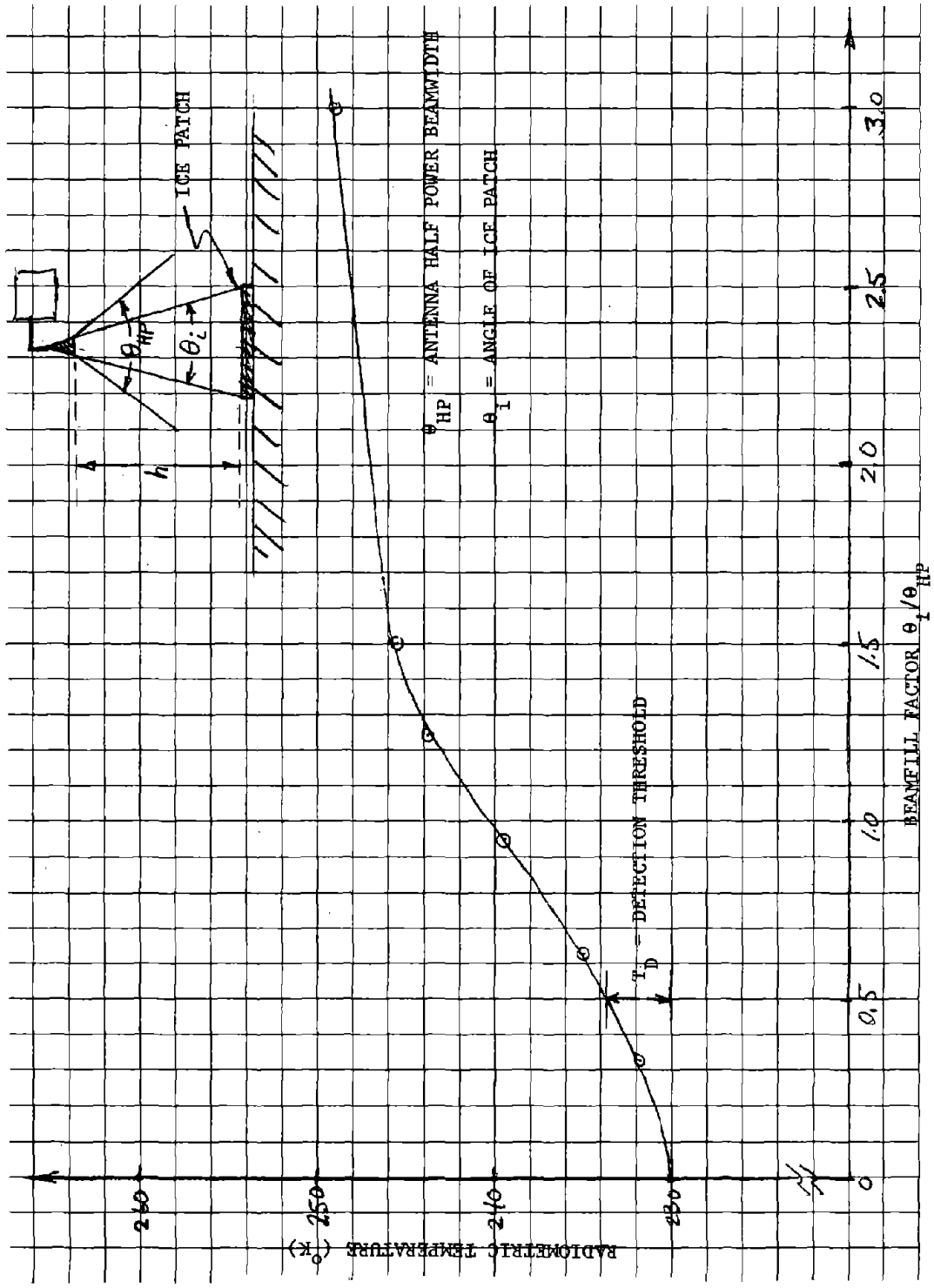


FIGURE 9. RADIOMETRIC TEMPERATURE VS. ANTENNA BEAMFILL

Plotted in Figure 10 is the projected production cost per system versus T_{ϵ} . The most accurate system indicated is a Dicke type radiometer with the reference housed in a precise temperature-controlled environment similar to systems used for radio astronomy. On the other end of the scale is a total power type radiometer with one temperature calibration. Note placement of the breadboard radiometer on the curve of Figure 10 and the range of values for radiometers of this type.

The ΔT_{\min} tradeoffs for a radiometer of the breadboard configuration as a function of RF bandwidth and receiver noise figure versus production cost are shown in Figures 11 and 12, respectively.

This tradeoff analysis was performed based on a limited data base of actual radiometric temperature measurements (prior to Phase II test activities). Major simplifying assumptions have been made on what an alarm mechanization might be and have excluded real world environmental effects that can have a major impact on the alarm mechanization.

3.2.4 Example of Use of System Tradeoffs

The following example is given to illustrate the interrelation of these tradeoffs. Assume the snow and ice detector system is required to provide a false alarm rate of one per year and a missed alarm probability of 0.1. It is also required to monitor an area of 15 ft. (4.6 m) diameter and detect an ice patch of 4 ft. (1.2 m) diameter.

From Figure 6, for a missed alarm probability of 0.1, $\frac{T_D - T_I}{\epsilon} = -0.6$. For a false alarm rate of 1/year ($T_{FA} = 8,770$ hrs) and a required response time of $\tau = 1$ second, Figure 7 indicates $T_D/\epsilon = 2.76$. Next, assume that we are using the breadboard radiometer sensor at 10 GHz and its antenna is mounted 30 ft. (9.1 m) above the roadway. The required half-power beamwidth would be $\theta_{HP} = 2 \tan^{-1} \left(\frac{15}{2(30)} \right) = 28.1^\circ$.

From Figure 8, the required antenna aperture for this beamwidth is about 3.5 in. (8.9 cm) diameter. At this antenna height, the ice patch will subtend an angle of 7.6° , giving a beamfill factor $\frac{\theta_i}{\theta_{HP}} = 0.27$.

From Figure 9, for the beamfill factor of 0.27, the radiometer temperature difference is 1.5° . Then, from the missed alarm criteria $\frac{T_D - T_I}{\epsilon} = -0.6$ and the false alarm criteria of $T_D/\epsilon = 2.76$ and substituting $T_I = 1.50$ (the temperature difference needed for detection), the resulting requirement is that the accuracy ϵ of the radiometer must be less than 0.45°K and the threshold setting T_D should be at 1.23°K . These ϵ and T_D values are obtained from solving $(T_D - 1.5)/\epsilon = -0.6$ and $T_D/\epsilon = 2.76$. From Figure 10 it is seen that this ϵ requirement is not within the current radiometer accuracy range. Therefore, the most restrictive requirement is the value of ϵ .

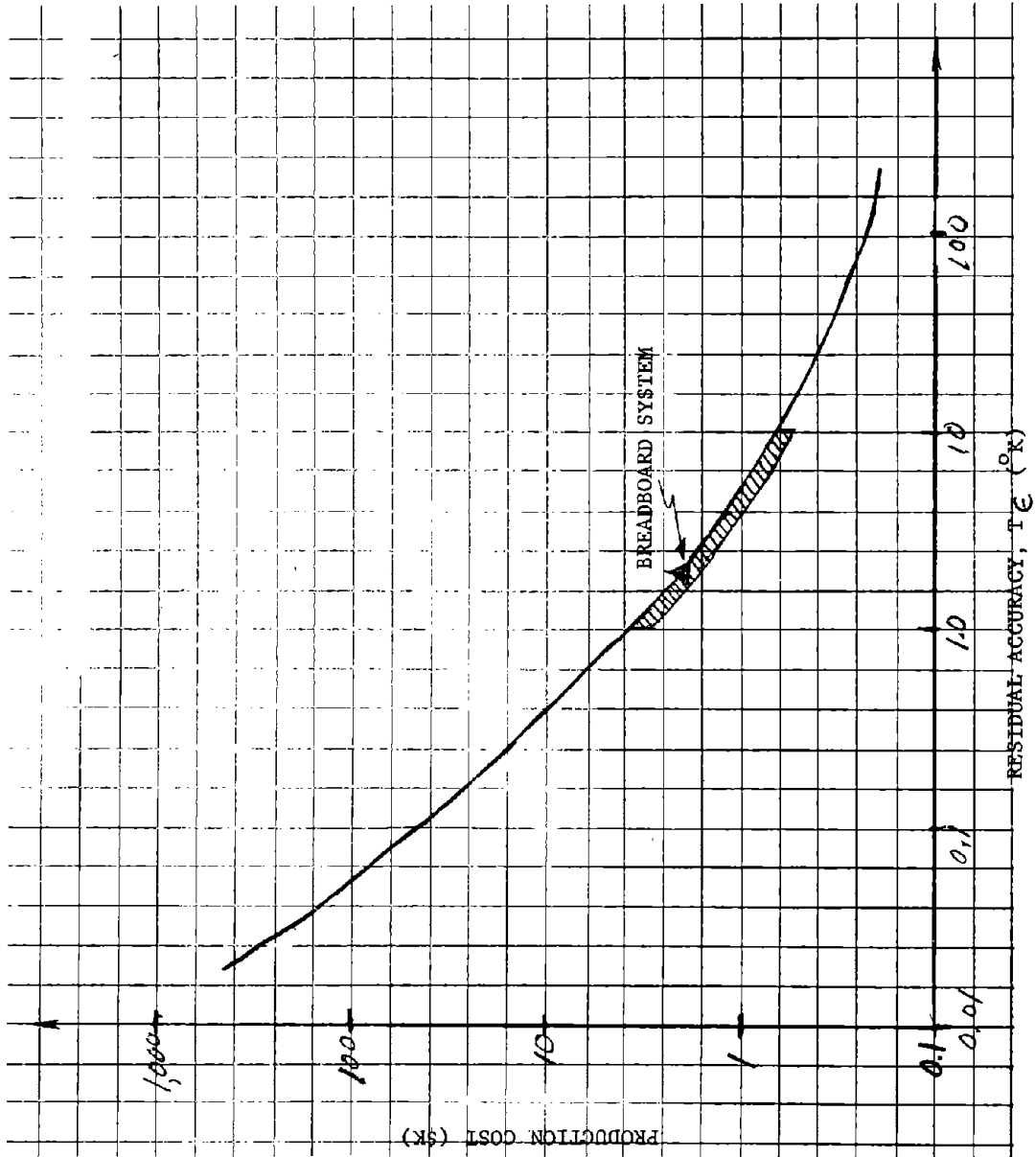


FIGURE 10. RADIOMETER ACCURACY VS. PRODUCTION COST

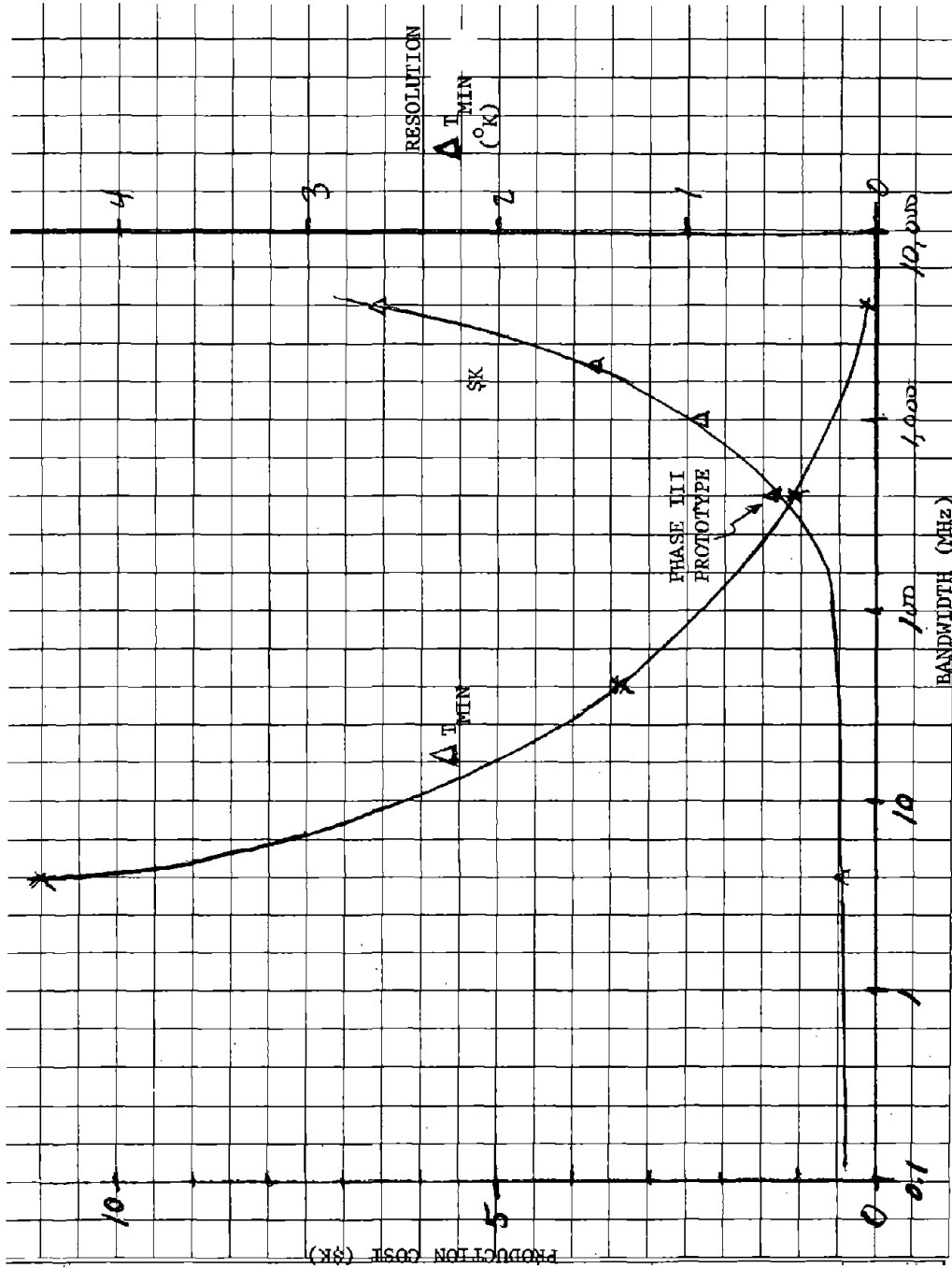


FIGURE 11. RF BEAMWIDTH VS. RESOLUTION AND COST

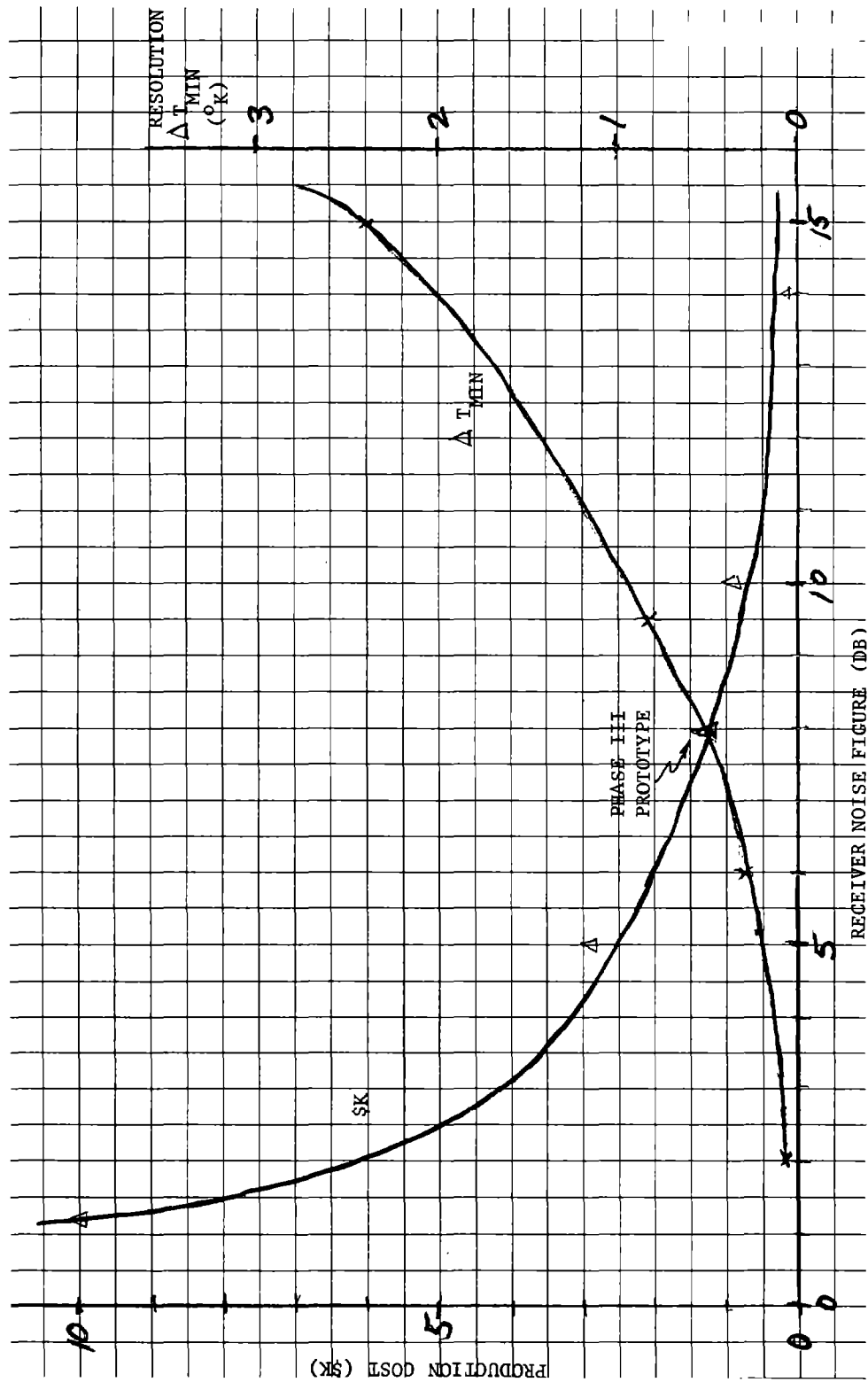


FIGURE 12. RECEIVER NOISE FIGURE VS. RESOLUTION AND COST

Now treating the tradeoffs from an achievable ϵ standpoint, say $\epsilon = 2^\circ\text{K}$, then to maintain the same false alarm/missed alarm criteria, the only tradeoff parameter left is the beamfill factor $\frac{\theta_i}{\theta_{\text{HP}}}$. For $\epsilon = 2^\circ\text{K}$, solving $\frac{T_D - T_I}{T_I} = -0.6$ and $T_D/2 = 2.76$, we obtain $T_I = 6.72^\circ\text{K}$. From Figure 9, this T_I requires a $\frac{\theta_i}{\theta_{\text{HP}}} = 0.77$. This, in turn, requires that the half power beamwidth θ_{HP} be 9.7° which requires an antenna aperture of about 8.5 in. (21.6 cm) diameter. However, in this example, the surveillance area has been reduced to 5.1 ft. (1.6 m) diameter.

From the exercises given above, it is clear that conducting a tradeoff analysis is an iterative process where often the system desires are unrealizable. Hence, the system designer must weigh each system parameter and, with the aid of the tradeoff curves, come up with the optimum realizable system.

3.2.5 Reliability Analysis

Along with the system tradeoff investigations discussed above, a reliability analysis was performed. This analysis is contained in Appendix A which has been separately transmitted. In summary, the analysis provides a breadboard radiometer block diagram comprised of three major sections; states the assumptions used to facilitate modeling and computations; defines a reliability probabilistic model; presents applicable calculations and a reliability vs. time plot; and provides conclusions and recommendations. A reliability of 0.930 is indicated at 1 year, degrading to 0.865 at 2 years.

3.3 THEORETICAL ANALYSES

3.3.1 General

During the breadboard radiometer design optimization and the general system tradeoff investigation tasks of Phase I, specific theoretical analyses were made to obtain additional insight on factors affecting the design and performance of a radiometric hazard detection system. These analyses are contained in Appendices B1 through B6 which have been separately forwarded. Summary descriptions of each appendix are provided below.

3.3.2 Description of Analytical Reports

The salient features and principal findings of the Appendix B reports are as follows:

- o B1. Comparison of Background and Sun Temperatures. Antenna beamwidth and sun brightness temperature values are given to illustrate the effect of the sun on the performance of a 10 GHz radiometer. The radiometric temperature error is of the order of 1° to 2° K even with an overhead (zenith) sun.
- o B2. Radiometric Temperature vs. Time-Car On Asphalt. The case treated here is a car at 30 mph (48.3 Kmph) speed on an asphalt road observed by a vertically-mounted 10 GHz radiometer antenna of 13° beamwidth. A radiometric temperature vs. time function is derived and plotted. A temperature drop in excess of 160°K from a starting reference of 224°K results as the car, being the "colder" object, completely fills the antenna beam. The smoothing effects of non-idealized antenna patterns and finite response time radiometer processors are also noted.
- o B3. The Concept and Calculation of Skin Depth. In this analysis, skin depth is defined in terms of penetration of an electromagnetic wave into a medium. A complex propagation constant is derived in terms of a complex relative dielectric constant. Skin depth calculations are made at 10 GHz for water at 20° and 9°C (0.2 and 0.3 cm); asphalt (1.7 cm); concrete (2.6 cm); brick (18.6 cm); dry and wet loam (5.1 and 0.6 cm); and dry and wet sand (1.7 and 0.4 cm).
- o B4. Radiometric Temperature for Ice on Concrete. A two-layer, smooth surface expression is derived which permits the calculation of radiometric temperature for a normal incidence case. An example of ice over concrete is treated with the thickness of the ice layer as a variable. The result is shown to be a cyclic temperature function with a period approximately equal to $\lambda/4$ (0.8 cm).
- o B5. Radiometric Temperatures for Rough Surfaces. The equation for the radiometric temperature, T_R , of a slightly rough surface is given for a radiometer at normal incidence. Equation terms are derived for computation purposes and the function h (rms amplitude of surface variations) and λ (correlation length of surface variations) are introduced. As an example, T_R is calculated at 10 GHz for an asphalt road at a surface temperature of 21°C with h values from 0.05 to 0.2 cm and λ values from 0.05 to 0.6 cm. Over this range of values, temperature increases up to 36°K are noted as compared to the smooth surface case, namely, $T_R = 241.5^\circ\text{K}$. Equations are also provided for the general case of non-normal incidence angles.
- o B6. Effects of Antenna Aperture Size - Ice Patch Example. A conical horn with half-power beamwidth of 12° is selected to illustrate antenna aperture effects. The coordinate reference system and antenna pattern are analytically defined and plotted.

Antenna percent beamfill is also plotted as a function of half beamwidth value. A scenario is selected with this antenna at vertical incidence 20 feet (6.1 m) above a concrete roadway observing an ice patch of diameter 2 r. The expression for T_R as a function of ice patch diameter is given, derived in terms of the percent antenna beamfill function, and plotted. Limits were determined experimentally for an "infinite length" road at a surface temperature of 0°C ($T_R = 225^{\circ}\text{K}$) and an "infinite diameter" ice patch 0.4 cm thick ($T_R = 225^{\circ}\text{K}$). For this example, with an ice patch less than about 10 feet (3.0 m) in diameter, corresponding to an antenna half-angle value of 15° or 88% beamfill, the radiometer temperature starts to approach the dry (no ice) road condition.

3.4 TEST PLAN

3.4.1 Objective

The overall objective of the test plan was to demonstrate the feasibility of detecting hazardous roadway conditions using a passive microwave radiometer system. The plan was developed to provide the guidelines and testing requirements necessary to utilize a breadboard unit in a systematic and progressive manner, allowing some degree of flexibility so that changes to the test sequence could be incorporated as test results were interpreted. The test plan defined the test schedule; tests to be conducted; objectives and requirements; and the test approach, including detailed test procedures. The complete test plan is identified as: LMSC/D556180, Test Plan - Area Detectors for Snow and Ice, dated November 18, 1977. A brief synopsis of the testing portion of this plan is outlined in the following sections.

3.4.2 Laboratory Test Plan

The testing portion of the test plan was comprised of two major sections: a laboratory test plan and a field test plan. Major emphasis was placed on the laboratory tests with the bulk of the testing performed during that phase. The laboratory tests were further subdivided into:

Preliminary Tests

Bench Test:

- Verify proper radiometer/processor operation.
- Set internal adjustments.

Calibration:

- Verify performance and scale factor.

Stability:

- Measure equipment stability for input voltage variation, temperature change, and time.

Simulator Tests

Accumulate radiometric temperature data for hazardous conditions.
Determine threshold levels for design of alarm logic circuits.

The preliminary bench tests were to be accomplished under the direct supervision of the design engineer and were intended mainly to consist of "factory adjustments". Since the breadboard unit is a single unique item, various adjustment techniques were purposefully omitted from the test plan as a cost saving measure. For a "one of a kind" unit, this approach is normally more economical.

The calibration procedure was detailed in the test plan so that personnel who were unfamiliar with the equipment could accomplish this vital task. In the beginning, the time span for which the breadboard unit would maintain a valid calibration was unknown. Original thoughts on this subject ranged from days to weeks. When the temperature instability problem was uncovered during later testing, frequent recalibration of the radiometer was necessary to counteract the effects of temperature drift. This procedure eliminated the need for complicated data correction methods.

The stability tests during the preliminary portion of the test plan were considered very important due to the uncontrollable nature of the environment and the range of input voltage within which the breadboard unit must operate. Diurnal stability (sun position) was considered of lesser importance due to the small increment of radiometric temperature affected by effective sky temperature. The test plan included test procedures to evaluate specific stability requirements for input voltage and ambient temperature change.

The roadway surface simulator test portion of the test plan was considered to be of primary importance to the entire program. Considerable time was to be spent on this activity so that meaningful data could be obtained prior to the field test portion of the program. As outlined in the test plan, the simulators were to be fabricated as described below.

One simulator was to be fabricated per Figure 13 for each of the following specimen types: (a) asphalt; (b) rough concrete; and (c) smooth concrete. The asphalt and rough concrete simulators were to be used as simulated road surfaces, and the smooth concrete simulator was to provide reference data to relate the theoretical analysis with empirical data obtained from the asphalt and rough surface measurements.

The simulators were to be fabricated by constructing three shallow wooden boxes, each on top of a standard wooden pallet. A cooling grid of 5/8" (15.9 mm) OD copper tubing was to be placed in the bottom of the boxes and the boxes were to be filled with the appropriate sub-

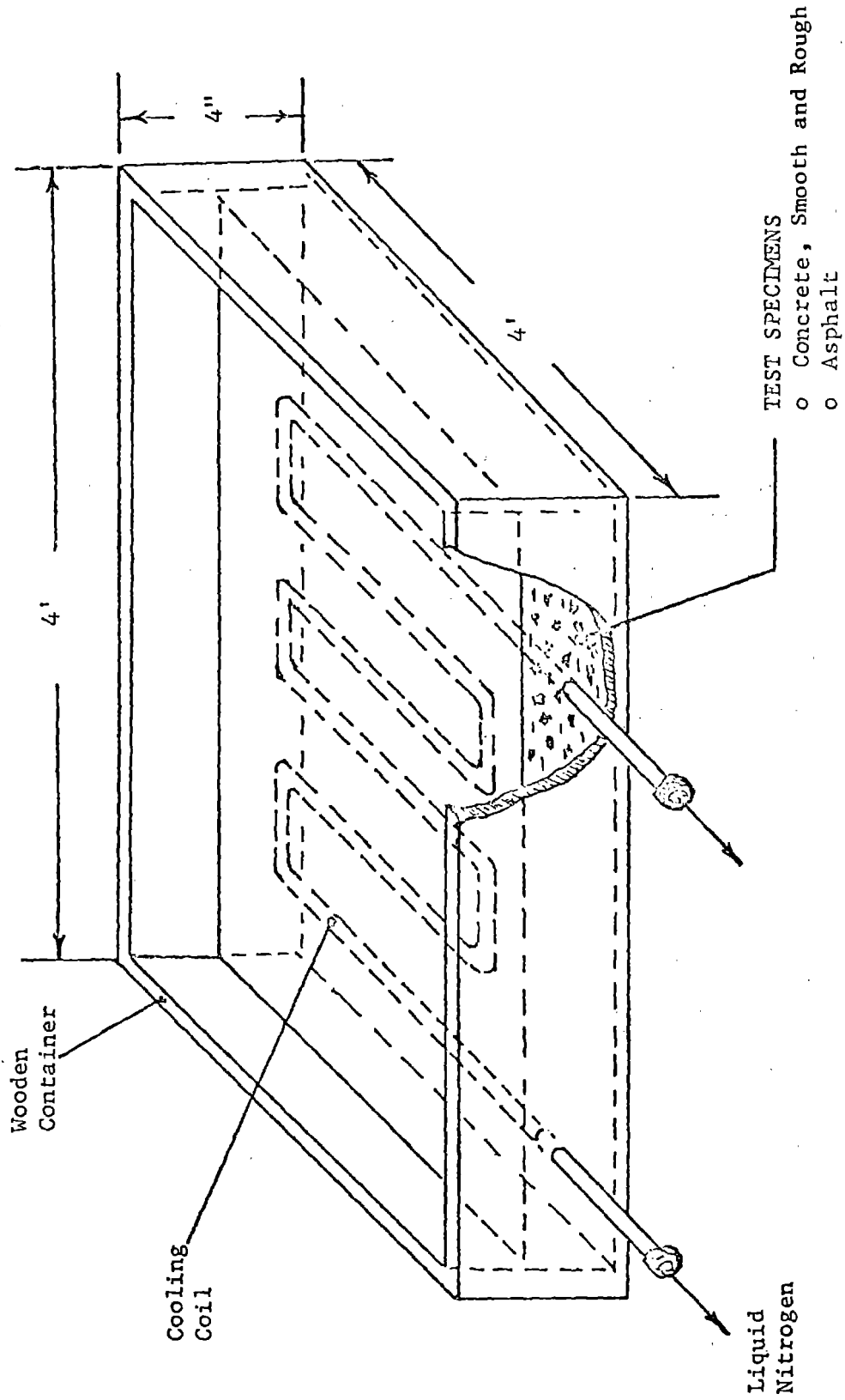


FIGURE 13. ROADWAY SURFACE SIMULATOR

strate material. Thermocouples were to be embedded near the surface of the substrate to provide substrate temperature data. Provision was to be made to contain the water necessary to form an appropriate precipitation layer.

Liquid Nitrogen (LN₂) was to be applied to the cooling coils from a 160 liter dewar to cool the simulator to a temperature lower than the freezing point of water.

Figure 14 shows the series of simulator tests which are outlined in the test plan. The "X" symbols of the table denote the specific tests to be run. The tests are ordered in a logical sequence so that radiometric temperature data pertaining to the majority of anticipated hazardous conditions could be obtained. This was deemed important to the definition and development of the alarm logic circuits. The test sequence consists of five major groupings of tests which would yield the most useful data within the economic and schedule constraints of the program. The major groupings are:

- (1) Basic Signatures - Test radiometer performance on two types of road surface with a theoretical cross-reference to a known surface. Provide basic data for preferred polarization determination, and a usable range of angles off vertical.
- (2) Simple Conditions - Test simple hazardous condition detection capabilities and provide data for determination of alarm logic circuit thresholds. Test 4 provides the same cross-reference information as the basic signatures tests.
- (3) Complex Conditions - Determine the amount of modification to basic radiometric temperature data by the introduction of de-icing/anti-icing materials.
- (4) Beamfill - Establish minimum detectable patch size. Provide data for determination of antenna beamwidth requirements for the prototype unit.
- (5) Optional - Ice on water test would require a housing placed over the simulator to facilitate freezing from the top down. The alarm logic tests would evaluate the ability of the alarm circuit to energize when hazardous conditions are detected and identified. The alarm logic test may be performed earlier in the test sequence, when the alarm logic unit is completed.

The test sequence did provide a useful starting point for the simulator tests, but was modified in the early stages of testing when the theoretical analysis of "Radiometric Temperature of Ice on Concrete" (see Sec. 3.2.2 B4) was developed. This modification was accomplished so that more realistic hazards involving thin ice layers would be tested.

TEST NO.	TEST TYPE	SIMULATED CONDITIONS	SMOOTH CONCRETE					ROUGH CONCRETE					ASPHALT					POLARIZATION	
			0°	10°	20°	30°	40°	0°	10°	20°	30°	40°	0°	10°	20°	30°	40°	HORIZ	VERT
1	BASIC SIGNATURES	DRY, AMBIENT TEMPERATURE	X	X	X	X	X	X	X	X	X	X	X	X	X	X	X	X	X
2		DRY, -30 C	X	X	X	X	X	X	X	X	X	X	X	X	X	X	X	X	X
3		WET, AMBIENT TEMPERATURE	X	X	X	X	X	X	X	X	X	X	X	X	X	X	X	X	X
4	SIMPLE CONDITIONS	ICE, 1 inch thick (2+5 cm)	X	X	X	X	X	X	X	X	X	X	X	X	X	X	X	X	X
5		" 2 " " (5.1 cm)																	
6		" 1 " " (1.3 cm)																	
7		" 1/2 " " (0.6 cm)																	
8		" GLAZE																	
9	FROST																		
10	SLUSH, 1 inch thick (2.5 cm)																		
11	COMPLEX CONDITIONS	ICE with SAND																	
12		" " DIRT																	
13		" " GRAVEL																	
14		" " SALT																	
15		" " UREA																	
16		SLUSH with SAND																	
17		" " DIRT																	
18		" " GRAVEL																	
19	" " SALT																		
20	" " UREA																		
21	BEAMFILL	MINIMUM PATCH SIZE																	
22		MULTIPLE PATCH DETECTION																	
23		ICE ON WATER*																	
24	ALARM UNIT TEST																		

* This test will require fabrication of a polystyrene housing to cover the simulator.

FIGURE 14. ROADWAY SURFACE SIMULATOR TESTS

3.4.3 Field Test Plan

A total field test plan was not completely definitized within the overall test plan. The intention was to gather the simulator test data and allow equipment operational familiarization prior to embarking on any specific field tests.

The overall objective of the field tests was to verify the performance of the breadboard radiometer system under cold weather operational conditions where the system is used to detect ice and snow on a highway bridge deck. The following specific objectives were designated to demonstrate that the system is ready for prototype evaluation tests:

- o Collect data to demonstrate that the system can detect and identify ice and snow on a roadway.
- o Verify that the system's performance in the field can be related to the performance achieved under laboratory simulated conditions.

In addition, snow signature data was to be gathered to provide a data base for future test activities.

Activities and planning relating to the above objectives occurred after completion of the laboratory simulator tests and are described in more detail in Section 4.2 (Breadboard Field Tests) of this report.

Section 4.0

DESCRIPTION OF PHASE II EFFORT

This section describes the laboratory and field tests conducted and the test results obtained under Phase II. Additionally, recommendations for the prototype system to be delivered under Phase III are provided.

Section 4.1 below addresses the bench tests, calibration technique, input voltage and thermal stability tests, and, finally, the tests performed using concrete and asphalt roadway simulators which were fabricated under this contract. Section 4.2 describes a field test site survey and measurements taken during two field trips on roads under ice, slush, and snow cover conditions. Section 4.3 contains the basis for selection of logic for a hazard alarm and development and test details on a breadboard alarm unit. Radiometer proposed modifications for Phase III are found in Section 4.4.

4.1 BREADBOARD LABORATORY TESTS

4.1.1 Bench Tests

The X-Band Radiometer developed by LMSC on an earlier Independent Development program was updated to the revised configuration shown in Figure 15. These modifications were incorporated to provide a configuration suitable for performing both the simulator tests and the field tests. This configuration would also easily correlate in performance with the anticipated Phase III radiometer prototype.

The bench tests verified the interface parameters of the X-Band receiver with the 94 GHz radiometer processor and added power supply and L.O. driver circuits in the receiver. Adjustments were made and measurements were taken to ensure a compatible interface. Bench test adjustments included the following:

- 1) Receiver Gain
- 2) Processor Video Gain
- 3) AGC Threshold Limits
- 4) AGC Adjustment Range
- 5) Local Oscillator Voltages
- 6) Output Filter Time Constant Adjustment

These adjustments consisted of a combination of potentiometer adjustments and circuit component value changes in the processor circuit boards.

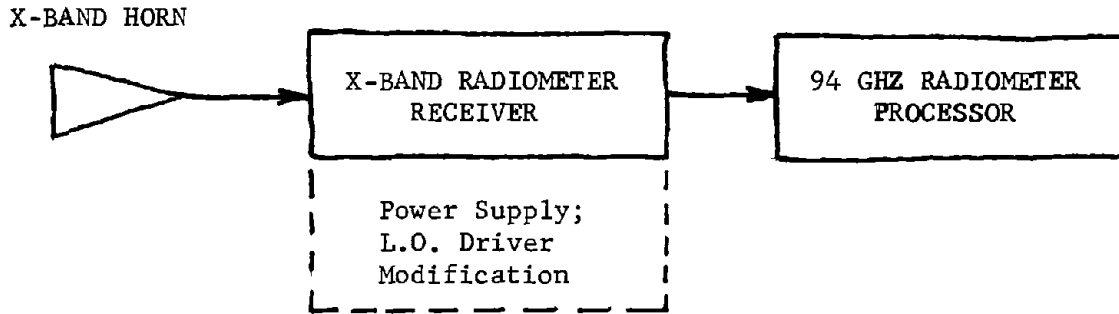


FIGURE 15 . REVISED RADIOMETER CONFIGURATION

4.1.2 Calibration

Calibration is accomplished by measuring sky temperature at zenith and then covering the horn with microwave absorber material and measuring the ambient temperature of this material. Sky temperature at X-Band frequencies is approximately 10°K and the microwave absorber temperature in °K is equal to air temperature in °C plus 273.

The calibration procedure was performed prior to beginning any series of tests and repeated at frequent intervals so that the task of data reduction would be simplified. The frequency of calibration checks during the test program was necessary due to the breadboard radiometer temperature drift problem which is discussed in paragraph 4.1.3.2.

The following calibration procedure was used throughout the test program (refer to Figure 16 for location of adjustment trim pots):

- 1) Direct radiometer horn antenna toward the sky at zenith. Adjust R17A, Offset Adjust, for an output of 10°K (0.200 VDC).
- 2) Measure temperature of microwave absorber material and convert to °K (e.g., absorber temperature = 68°F; 20°C + 273° = 293°K). Adjust R42, Gain Adjust, for the calculated absorber temperature (293°K or 5.860 VDC).
- 3) The gain and offset adjustments interact with each other, so that steps 1 and 2 need to be repeated until no further adjustments are required; three sets of adjustments will generally provide this condition.

After completing this radiometer calibration procedure, the strip-chart recorder was adjusted so that its output is recorded in Volts D.C. which was then read directly in °K. Figure 17 is an example of the stripchart recording of the radiometer calibration to a scale of 1 inch (10 recorder sheet units) per 1 VDC per 50°K.

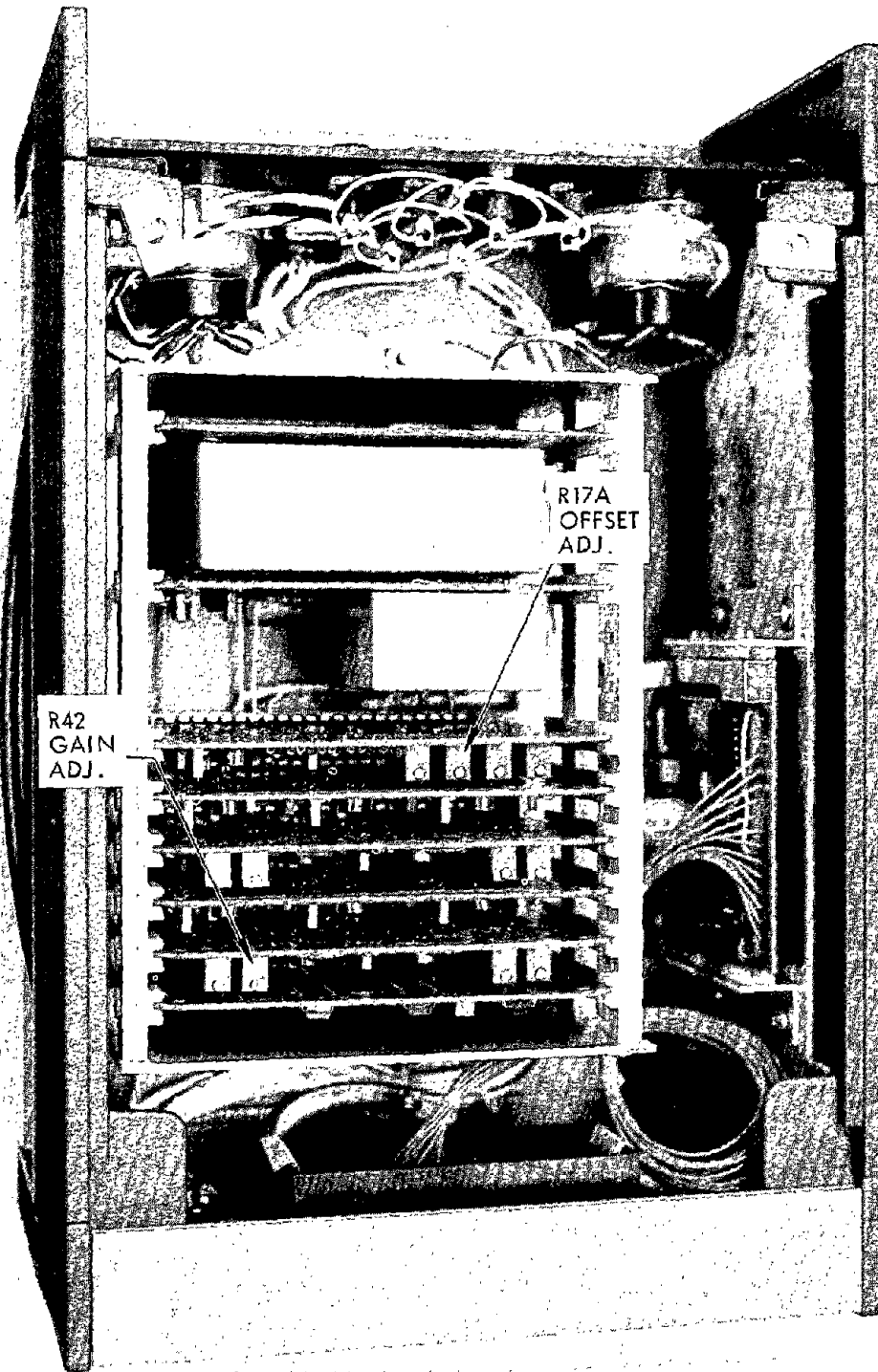
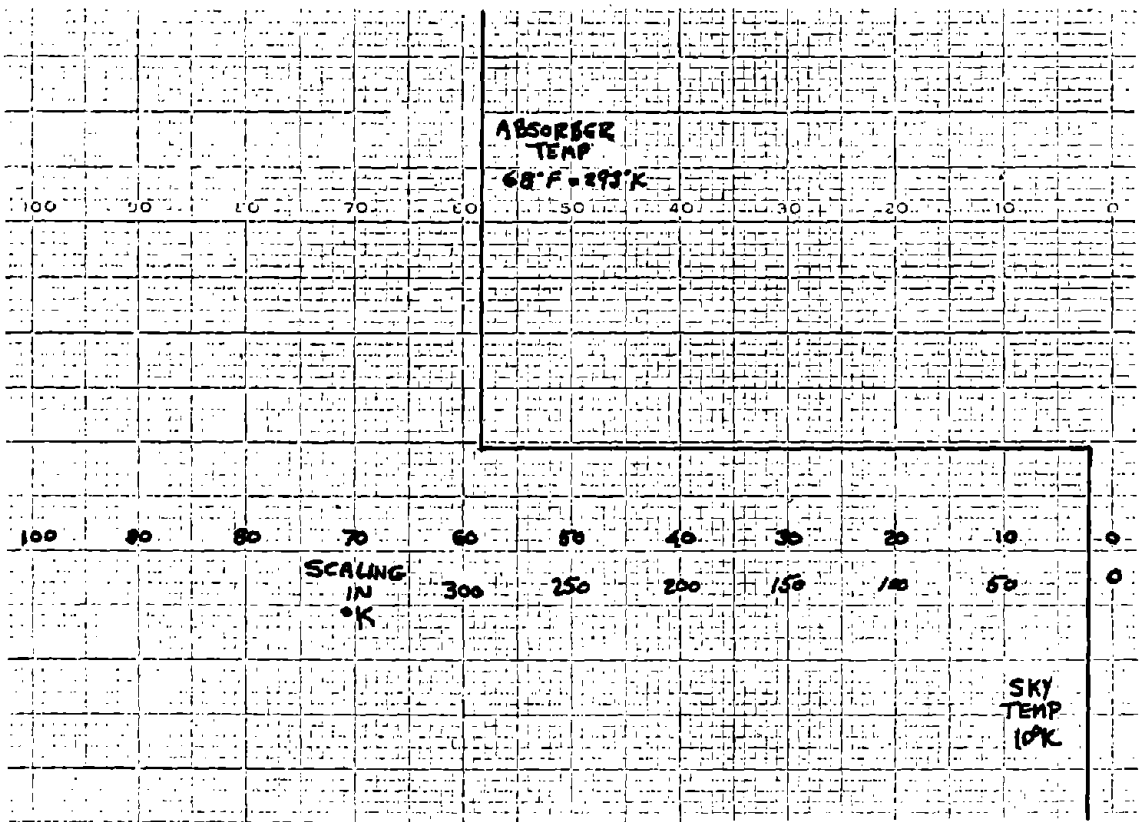


FIGURE 16. BREADBOARD PROCESSOR (TOP VIEW, COVER REMOVED)(PHOTO)



CALIBRATION DATA

ABSORBER TEMPERATURE: $68^{\circ}\text{F} = 293^{\circ}\text{K}$

SKY TEMPERATURE: 10°K

SCALING: $20 \text{ MVDC}/^{\circ}\text{K}$

FIGURE 17. STRIP CHART RECORDING OF RADIOMETER CALIBRATION

4.1.3 Stability Tests

4.1.3.1 Input Voltage Stability

- o Purpose - The radiometer output was tested for output stability over an input voltage range of 100 to 125 VRMS. It is essential that the equipment remain stable over this range to eliminate any errors induced by line voltage fluctuations.
- o Configuration - The radiometer and test equipment was set up as shown in Figure 18. The Variac was used to control line voltage to the radiometer electronics only. Line voltage was varied from 100 to 125 VRMS in 5 VRMS increments. Sky temperature and absorber temperature data were recorded for each increment of input line voltage change.
- o Results - Two tests were performed.
 - a) Test #1 - Results of Test #1 proved the radiometer to be unstable over the input line voltage variation range. Radiometric temperature output of the absorber temperature varied at a rate of $4.2^{\circ}\text{K}/\text{volt}$ over the range of 100 to 115 VRMS. An additional variation of $1.2^{\circ}\text{K}/\text{volt}$ was noted over the 115 to 125 VRMS range. The total instability measured over the entire line variation range was 25%. Figure 19a is a plot of radiometric temperature vs. input line voltage for this test. Further testing proved the cause of the instability was the 28 VDC power supply. This power supply was changed and the test was rerun.
 - b) Test #2 - Results of Test #2 were completely satisfactory. Total instability over the entire input voltage range was under 2°K . This is less than 1% instability over the range of input voltage variation. Figure 19b is a plot of the results of this test. This remaining instability was not isolated further; probable causes are short-term component instabilities (IF amplifiers, noise generator, etc.) and the regulation of other power supplies ($\pm 15\text{ V}$, $+ 5\text{ V}$).
- o Conclusion - Radiometric temperature output drift caused by a change in input line voltage from 100 to 125 VRMS represents an insignificant error in further testing and data analysis with the breadboard radiometer.

4.1.3.2 Temperature Stability

- o Purpose - Temperature stability tests were performed on the radiometer receiver to determine the scale factor drift rate caused by changes in ambient temperatures.
- o Configuration - The breadboard radiometer was configured as shown in Figure 20. The receiver portion was enclosed on all sides with sheets of Polystyrene foam approximately 2" (5.1 cm) thick. Liquid Nitrogen gas was injected into the receiver enclosure to cool the receiver to low ambient temperatures.

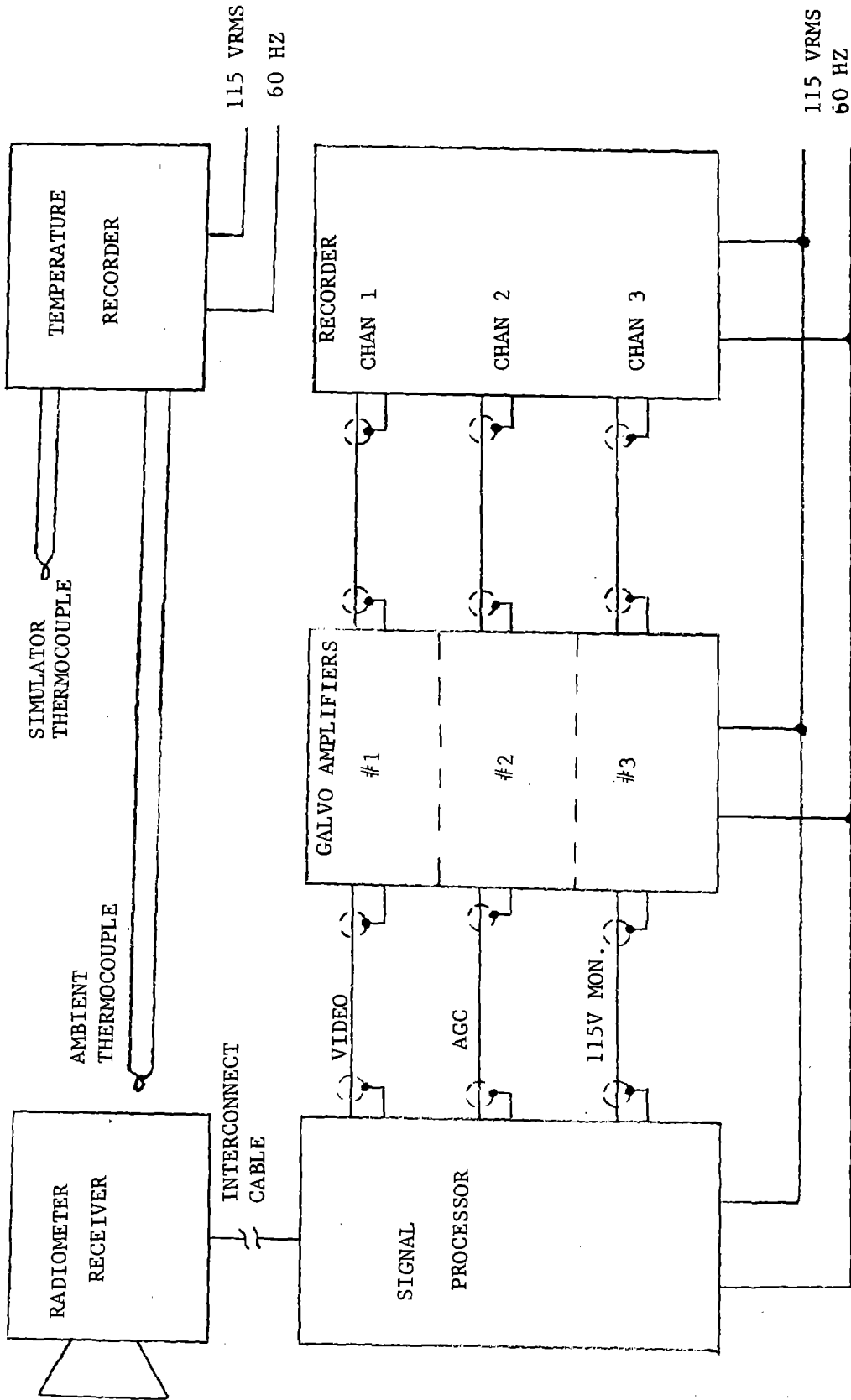


FIGURE 18. DATA RECORDING SYSTEM

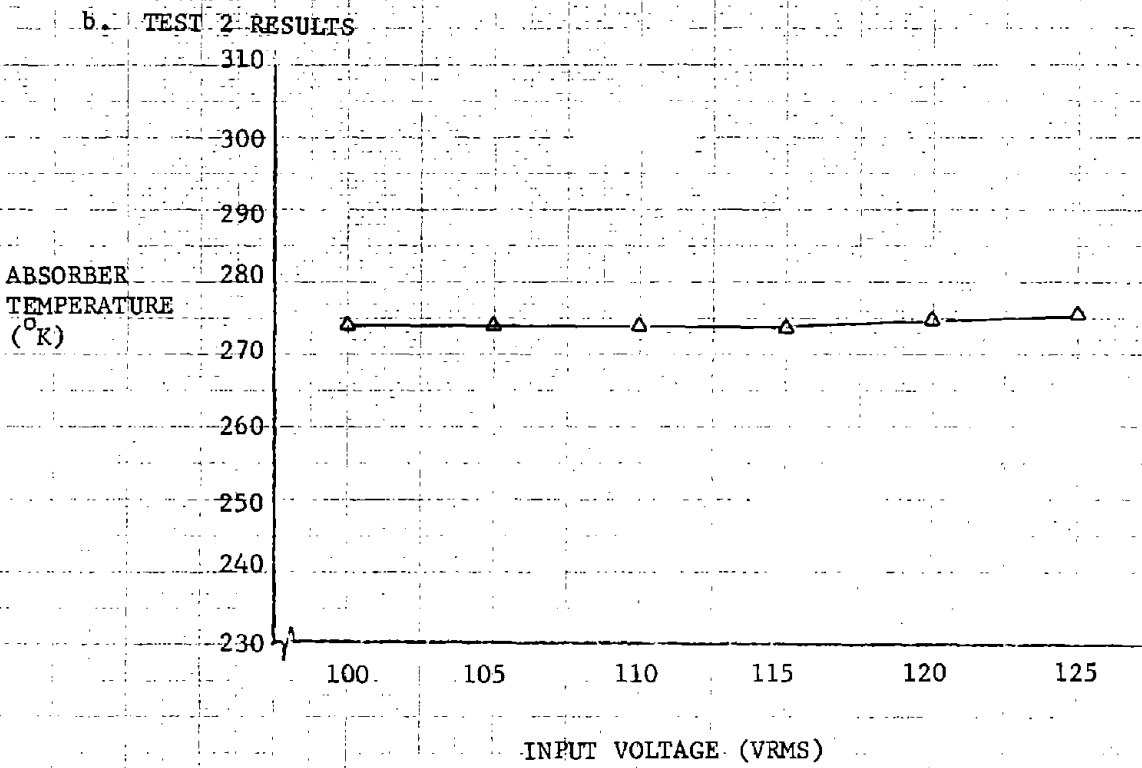
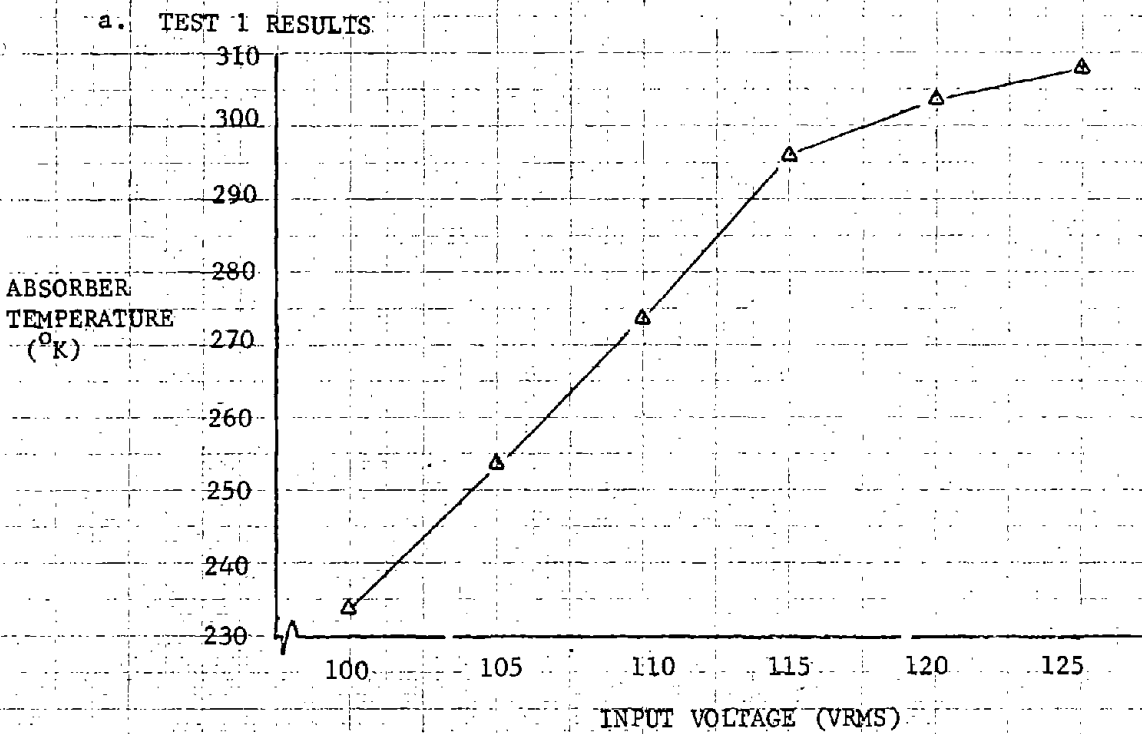


FIGURE 19. INPUT VOLTAGE STABILITY TESTS (TESTS 1 AND 2)

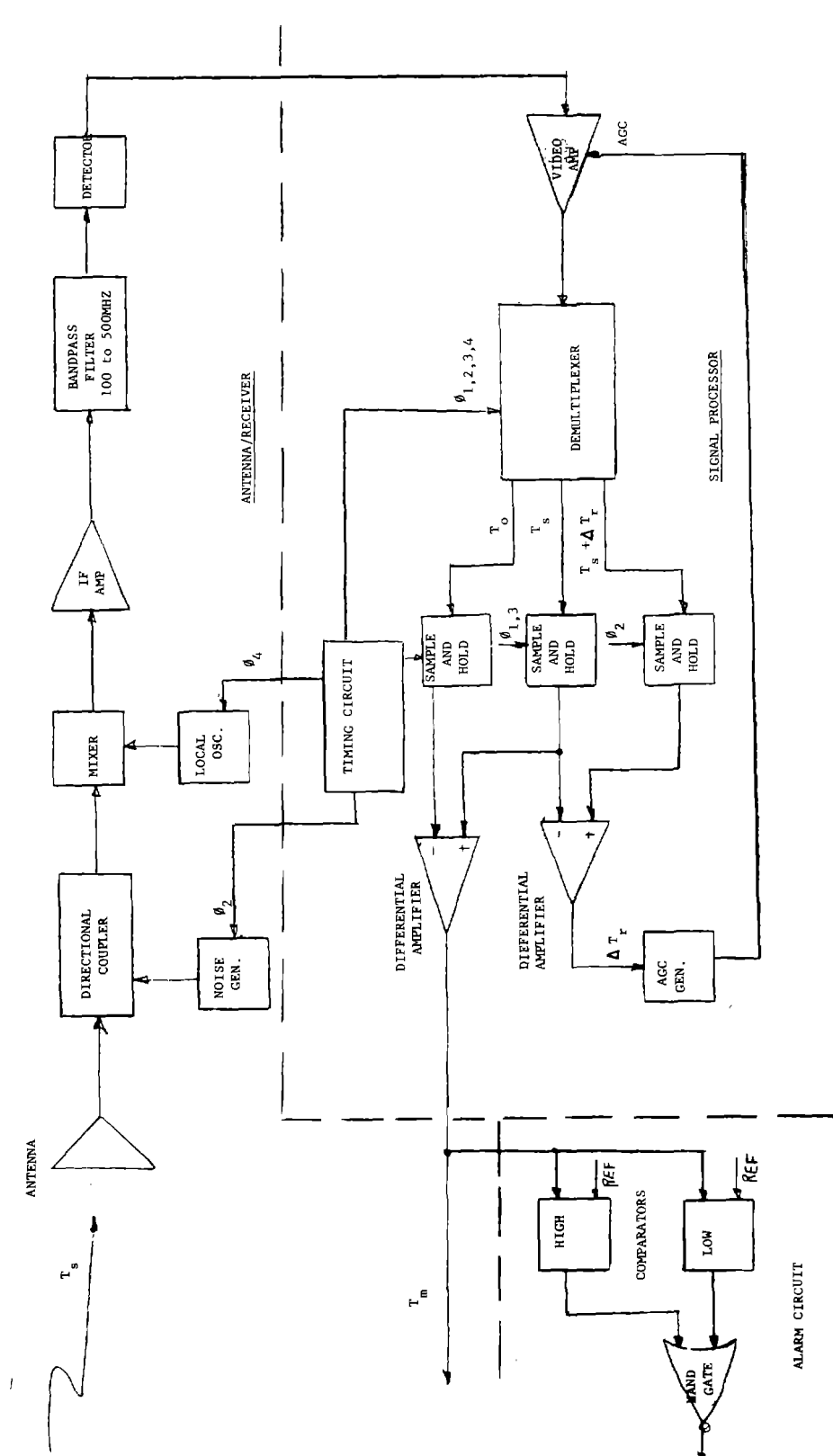


FIGURE 20. LOCKHEED RADIOMETER BLOCK DIAGRAM

Temperatures of three points on the receiver were monitored, along with radiometric temperature data. The three points monitored were: (1) detector; (2) noise generator; and (3) mixer.

- o Results - Temperature stability of the breadboard radiometer was found to be unsatisfactory. Temperature monitoring of several points on the radiometer receiver determined that the mixer is the component that is most sensitive to ambient temperature changes. Several methods of correction were tried, and the test was rerun after each "fix" was incorporated. None of these fixes provided satisfactory results.

Due to schedule impacts on the simulator test program, work on correcting this problem was deferred and the radiometer was used "as is". For the balance of the test program, the radiometer was allowed ample warm-up time prior to testing. The warm-up time allowed the internal receiver temperature to stabilize at about 100°F (due to internal heat dissipation) at which time the scale factor became stable. In addition, scale factor checks were performed at frequent intervals during the tests.

Scale factor drift rate versus receiver temperature change was determined to be approximately 1°K per 1°C. Figure 21 is a plot of the test data used for determining this correction factor. In cases where it was not feasible to allow the necessary warm-up time (i.e., field tests), the correction factor was applied as a correction to the raw data.

- o Conclusions - Radiometer receiver drift must be negligible (e.g., within 2°K) as internal receiver temperatures change. As a minimum requirement, the scale factor should remain constant over a temperature range which can be maintained within the receiver enclosure when an auxiliary heating device is used for stabilization.

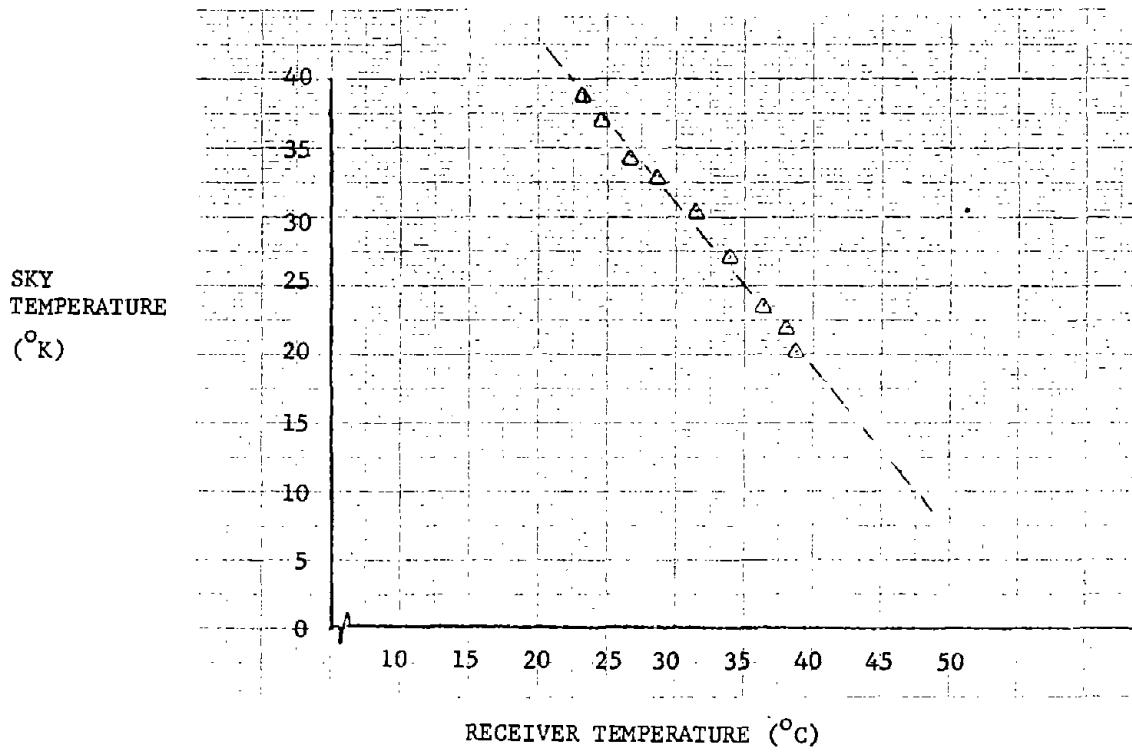
4.1.3.3 Diurnal Sun Position Stability

This test was deleted from the breadboard test program since the sky temperature contribution to overall radiometric temperature is very small at the 10 GHz operating frequency (Section 3.3.2 B1, "Comparison of Background and Sun Temperatures"). Additionally, meaningful results of diurnal tests would only be obtained with a temperature-compensated radiometer system.

4.1.4 Simulator Tests

4.1.4.1 Purpose, Configuration and Test Geometry

- o Purpose - The simulator tests were primarily intended to evaluate the feasibility of using an X-Band radiometer to detect



DATA POINTS FROM APPENDIX A. SLOPE IS $-1.05^{\circ}\text{K}/^{\circ}\text{C}$.
 INTERCEPT IS 63°K .

FIGURE 21. SCALE FACTOR DRIFT VS. RECEIVER TEMPERATURE

hazardous driving conditions on typical road surfaces. To achieve this goal, a series of specific tests were performed to determine exactly what radiometric temperature information was available when hazardous conditions were present.

o Configuration

- a) Stripchart Recorder - Two recorders were used throughout the test sequence. Early data was recorded on a Honeywell Model 1858 multi-channel recorder. Later data was recorded on a Honeywell Electronic 19 single channel recorder. The Electronic 19 recorder had the advantage of using pre-printed grid paper. Both recorders were set up to record 1 volt/inch (0.39 volt/cm) deflection over the total radiometric temperature range of 0 to 300°K. Data from both recorders was satisfactory but the Electronic 19 was preferred because it simplified data reduction with its preprinted paper and produced more permanent, legible records.
- b) Radiometer Receiver - The receiver and horn antenna are shown in Figure 22. A block diagram of this receiver configuration was shown in Figure 20. The receiver components were mounted on a rigid aluminum plate approximately 9 x 9 inches square (22.9 x 22.9 cm). An angle bracket was added to allow both vertically and horizontally polarized mounting positions. The entire receiver was then covered with polystyrene foam about 2 inches (5.1 cm) thick so that internal heat would be retained and temperature stability would be improved. The receiver unit was then mounted on an aluminum "I" beam so that it was approximately 6 feet (1.8 m) above the test surface.
- c) Processor and Data Recording System - Figure 23 shows the stripchart recorder, a Honeywell temperature recorder, oscilloscope, digital voltmeter, and the processor electronics unit. These components were mounted on a push cart so that the entire system would be portable enough to move to the outside test area each day. The combination of using two separate recorders for thermometric temperature and radiometric temperature made the task of data reduction quite difficult because of a lack of synchronization between the two units. This problem was resolved late in the test program when a Fluke model 2240 B data logger was acquired. This unit is discussed in detail in Section 4.2.2.1.
- d) Simulator Test Set-Up - In addition to the microwave radiometer receiver/processor and the data recording system, three roadway surface simulators were used during the tests. Construction details are shown in Figures 13 and 24. Liquid Nitrogen was used to cool down the simulator



FIGURE 22. RADIOMETER RECEIVER AND HORN ANTENNA (PHOTO)

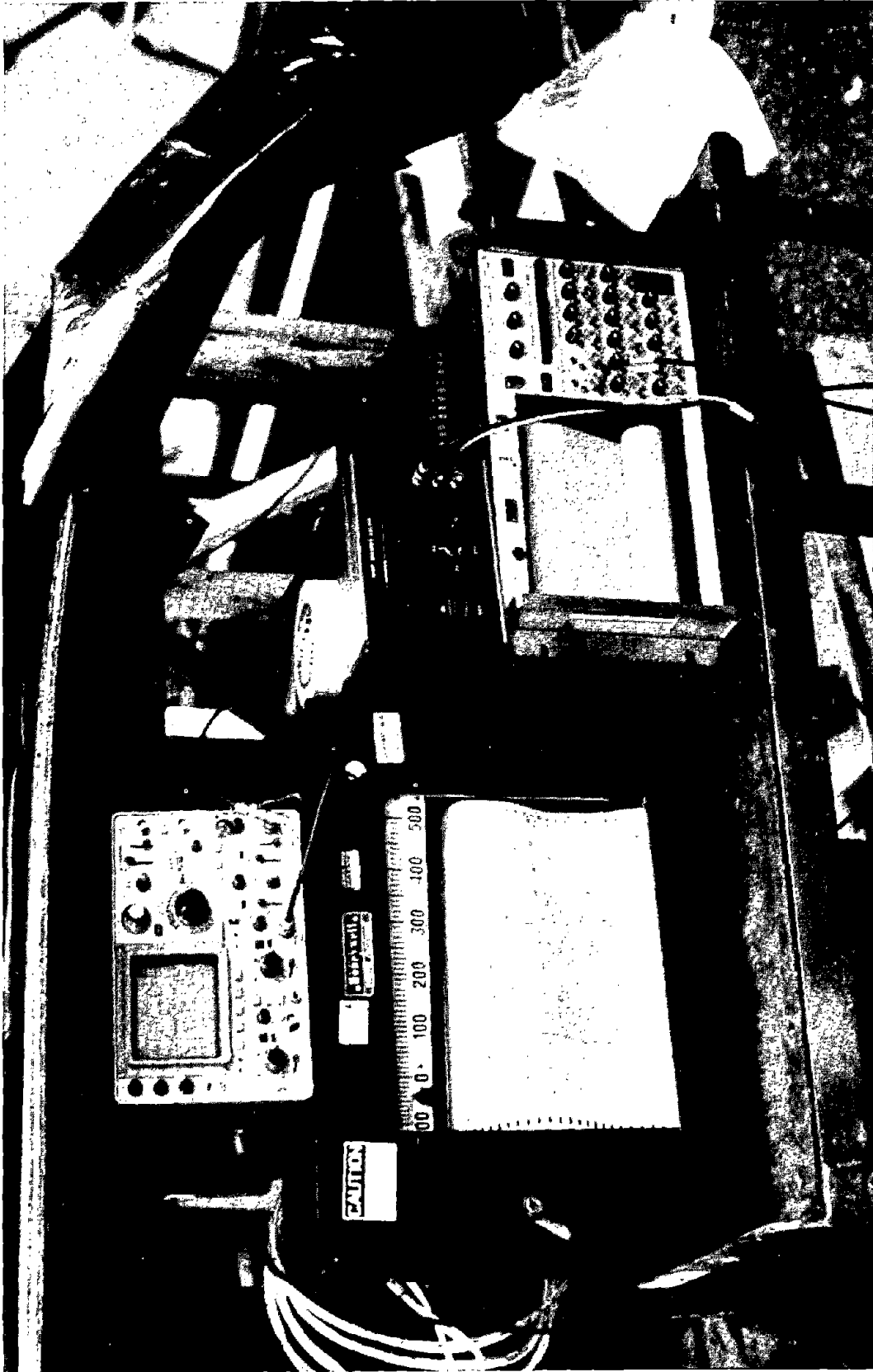


FIGURE 23. PROCESSOR AND DATA RECORDING SYSTEM (PHOTO)

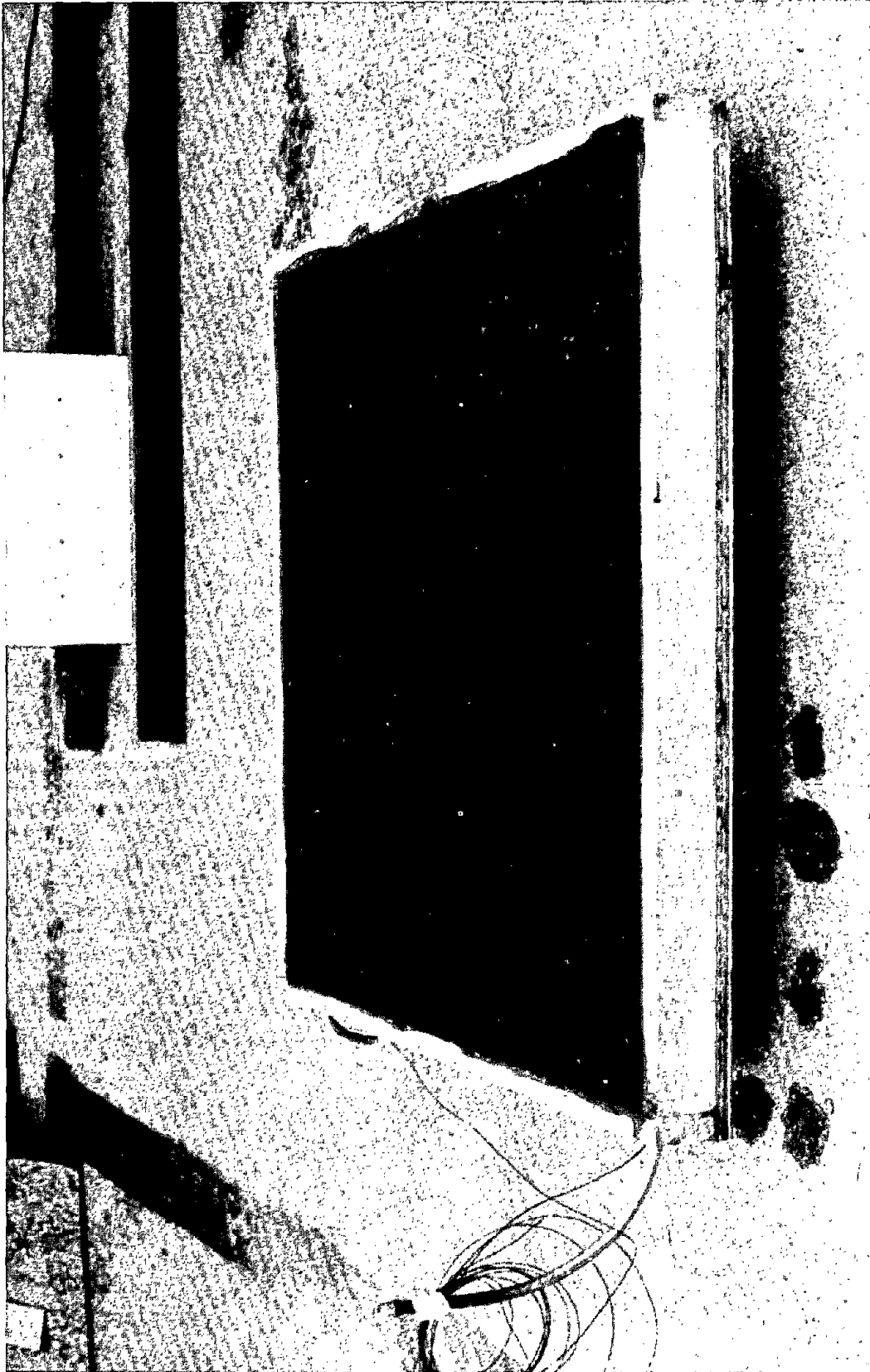


FIGURE 24. COMPLETED ASPHALT ROADWAY SURFACE SIMULATOR (PHOTO)

surfaces to the point at which water would freeze. About 160 liters of LN₂ were required for each test. The simulator test set-up is shown in Figure 25.

- o Test Geometry - The receiver with attached horn antenna was mounted above the simulator with the horn pointed downward at an angle which could be varied from zero to 40 degrees from the vertical. The horn antenna has a half-power beamwidth of 13 degrees and a 70 percent power beamwidth of 16 degrees. To insure that the simulator surface "represents" at least 70 percent of the total power sensed by the radiometer for all of the tests, a maximum test height of 7.5 feet (2.3 m) for radiometer installation was adopted, corresponding to the 4 ft. x 4 ft. (1.22 x 1.22 m) simulator. Then, with the radiometer canted 40 degrees from the vertical at a distance of 7.5 feet (2.3 m) above the simulator, the portion of the radiometer beam pattern intercepted by the simulator surface will never be less than the 70 percent power beamwidth. Figure 26 illustrates this test geometry and provides the applicable mathematical relationships.

4.1 4.2 Test Sequence

The sequence of tests presented in the test plan, as shown in Table 2, was followed through Test 3 (Basic Signatures) for all three roadway surface simulators and through Test 7 for the smooth concrete simulator. The test sequence was then altered so that test data gathered from icy surfaces could be correlated with the theoretical analysis, "Radiometric Temperature for Ice on Concrete" (ref. Section 3.3.2 B4). This test sequence which is discussed further in paragraph 4.1.4.3, Test Results, Icy Surfaces.

4.1.4.3 Test Results

- o Dry Surface, Warm Temperatures (70°F)

This test was intended to meet the following goals: (1) obtain radiometric temperature data on warm surfaces at both horizontal and vertical polarization at various angles off vertical; (2) provide a check on radiometer performance as compared with previously published radiometer test data; and (3) familiarize test personnel with bread-board radiometer and data recording system operation.

Figure 27 is a graphical representation of the test data obtained on dry, warm, surfaces. The data points on the curves compare favorably with previously published radiometer temperature data for concrete and asphalt surfaces. The curves for vertical and horizontal polarization at angles out to 50 degrees off vertical correspond to all available previously published data. The data comparison is made by deriving the surface emissivity figures for the test surfaces

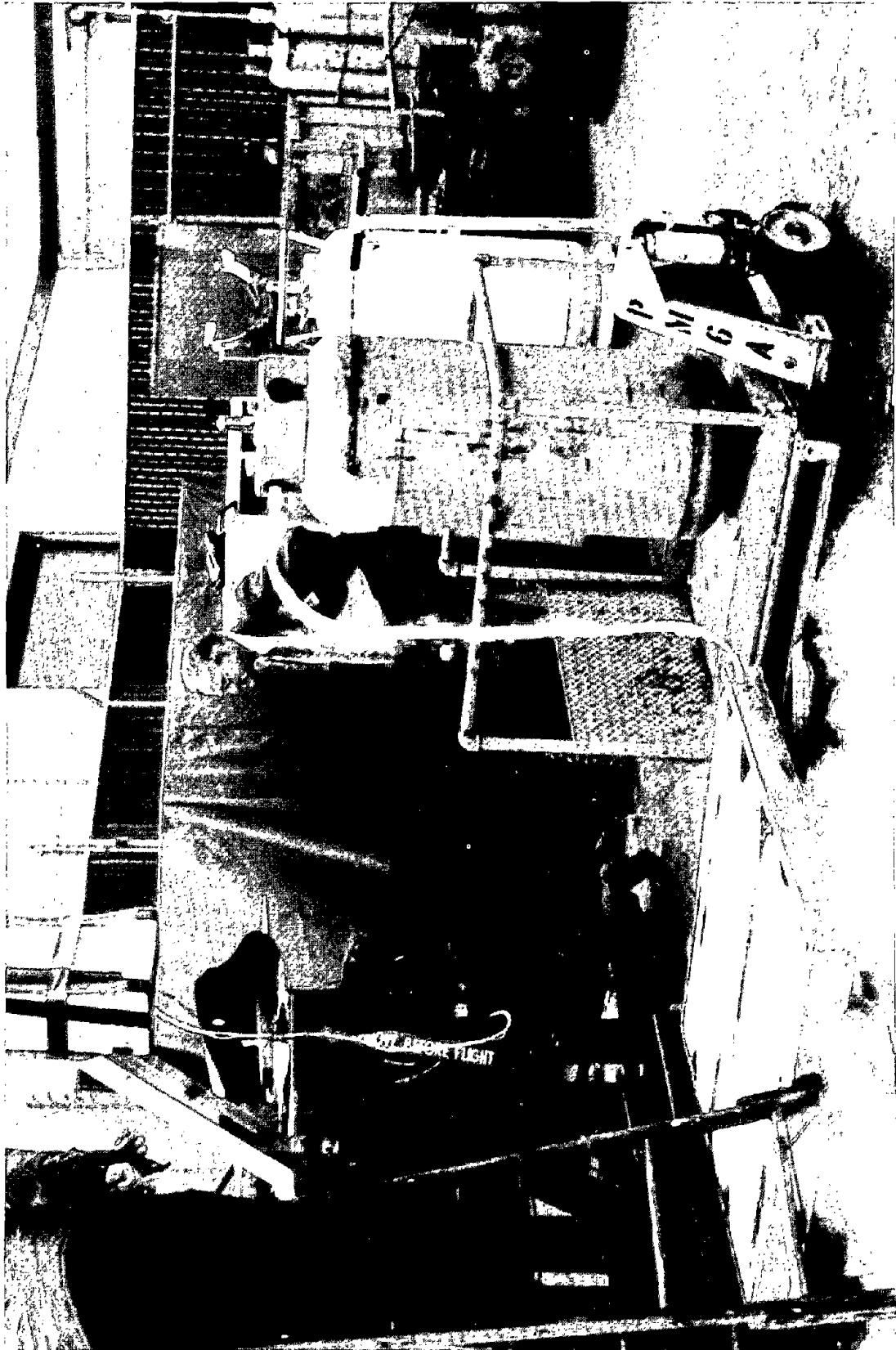


FIGURE 25. SIMULATOR TEST SET-UP (PHOTO)

RADIOMETER

Where: h = height of antenna

ϕ = angle of antenna off vertical

$\gamma = 90^\circ + \phi$

$\alpha = \frac{1}{2}$ beamwidth for 70% sensed area

$\theta = 90^\circ - \phi$

$D = \frac{h}{\tan \theta}$

$$c = \frac{h}{\cos(\alpha + \phi)}$$

$$r = \frac{c \sin \alpha}{\sin \gamma}$$

$$\therefore r = \frac{h}{\cos(\alpha + \phi)} \frac{\sin \alpha}{\sin \gamma}$$

and

$$h = r \cos(\alpha + \phi) \left(\frac{\sin \gamma}{\sin \alpha} \right)$$

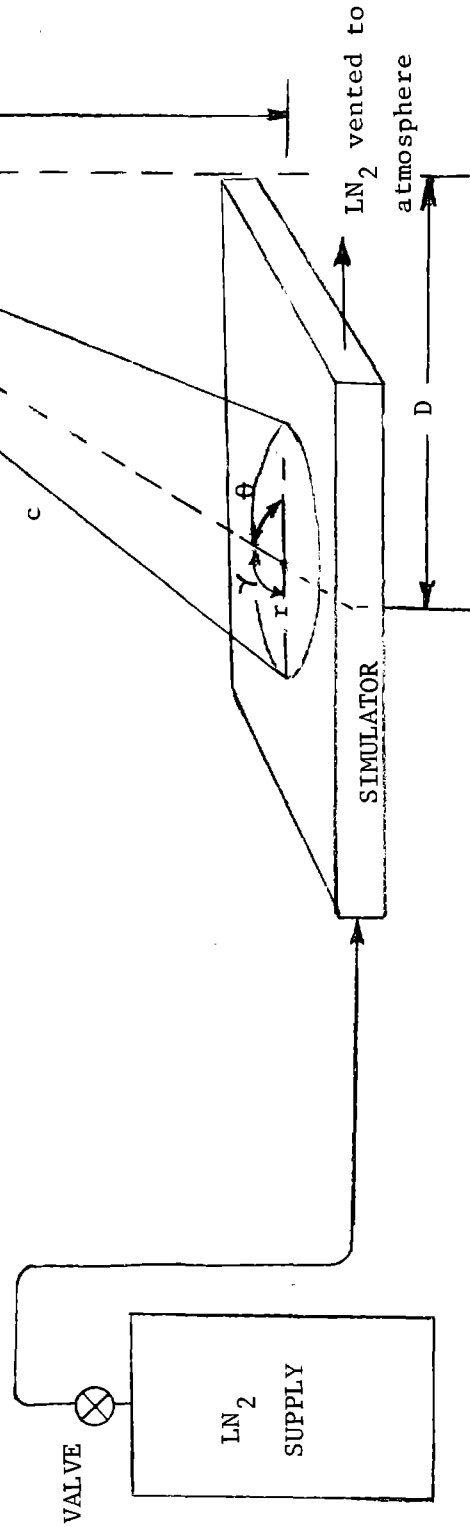


FIGURE 26. SIMULATOR TEST SET-UP AND GEOMETRY

Reproduced from
best available copy.

TABLE 2. TEST PLAN TEST SEQUENCE

TEST NO.	TEST TYPE	SIMULATED CONDITIONS	SMOOTH CONCRETE					ROUGH CONCRETE					ASPHALT					POLARIZATION		
			0°	10°	20°	30°	40°	0°	10°	20°	30°	40°	0°	10°	20°	30°	40°	HORIZ	VERT	
1	BASIC SIGNATURES	DRY, AMBIENT TEMPERATURE	X	X	X	X	X	X	X	X	X	X	X	X	X	X	X	X	X	X
2		DRY, -30 C	X	X	X	X	X	X	X	X	X	X	X	X	X	X	X	X	X	X
3		WET, AMBIENT TEMPERATURE	X	X	X	X	X	X	X	X	X	X	X	X	X	X	X	X	X	X
4	SIMPLE CONDITIONS	ICE, 1 inch thick (25.4 mm)	X	X	X	X	X	X	X	X	X	X	X	X	X	X	X	X	X	X
5		" 2 " " (50.8 mm)	X	X	X	X	X	X	X	X	X	X	X	X	X	X	X	X	X	X
6		" 1 " " (12.7 mm)	X	X	X	X	X	X	X	X	X	X	X	X	X	X	X	X	X	X
7		" 1 " " (6.4 mm)	X	X	X	X	X	X	X	X	X	X	X	X	X	X	X	X	X	X
8	" GLAZE	X	X	X	X	X	X	X	X	X	X	X	X	X	X	X	X	X	X	
9	EROST	X	X	X	X	X	X	X	X	X	X	X	X	X	X	X	X	X	X	
10	SLUSH, 1 inch thick (25.4 mm)	X	X	X	X	X	X	X	X	X	X	X	X	X	X	X	X	X	X	
11	COMPLEX CONDITIONS	ICE with SAND	X	X	X	X	X	X	X	X	X	X	X	X	X	X	X	X	X	X
12		" " DIRT	X	X	X	X	X	X	X	X	X	X	X	X	X	X	X	X	X	X
13		" " GRAVEL	X	X	X	X	X	X	X	X	X	X	X	X	X	X	X	X	X	X
14		" " SALT	X	X	X	X	X	X	X	X	X	X	X	X	X	X	X	X	X	X
15		" " UREA	X	X	X	X	X	X	X	X	X	X	X	X	X	X	X	X	X	X
16		SLUSH with SAND	X	X	X	X	X	X	X	X	X	X	X	X	X	X	X	X	X	X
17	" " DIRT	X	X	X	X	X	X	X	X	X	X	X	X	X	X	X	X	X	X	
18	" " GRAVEL	X	X	X	X	X	X	X	X	X	X	X	X	X	X	X	X	X	X	
19	" " SALT	X	X	X	X	X	X	X	X	X	X	X	X	X	X	X	X	X	X	
20	" " UREA	X	X	X	X	X	X	X	X	X	X	X	X	X	X	X	X	X	X	
21	BEANFILL	MINIMUM PATCH SIZE	X	X	X	X	X	X	X	X	X	X	X	X	X	X	X	X	X	
22		MULTIPLE PATCH DETECTION	X	X	X	X	X	X	X	X	X	X	X	X	X	X	X	X	X	X
23	OPTIONAL	ICE ON WATER*	X	X	X	X	X	X	X	X	X	X	X	X	X	X	X	X	X	X
24		ALARM UNIT TEST	X	X	X	X	X	X	X	X	X	X	X	X	X	X	X	X	X	X

* This test will require fabrication of a polystyrene housing to cover the simulator.

CROSS-HATCHED AREA INDICATES TESTS PERFORMED PRIOR TO TEST SEQUENCE MODIFICATION

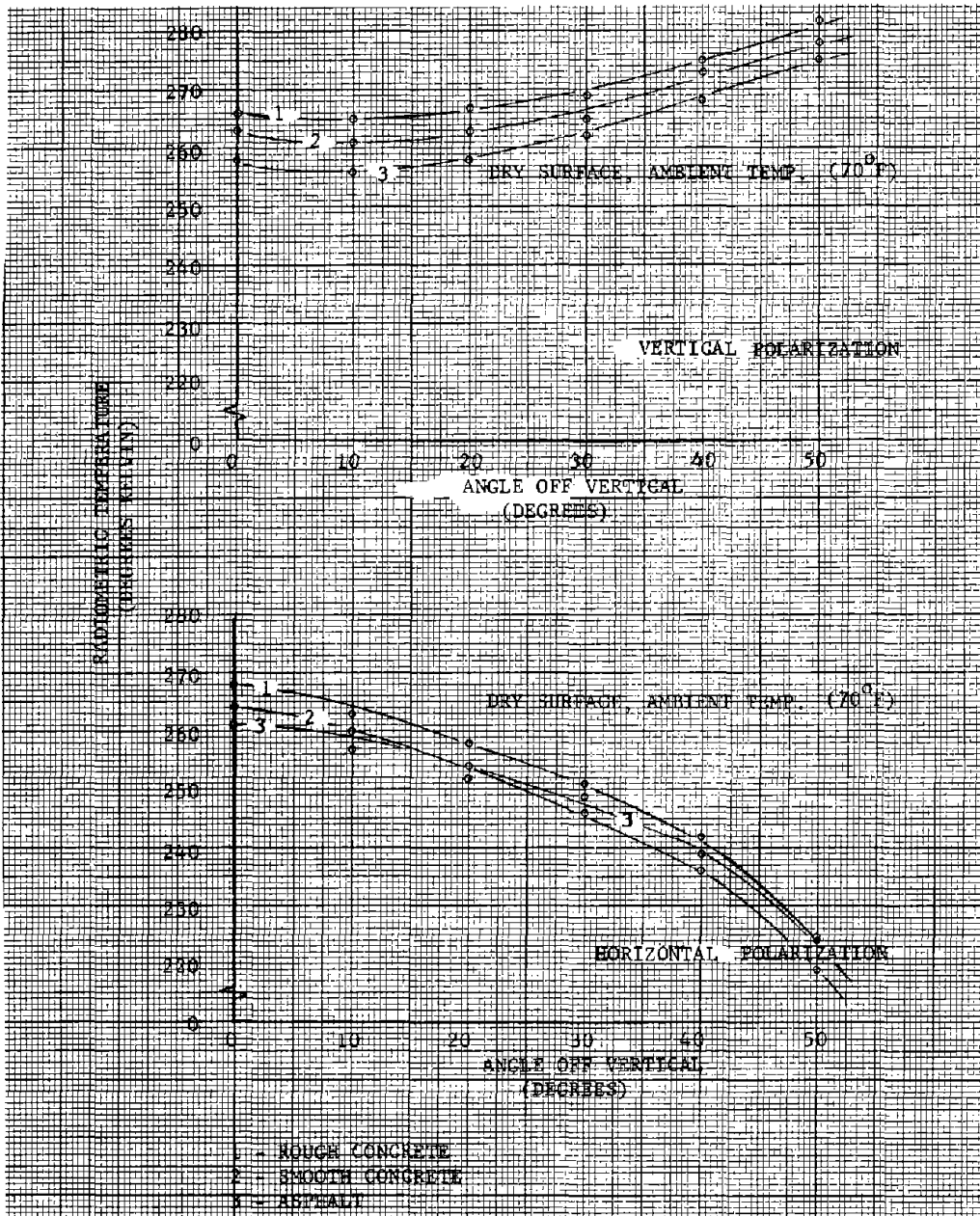


FIGURE 27. TEST 1 - DRY, WARM SURFACE

and comparing these values with other published emissivity figures.

An approximation of surface emissivity for a known radiometric temperature is obtained from the simple formula:

$$\epsilon \approx \frac{T_R}{T_g}$$

where:

ϵ = surface emissivity

T_R = measured radiometric temperature in $^{\circ}\text{K}$

T_g = measured thermometric temperature in $^{\circ}\text{K}$

This approximation is derived from the smooth surface formula:

$$T_R = T_s(1 - \epsilon) + T_g \epsilon$$

where:

T_s = radiometric sky temperature in $^{\circ}\text{K}$

Since T_s is normally 10°K (at X-band frequencies) and emissivity values for concrete and asphalt are in the range of 0.85 to 0.90, the term $T_s(1 - \epsilon)$ is ignored because its overall contribution to T_R is negligible.

Approximate emissivities of the simulator test surfaces are shown in Table 3.

TABLE 3 . EMISSIVITIES OF SIMULATOR TEST SURFACES

<u>Simulator</u>	<u>T_R 0°, Vert. Pol.</u>	<u>T_g 70°F</u>	<u>ϵ</u>
Rough Concrete	266 $^{\circ}\text{K}$	294 $^{\circ}\text{K}$	0.90
Smooth Concrete	263 $^{\circ}\text{K}$	294 $^{\circ}\text{K}$	0.89
Asphalt	258 $^{\circ}\text{K}$	294 $^{\circ}\text{K}$	0.88

The rough approximation method of determining surface emissivity is important to the set-up and operation of the alarm circuits; this point will be discussed in a later section.

The data shown in Figure 27 further indicates that T_R remains relatively constant through the range of 0 to 20 degrees off vertical for vertical polarization measurements, while measurements taken with horizontal polarization show a greater change over this same range of angles. This information implies that any future system employing scanning techniques would have a usable scan angle of ± 20 degrees

off vertical, for a total scan range of 40 degrees, without degradation to system performance, and without using any type of self-correcting circuitry. This usable scan angle could probably be increased significantly by employing simple microprocessor-based correction techniques.

It is then concluded from Test 1, that:

- a) Breadboard radiometer system performance is comparable to other radiometric systems which have been built and tested, and for which some published test data is available.
 - b) Vertical polarization of the horn antenna will probably be more useful than horizontal polarization in detecting hazardous conditions.
 - c) Differences in angle off vertical up to $\pm 20^\circ$ do not significantly alter the T_R of any homogeneous test surface.
 - d) A scan range of $\pm 20^\circ$ off vertical (40° total) may be employed in any future system without any additional correction factors.
- o Dry Surface, Cold Temperature

The purpose of these tests was to determine the effects of simulator surface thermometric temperature change on measured radiometric temperature. Some problems were encountered in analyzing the measured data from seven test runs on the different surfaces until a determination was made that the ϵ values for the various test surfaces were different for each test due to a change in moisture content of the surface material.

The tests were accomplished by pointing the antenna at the test surface (0° off vertical) and continuously recording both thermometric and radiometric temperature data while cooling the test surface down to some temperature lower than the freezing point of water. This condition was achieved by applying Liquid Nitrogen to the cooling coils of the simulator. Thermometric temperature information was recorded using a type J thermocouple imbedded beneath the surface of the simulator.

Results of the seven cold temperature tests are shown in Table 4. Starting radiometric and thermometric temperatures are shown in the column marked T_R and T_g , respectively. Calculated ϵ values (from $\epsilon = \frac{T_R}{T_g}$) are listed in the middle column.

Expected and measured radiometric temperatures for the freezing point of water (273°K) are then listed in their respective columns. (The expected radiometric temperature is: $273^\circ\text{K} \times \epsilon$). Percent error of measured T_R from expected is listed in the last column. The percent error in 5 of the 7 tests is less than 1%. The maximum error is 2.4%.

TABLE 4. DRY, COLD TEMPERATURE TESTS

Test #	Surface Type	Starting Temperatures		(1)		(2)		% Error
		T _R (°K)	T _g (°K)	Calculated ϵ Value	273°K Point Expected	273°K Point Measured		
1	Asphalt	258	299.7	0.86	235	237	+0.8%	
2	Smooth Concrete	264	291.3	0.91	247	241	-2.4%	
3	Asphalt	264	288.6	0.91	250	254	+1.6%	
4	Smooth Concrete	243	285.8	0.85	232	231	-0.4%	
5	Asphalt	271	297.4	0.91	249	251	+0.8%	
6	Rough Concrete	261	293	0.89	243	244	+0.4%	
7	Rough Concrete	242	293	0.83	225	224	-0.4%	

NOTES:

(1) CALCULATED ϵ VALUE APPROXIMATED BY :

$$\epsilon = \frac{T_R}{T_g}$$

(2) EXPECTED 273°K POINT = 273°K X CALCULATED ϵ .

Figure 28a is a plot of the continuous temperature change on the asphalt surface. As the temperature goes below the freezing point of water, the slope of the curve changes and tends to flatten out. This effect is probably due to freezing of moisture in the simulator, causing a change in the effective emissivity value of the asphalt. Figure 28b shows two tests where angle off vertical was varied for two different surface temperatures. Figure 28b substantiates the fact that thermometric temperature of the surface changes the radiometric temperature (T_R) through the range of angles out to 50° off vertical. However, T_R changes over a $\pm 20^\circ$ angular region are nominal, as discussed in the previous section on dry, warm surfaces.

o Wet Surface

The primary purpose for performing this test was to determine the effects of a wet surface on radiometric temperature. The amount of water present on a surface in sufficient quantity to constitute a hazardous condition would vary for different degrees of surface smoothness; the criteria for making this determination for our simulator surfaces was not available. For purposes of the wet surface tests, the surface was considered wet when water in sufficient quantity to either flow across or stand upon the surface was present (less than 0.1 inch or 2.54 mm). This would probably constitute a hazard condition in the majority of roadway surface smoothness conditions and would produce an icing condition if surface temperature was cold enough.

Radiometric temperature data for wet surfaces is presented in Figure 29. In all cases out to ± 30 degrees off vertical, the radiometric temperature for a wet surface was below 150°K . This information was further substantiated during later tests when ice layers were built up by pouring water on previously formed ice layers.

o Frosty Surfaces

Tests on frosty surfaces were not performed on an individual basis. Frosty surface data was obtained during the tests of ice on the road surface simulators.

During a simulator temperature stabilization, frost was found to form on the cold surface. The moisture needed to form the frost layer was apparently condensed from the atmosphere which was in immediate contact with the cold surface. Dependent upon the time period involved (from 10 to 90 minutes), frost layers of various thicknesses were formed. After the frost had formed, the simulator surface was immediately cleared of the frost. The resultant radiometric temperature change in all cases appears to be of insufficient magnitude to detect with any degree of success (positive temperature differentials to 1°K maximum were recorded). Figure 30 shows a layer of frost on the asphalt simulator surface.

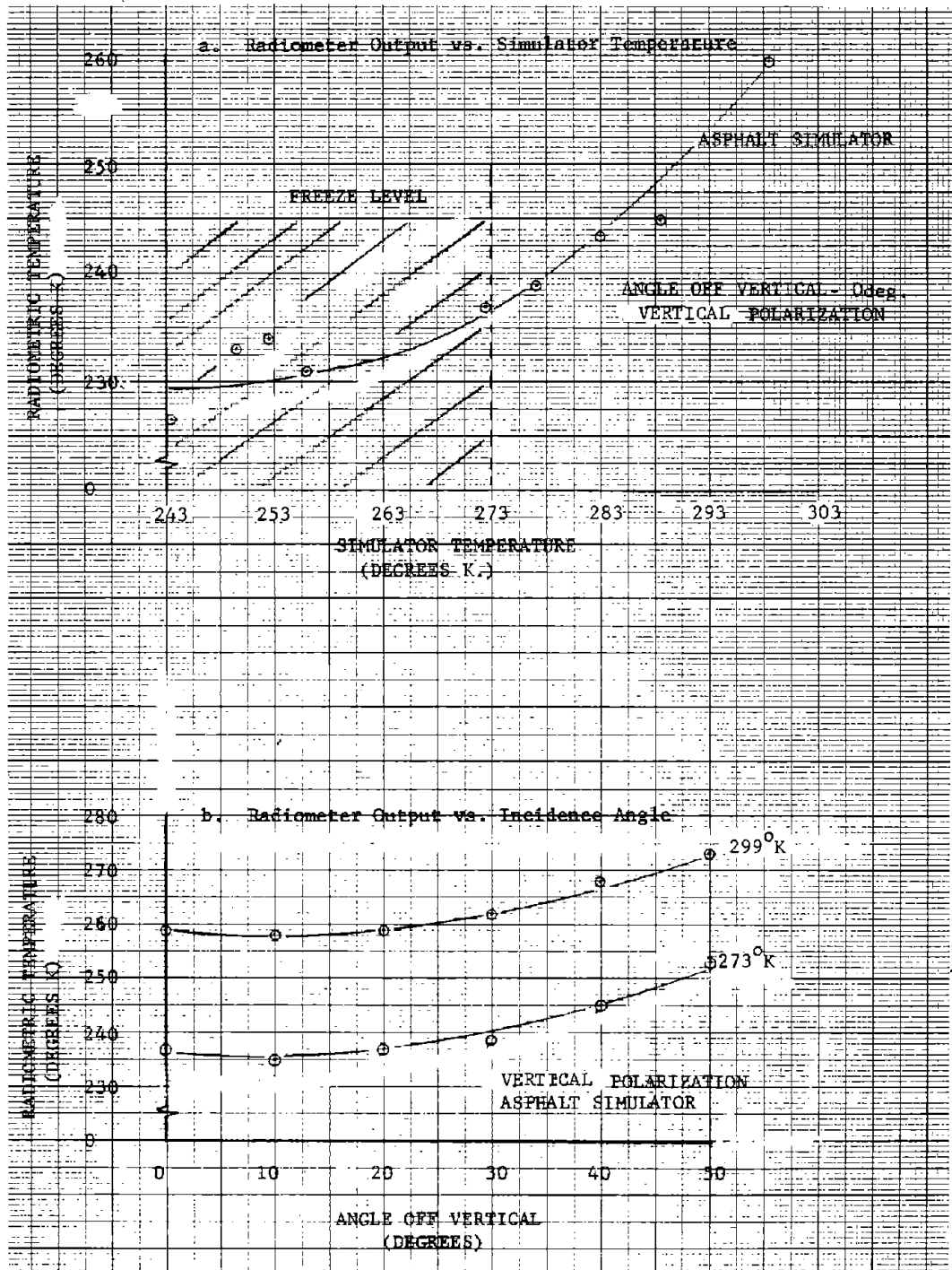


FIGURE 28. TEST 2 - DRY, COLD SURFACE
66

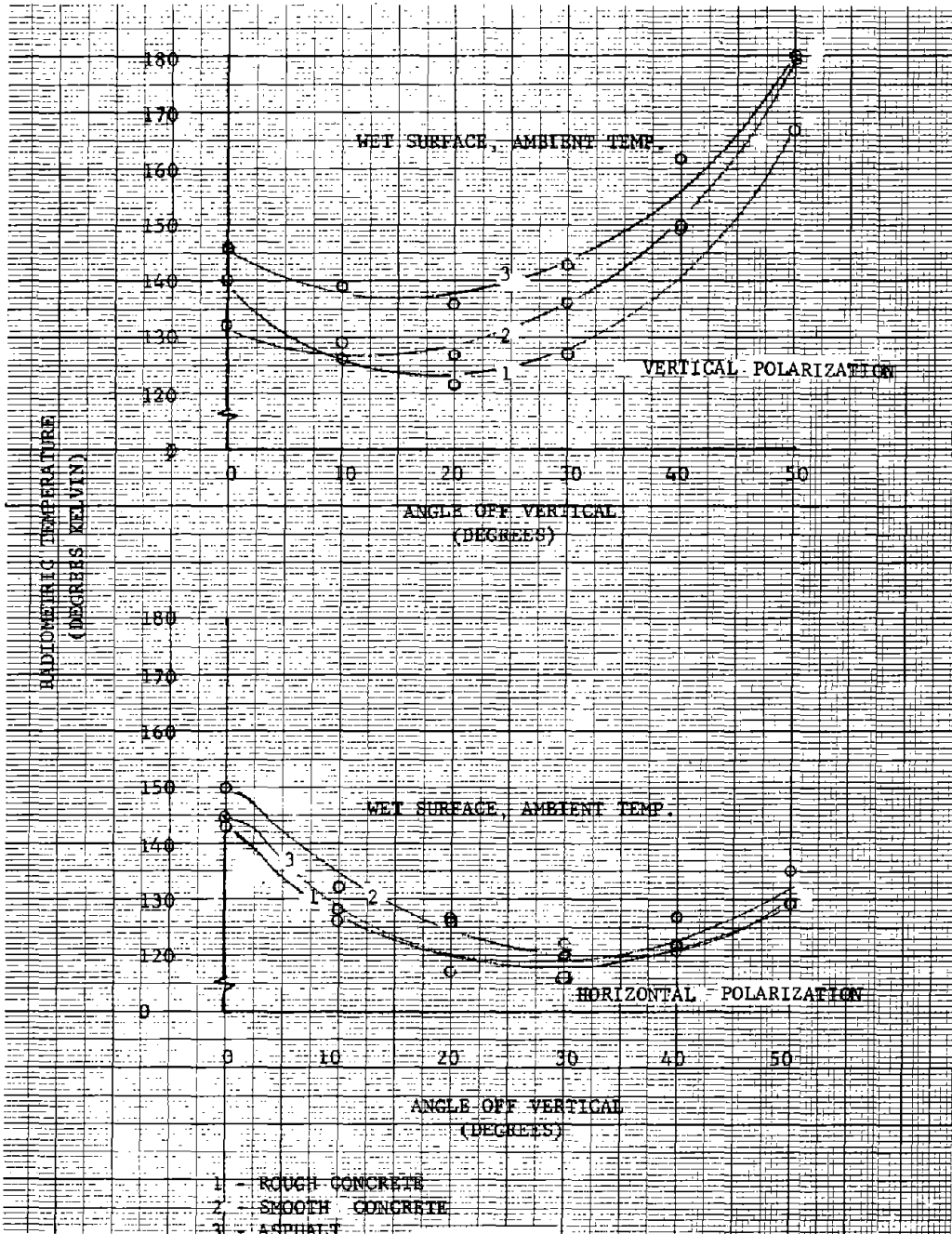


FIGURE 29. WET SURFACES



FIGURE 30. FROST ON ASPHALT SIMULATOR (PHOTO)

Figure 31 is the stripchart record from an icy surface test on smooth concrete. Results from three instances of frosty surfaces are tabulated in Table 5. A time scale of 10 minutes/inch (3.94 minutes/cm) is shown and each frosty surface event is annotated on the record. The "Time" column in Table 5 refers to approximate time of occurrence. Simulator temperatures are annotated on the stripchart in the column between 100°K and 150°K. Temperatures are given as two numbers which represent the temperature at 2 inch (5.1 cm) depth and the surface temperature (i.e., -20/17 = 2" or 5.1 cm depth/surface, in degrees F). Since very small radiometric temperature changes were anticipated, frequent calibration checks of sky temperature were performed. In addition, internal receiver temperature was monitored and recorded (105°F).

TABLE 5 . FROSTY SURFACE T_R VALUES

<u>Time</u>	<u>Frost</u>	<u>No Frost</u>	<u>Difference (°K)</u>
1250	233	232	1
1320	229	228+	< 1
1350	225	224	1

o Icy Surfaces

The primary purpose of these tests was to evaluate the feasibility of using a radiometer to detect ice on a roadway surface. It was also necessary to evaluate the effects of ice layers of various thicknesses on the radiometric temperature so that a detection and alarm circuit could be designed and fabricated.

Test Plan Tests 4 thru 7 (previously described in Table 2) were originally intended to serve this purpose with a high probability of success. However, these tests dealt with relatively thick ice layers and provided data which seemed inconclusive in the first analysis. The test plan was then modified to incorporate tests on thinner ice layers for ease of comparison to a theoretical analysis of ice on concrete.⁽¹⁾ The thinner ice layers also represent more realistic hazardous conditions which would be encountered on roadway surfaces.

The thin ice layers were formed by cooling the test simulator to a sub-freezing temperature. The simulator surface and its corresponding radiometric temperature was then allowed to stabilize prior to any addition of water. Water was then added in a spray which was fine enough to freeze upon contact with the simulator surface. This method produced an ice layer as thin as 10 mm and a positive radiometric temperature differential of 15°K on the smooth concrete surface (15°K

(1) Entitled Appendix B4, "Radiometric Temperature for Ice on Concrete" and submitted under separate cover.

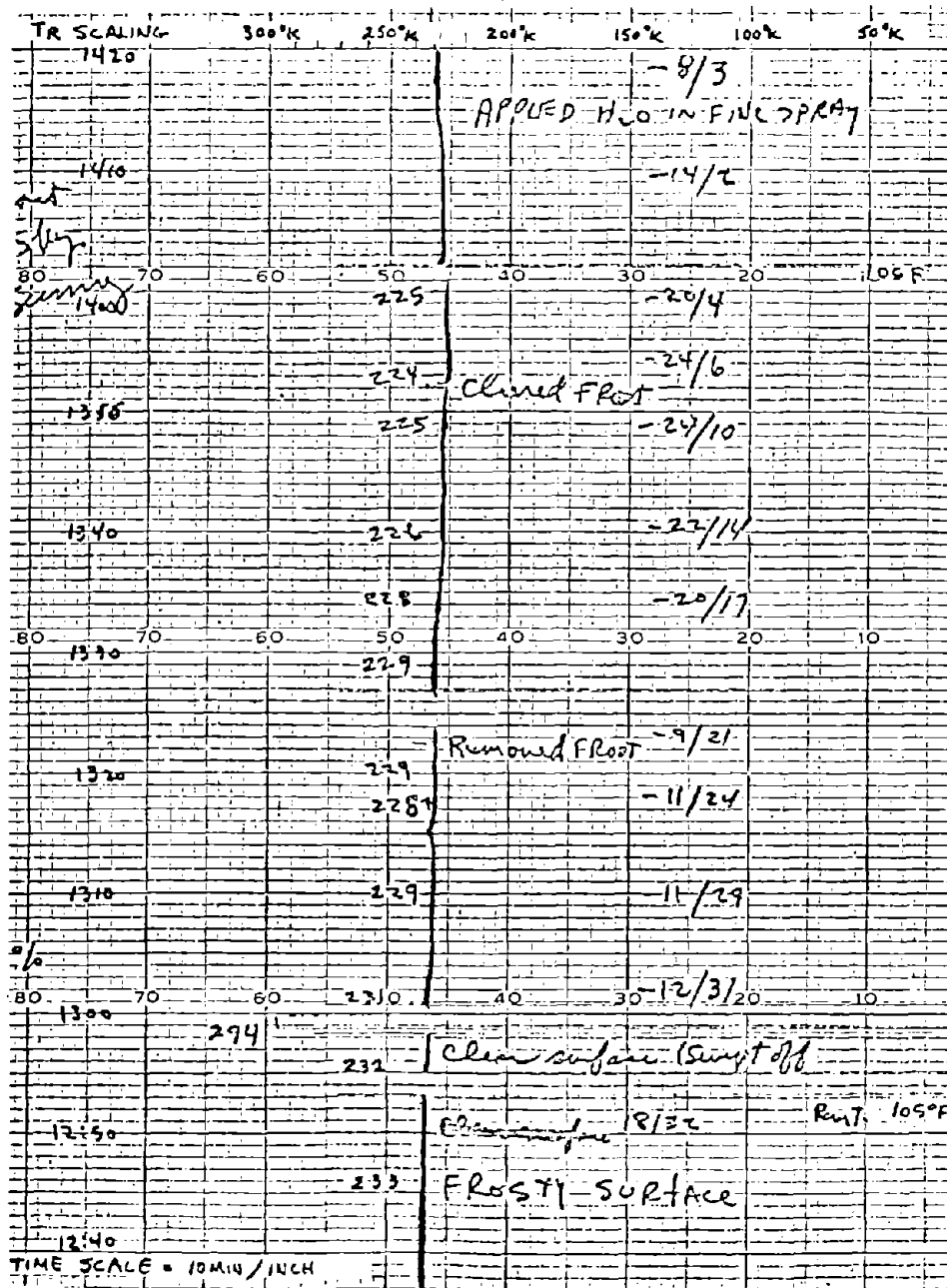


FIGURE 31. FROSTY SURFACE - STRIPCHART DATA

warmer than the no ice condition). Further additions of small amounts of water produced thicker ice layers until 1 cm thickness was approached and the test was stopped.

Ice layer thickness measurements were made at various times throughout the tests by taking eight measurements at different places (within the radiometer field of view) and finding the average thickness. A vernier caliper was used to make these measurements.

Simulator surface thermometric temperature was monitored continuously throughout the tests. The surface temperature was maintained to within 5°K of the "no ice" starting temperature throughout the tests.

Figure 32 shows the data from the first thin ice layer test plotted against the theoretical curve from Appendix B4. The test data has been normalized to the starting point of 235 °K so that the fit of test data to the theoretical curve is more apparent. From this test (and all other later tests) the oscillatory function of T_R as ice layer thickness increases is obvious. The most important feature of the test data plot is the fact that it immediately starts getting warmer upon formation of first ice. This fact will be utilized in the detection and alarm circuits.

Figure 33 is a plot of radiometric temperature vs time taken during the ice layer test of Figure 32. The ability of the radiometer to detect the change of state of water, from liquid to solid within very short time periods, is readily apparent. The lowest temperatures shown occur when the water was added. The amount of water added has a direct effect on the lowest T_R shown, and on the period of time required for the water to freeze. In all cases of ice layer buildup over the 3-hour time period, the radiometric temperature returned to a higher temperature than the dry surface starting temperature. Simulator surface temperature during the time interval was held relatively constant at approximately $255^{\circ} \pm 3^{\circ}\text{K}$. These variations in surface temperature are not high enough to cause the changes which occur in T_R . It also can be seen that thermometric temperature of the ice layer has an insignificant effect on T_R after the ice is formed because the T_R does not decrease as the ice layer gets colder, eventually stabilizing at the simulator surface temperature.

The ice layer tests were performed on all three simulator surfaces. Figure 34 is a plot of the raw data obtained on four tests of thin ice, and on Test Plan tests 4, 6 and 7 on thicker ice layers. This plot indicates a radiometric temperature increase at the occurrence of first ice in all cases and also shows the trend toward the theoretical oscillation as ice thickness increases. In this plot, no attempt was made to normalize the data to any specific value of surface temperature. Minimum, maximum, and mean thermometric surface temperatures during individual test runs are shown in Table 6 along with rough approxi-

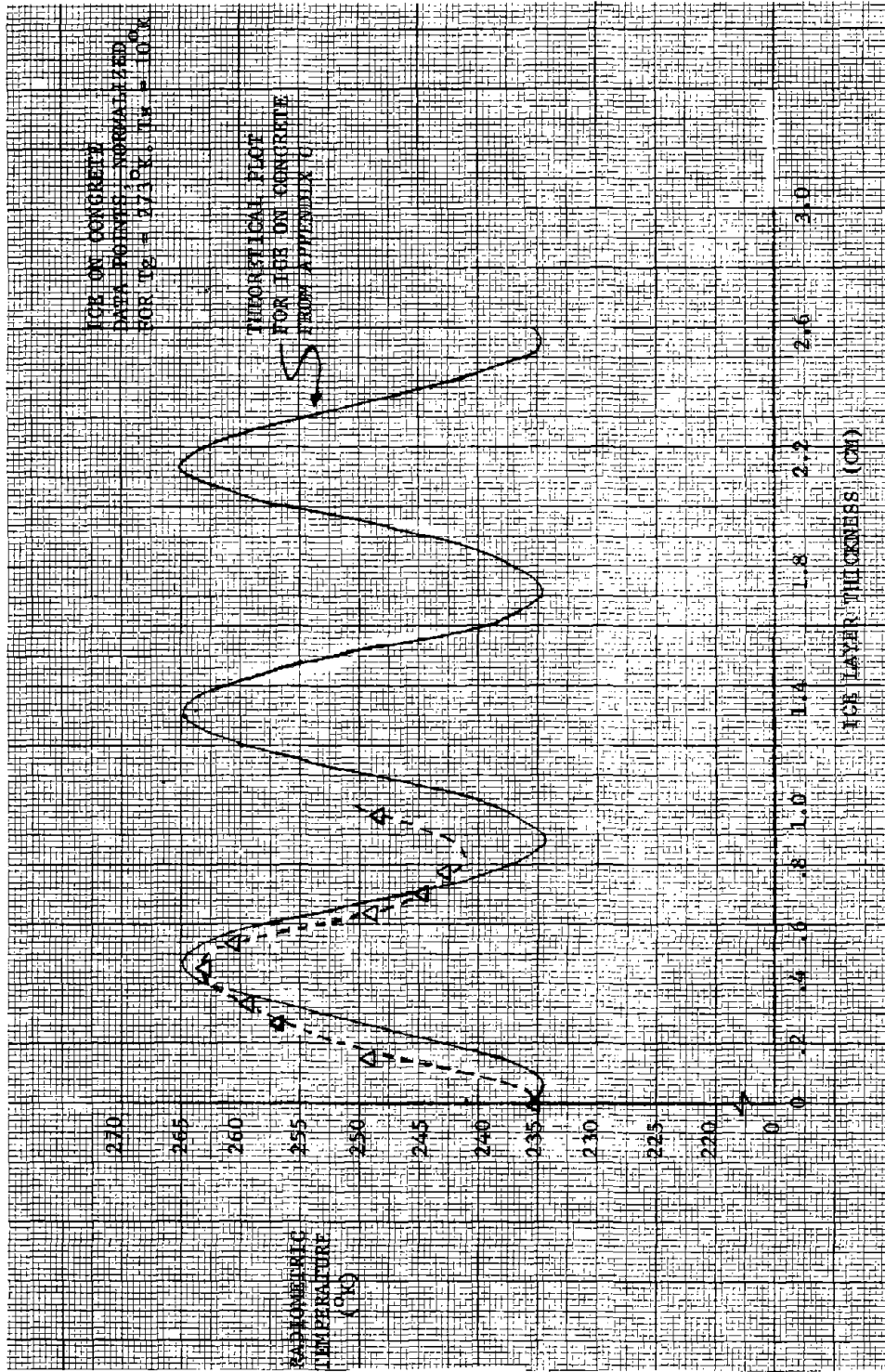


FIGURE 32. ICE ON CONCRETE

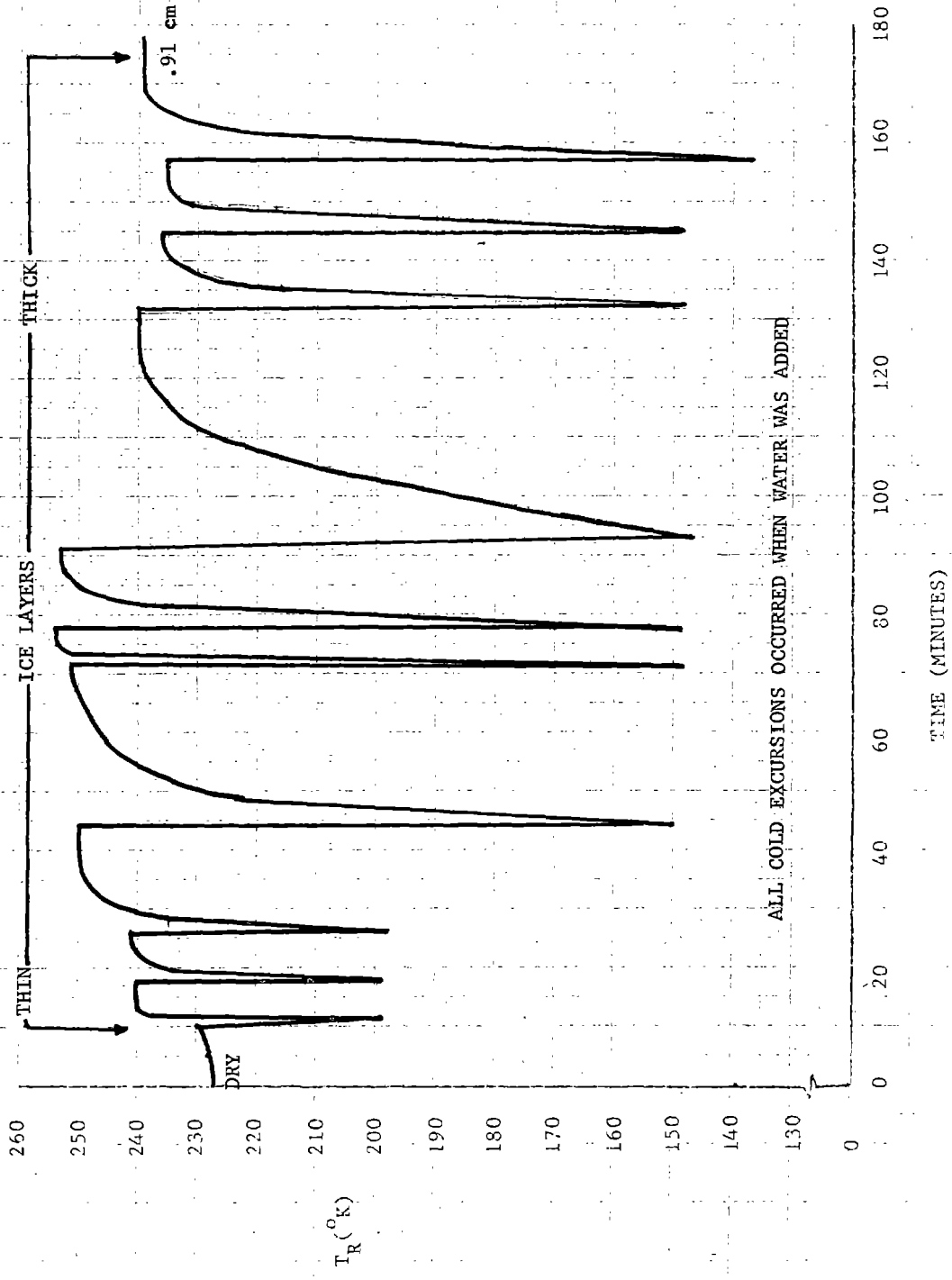


FIGURE 33. ICE LAYER BUILDUP VS. TIME

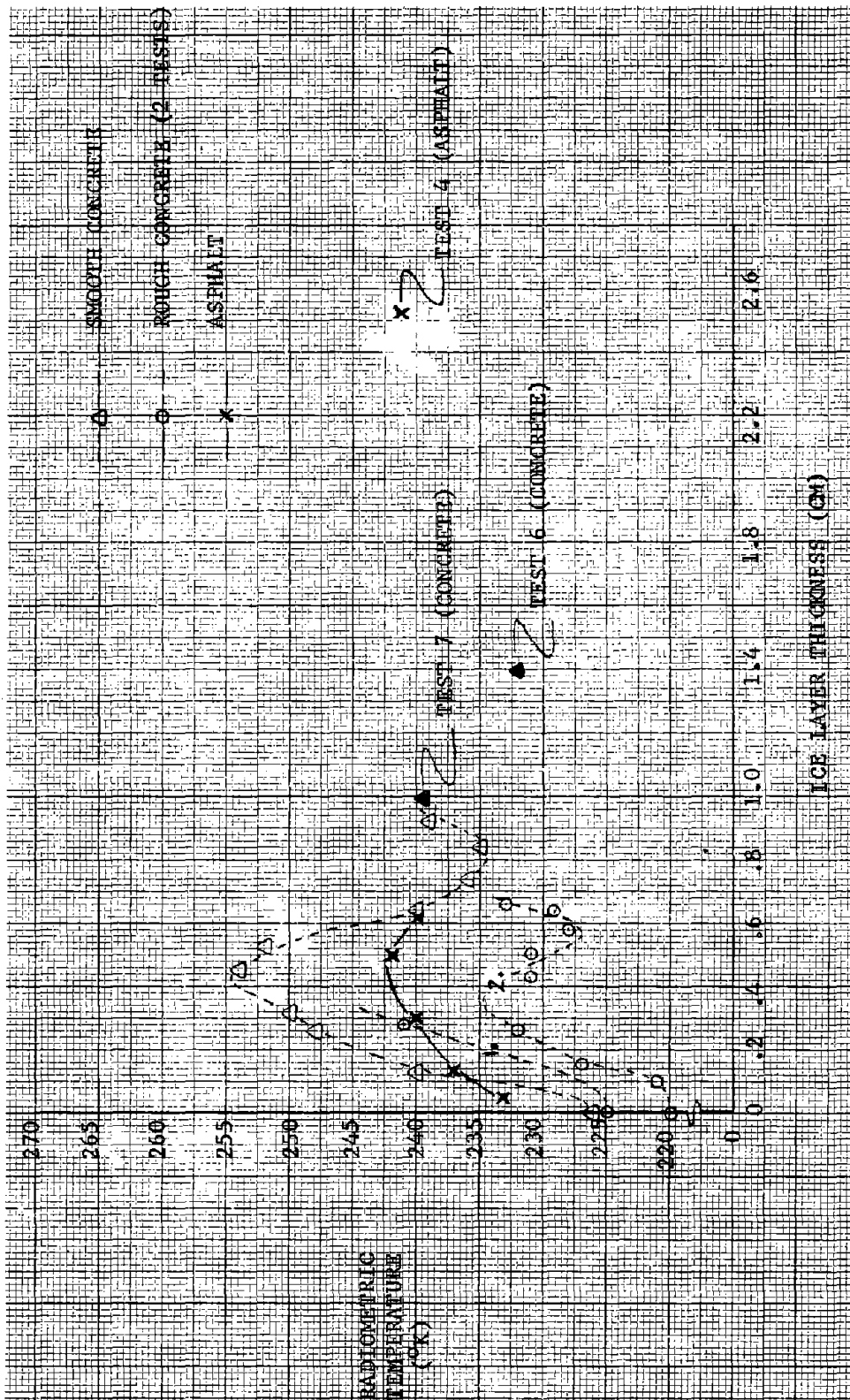


FIGURE 34. ICE TEST DATA (NOT NORMALIZED)

mations for emissivity ϵ by the formula $\epsilon = \frac{T_R}{T_A}$ for the "no ice" condition.

TABLE 6 . SIMULATOR TEMPERATURES AND EMISSIVITIES

<u>Simulator</u>	<u>T_A Surface Temperature</u>			<u>T_R</u> (°K)	<u>ε</u>
	<u>Min</u>	<u>Max</u>	<u>Mean</u>		
Smooth Concrete	256	264	260	226	0.87
Rough Concrete (1st test)	246	270	261	225	0.86
Rough Concrete (2nd test)	254	268	258	220	0.85
Asphalt	250	258	254	232	0.91

The ϵ values shown in the table fall within the range of 0.85 to 0.91, which is the basic range established in Table 4 (discussion of Dry Surface, Cold Temperature).

Tests to determine effects of incidence angle change at vertical polarity were performed during tests 4, 6, and 7. Results of these tests are plotted in Figure 35, and show that the range of usable angles off vertical is ± 20 degrees and the T_R curve behaves in the same manner as previously shown for other surface conditions

Radiometric temperature modifications due to the addition of salt or sand to the ice layer were investigated briefly. Salt, when added to a warm, dry surface increases the radiometric temperature about 5°K. This effect is probably a result of the increase in overall surface roughness and would vary in proportion to the amount of salt added. (In our test, the 5°K increase was caused by a salt layer one granule deep spread evenly and entirely over the surface; coarse water softener salt was used.) When the salt is added to an ice layer, it causes immediate melting, resulting in a lower radiometric temperature proportional to the amount of liquid water created. The resultant radiometric temperature is in a range of values equating to slush. Sand, when added to the ice surface in amounts up to 2 cm deep, does not effectively alter the radiometric temperature. These effects are shown in Figure 36.

Figure 36 illustrates the overall effects of varying conditions on a roadway surface; resultant thermometric and radiometric temperature changes are indicated. A summary of conditions is shown in Table 7 with the resultant T_A and T_R values and an estimate of detectability using the simple logic circuitry discussed in Section 4.3 of this report.

4.2 BREADBOARD FIELD TESTS

4.2.1 Site Survey

A survey trip was taken to the Sierra Nevada mountains during mid-March. This exploratory trip was intended to locate sites of high

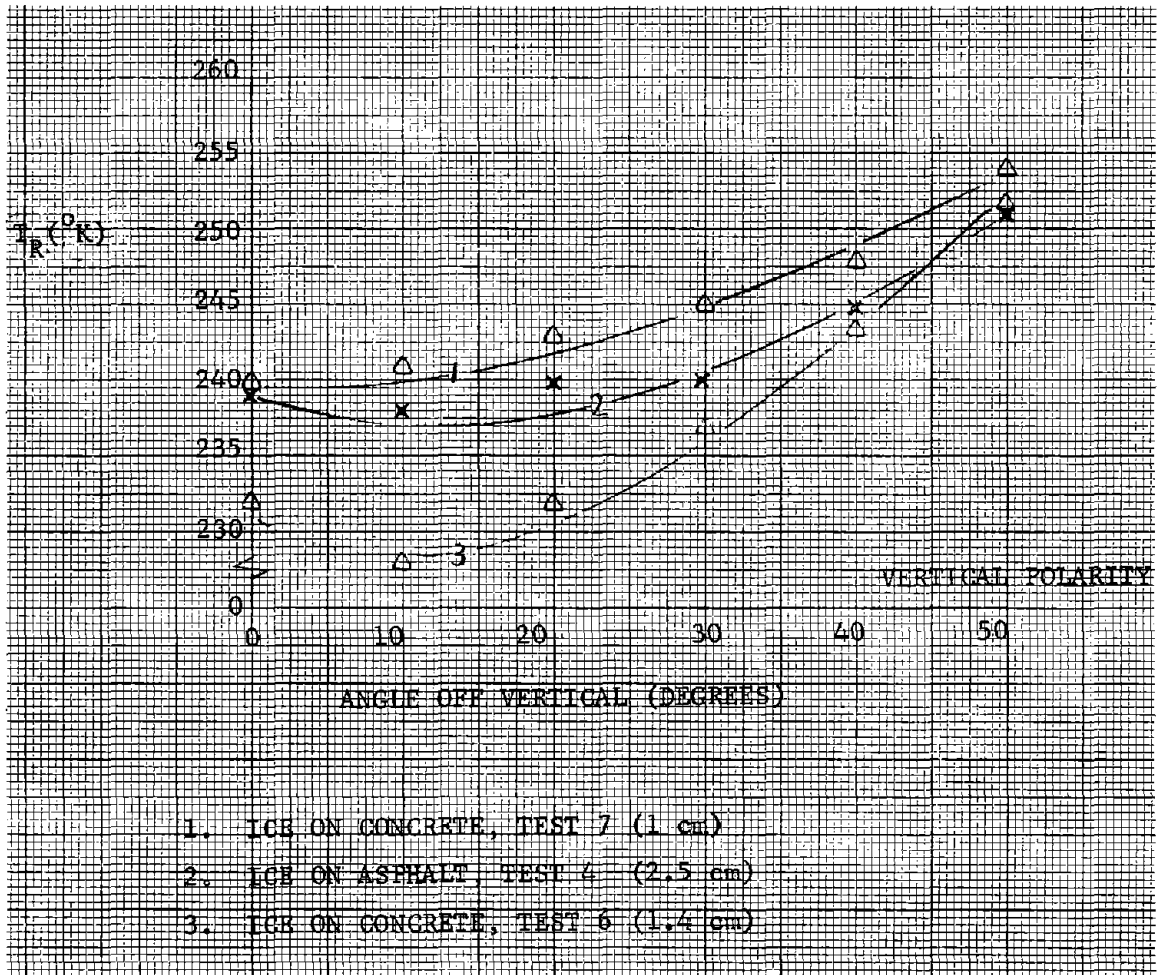


FIGURE 35. ICE SURFACE INCIDENCE ANGLE EFFECTS

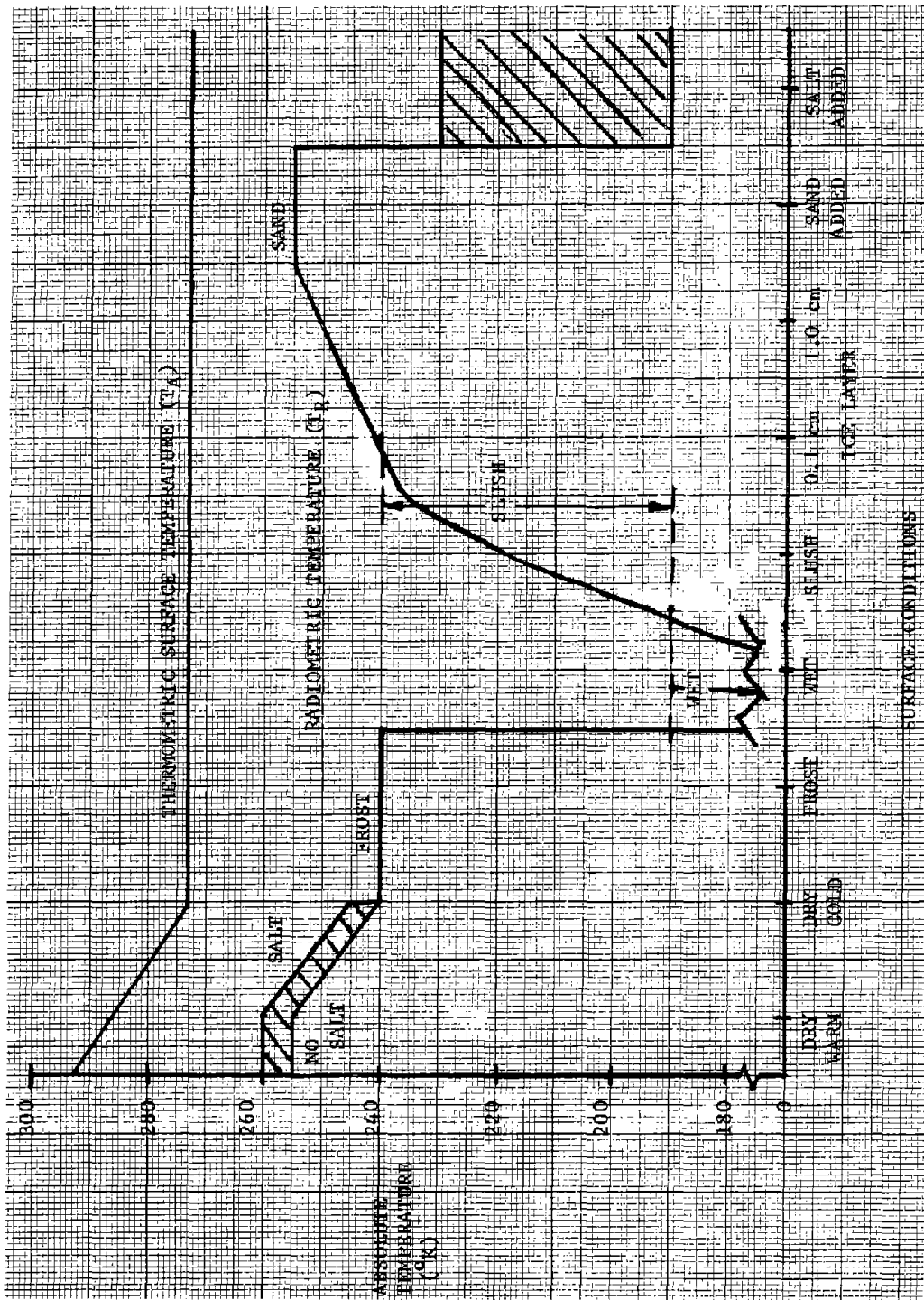


FIGURE 36. TEMPERATURE PROFILE FOR VARIOUS CONDITIONS

TABLE 7. SUMMARY OF CONDITIONS

<u>Condition</u>	T_A (°K)	T_R (°K)	<u>Detectable</u>	
			Yes	No
Dry, Warm	293	$T_A \in$	X	
Dry, Cold	273	$T_A \in$	X	
Frost	273	$T_A \in$		X
Wet	273	< 190	X	
Slush	273	$190 \text{ to } T_A \in$	X	
Ice Layer	273	$> T_A \in$	X	
Sand on Ice	273	$= \text{Ice } T_R$	Ice	Sand
Salt on Ice	273	$< \text{Ice } T_R$	*	

*Appears as Slush

enough altitude to encounter conditions appropriate to field testing of the breadboard radiometer. Although a large snowpack existed in the area of Donner Pass, unusually warm Spring weather had caused much of the snow cover to melt. The weather conditions also made it apparent that a storm of Arctic origin would be necessary to provide conditions of icing on the road surfaces.

Table 8 is a listing of the ten sites surveyed on the trip. Altitudes of the various sites are not listed in the table, but they are all over 5,000 ft (1,525 m) in elevation, the lowest being the concrete bridge at Floriston and the highest the Boreal Ridge rest area on Donner Pass. Exploratory trips were made up several side roads in search of an area where the snow had not melted, or been cleared by CalTrans. Site number 8 seemed the best prospective test area to find snow and slush remaining on the road surface.

The Prosser Creek bridge (site #6) used in previous FHWA sponsored tests was ruled out as a test site due to the high traffic volume and lack of nearby parking. This area was also barren of snow and ice because of the Spring-like weather.

After the site survey trip, several possible sites were selected as probable test sites where snow and ice would be found if cold weather conditions prevailed during subsequent field test trips. The selected sites are numbers 3, 4, 8, 9, and 10 of Table 8. Sites 3, 4, and 10 would require an encroachment permit from CalTrans, which was obtained from the district office located in Marysville, California. Field test sites of Trips 1 and 2 are shown in Figure 37.

4.2.2 Test Results

4.2.2.1 Configuration

Test configuration for the field test was essentially the same as that used for the simulator tests. The major difference was in the data recording system. A Fluke model 2240B Data Logger was obtained for the data recording function. This unit provided a distinct advantage over the multiple recorder system described previously, as it had the capability to record time, temperature, and voltage parameters on the same paper tape printout. Ten channels of recording capability were available, but only 4 or 6 channels were used during the field tests. (During later tests, with the breadboard alarm circuit, the 10 channel capability was utilized.)

Another deviation from the simulator test setup was the addition of a surface temperature sensor. The sensor unit used was an LX5600A from National Semiconductor Corporation. The unit is powered with + 15 VDC and provides an output of 10 MVDC per degree Kelvin. For use as a surface temperature sensor, the device was mounted on a small piece of aluminum "T" stock, wires were attached, and the unit

TABLE 8. TEST SITE SURVEY SUMMARY

<u>SITE #</u>	<u>LOCATION</u>	<u>SURFACE TYPE</u>	<u>COMMENTS</u>
1.	Hwy 80 - 8 miles (12.8 KM) East of Auburn (Park & Pool)	Parking Area Asphalt	Close to Hwy, easy access. Asphalt very thin (3/4") (1.9 cm) not representative of real road surface.
2.	Hwy 80 - 20 miles (32.2 KM) East of Auburn (Blue Star rest area)	Parking Area Asphalt	Close to Hwy, easy access. Good area for warm asphalt data. Two types asphalt.
3.	Eagle Lakes Rd - 1/4 mi. (0.4 KM) off Hwy 80	Bridge, Asphalt (extremely rough)	Close to Hwy, easy access. Probable ice in cold weather.
4.	Boreal Ridge Rest Area off Hwy 80	Parking Area Asphalt	Close to Hwy, easy access. Snow area. Melting snow on parking surface. Probable ice in early a.m.
5.	Prosser Dam Rd. off Hwy 89 NE of Truckee	Road Surface Asphalt	Road not plowed near Prosser Dam. Good area for snow on road surface. Possible ice in a.m.
6.	Prosser Creek Bridge Hwy 89 5 miles (8 KM) NE of Truckee	Bridge, Asphalt	Poor access, no nearby parking, very busy road.
7.	Boca Reservoir Rd - off Hwy 80 East of Truckee	Bridge, Wood Deck	Overhead girder construction. Probable ice in a.m. No real need for data on wooden deck.

TABLE 8. TEST SITE SURVEY SUMMARY (Continued)

<u>SITE #</u>	<u>LOCATION</u>	<u>SURFACE TYPE</u>	<u>COMMENTS</u>
8.	Boca Reservoir Rd - off Hwy 80 East of Truckee	Road Surface Asphalt	Road not plowed beyond Boca Reservoir, good area for snow on road surface.
9.	Hirschdale, off Hwy 80 SE of Truckee (Boca Reservoir Turnoff)	Bridge, Asphalt	Two bridges, 3 miles (4.8 KM) off Hwy 80, probable ice in a.m.
10.	Floriston Turnoff Hwy 80.7 miles (11.3 KM) East of Truckee	Bridge, Concrete	Easy access, good parking nearby. Only concrete test site found. Probable ice in a.m.

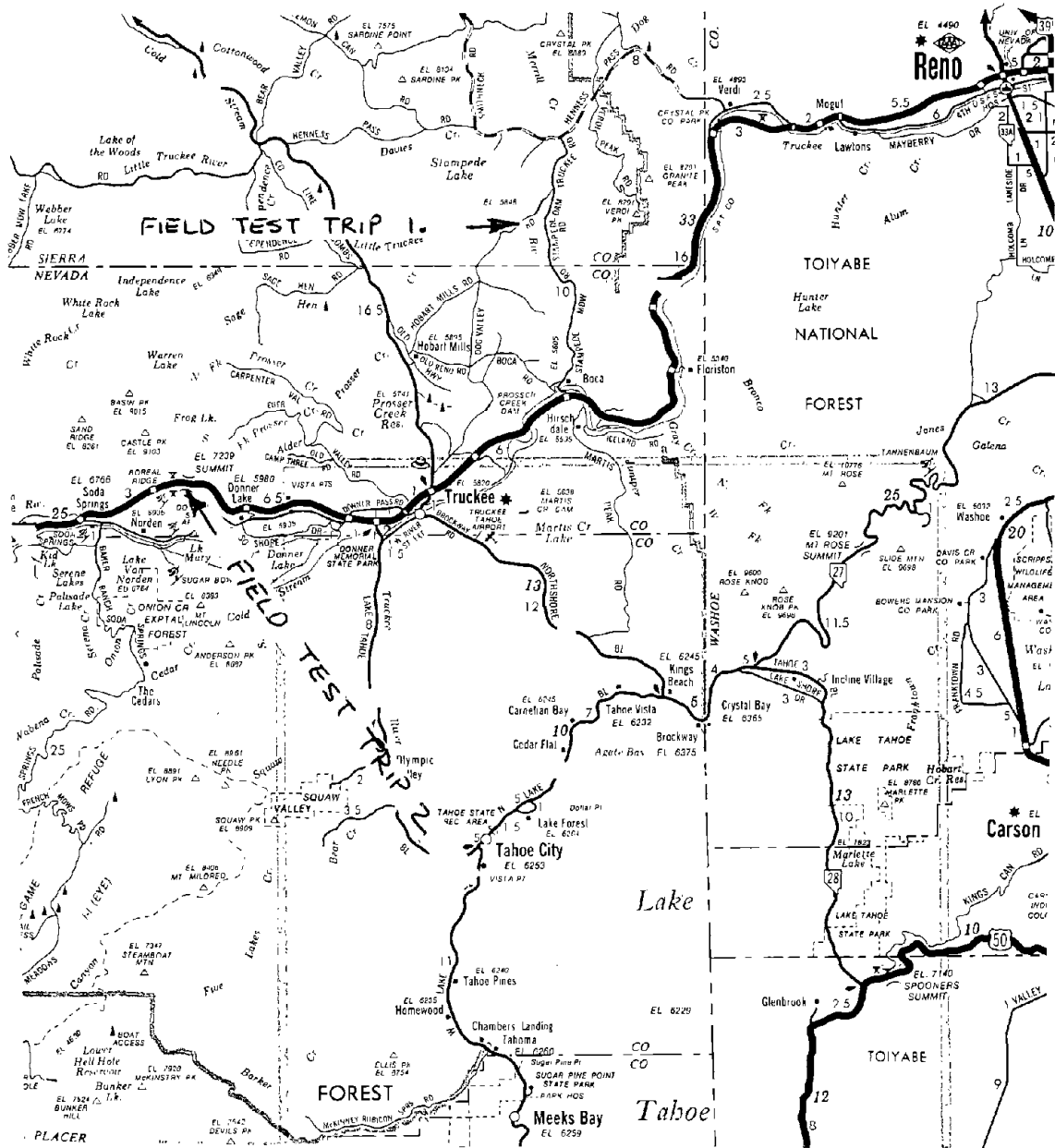


FIGURE 37. FIELD TEST AREA MAP

was completely encapsulated using an epoxy compound with good thermal transfer characteristics. Output calibration was checked by reading room ambient temperature of 70°F (21.1°C) with an output of 294°K, then immersing the unit in an ice bath at 32°F (0°C) with an output of 273°K.

Complete portability of the entire test setup was necessary due to the variable weather conditions existing in the Sierra Nevada region at this time of year (late March, early April). A four-wheel drive pickup truck with a camper shell seemed the best approach to providing equipment portability combined with easy access to the test site during inclement weather. A gasoline-powered portable generator was used to provide the necessary 115 V, 60 Hz power for the equipment. Because of the excellent results obtained from the input voltage stability tests, this power source proved entirely adequate for field tests.

Mounting holes were drilled in an aluminum "I" beam so that it could be attached to the front of the truck and serve as the receiver mounting in a manner similar to mounting during the simulator tests.

Prior to the departure to the field test site area, a complete test was performed utilizing the portable generator as a power source and a cold concrete simulator as test specimen. Data records for this test (including Data Logger printout) are shown in Figure 38. The verification test was completely satisfactory, even providing more data to substantiate the probability of detecting thin ice layers.

4.2.2.2 Field Test - Trip 1

Data from this trip proved very disappointing. Testing on icy surfaces was not possible due to either extremely warm temperatures or rain. Data which was obtained is shown in Table 9.

Data obtained during this trip proved useful in making the following determinations:

- a) Snow, although wet and melting, affects T_R in the same manner as ice of varying thickness.
- b) Slush appears in a range of T_R which is lower than the cold surface without ice, but warmer than a wet surface, and the T_R value of slush decreases as melting occurs.

Figure 39 provides photos of the test configuration and conditions encountered during this field test trip.

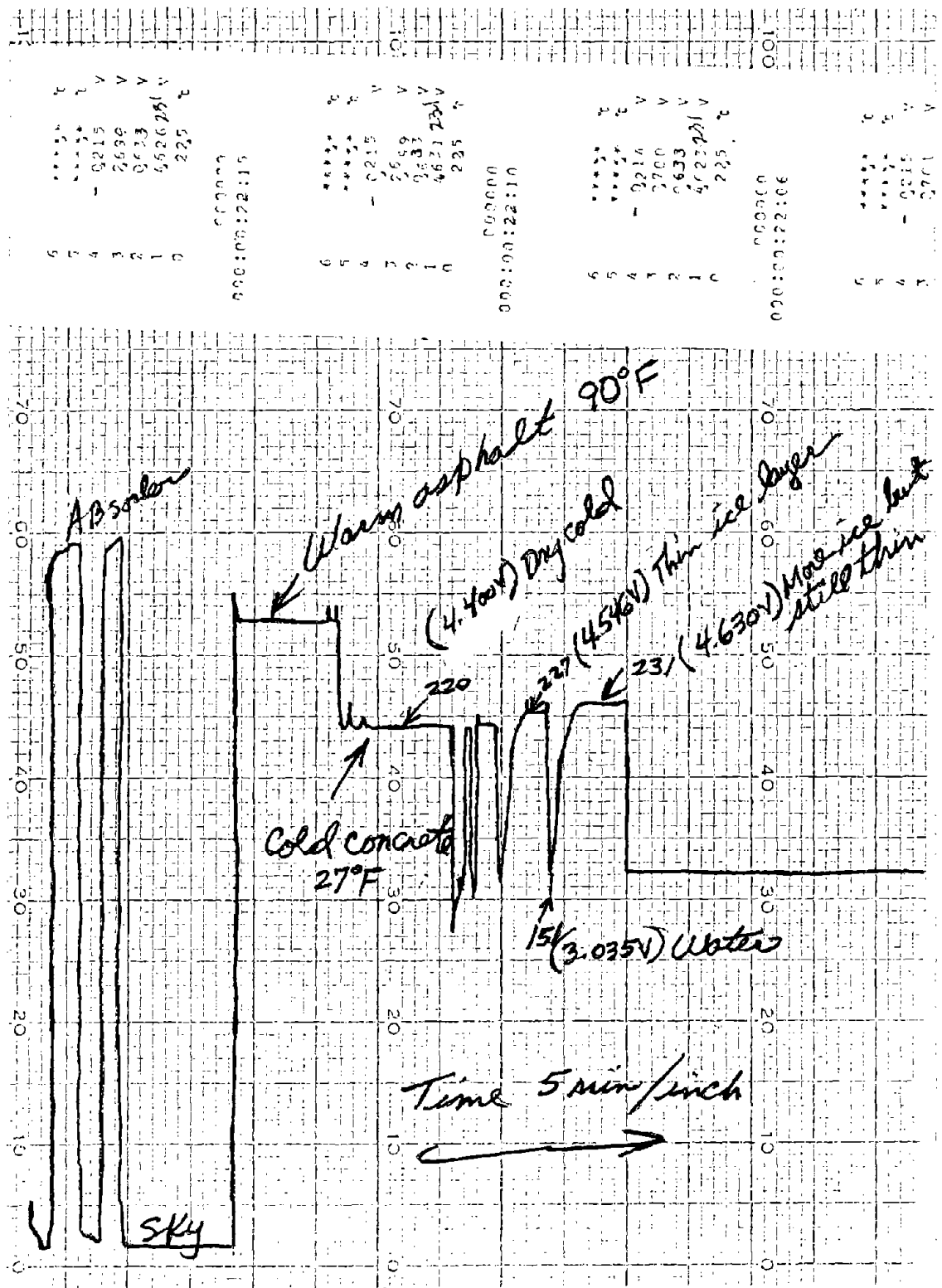


FIGURE 38. FIELD TEST CONFIGURATION VERIFICATION TEST

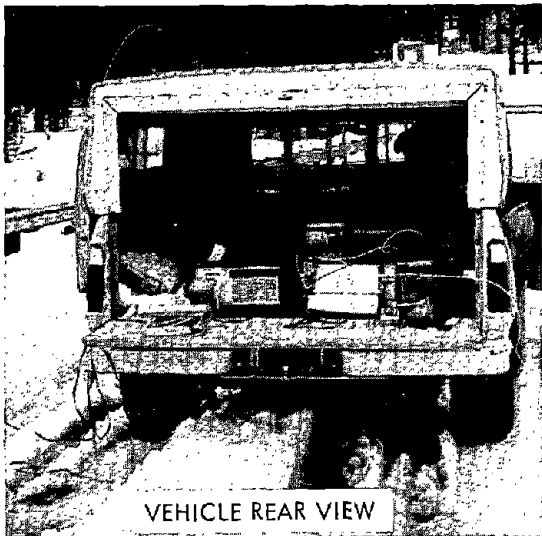
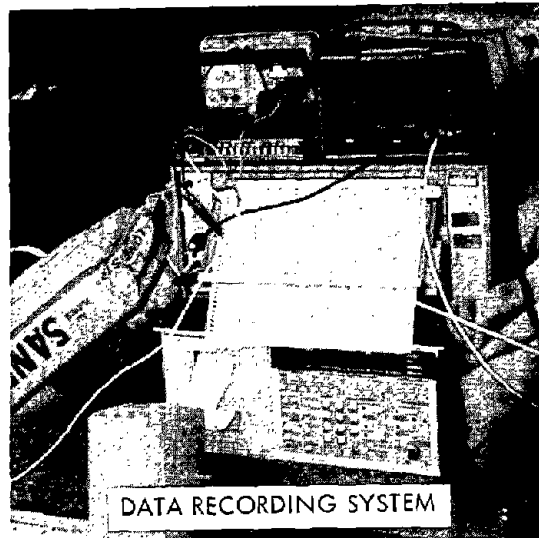


FIGURE 39. FIELD TEST 1 - TEST SET-UP PHOTOGRAPHS

TABLE 9, FIELD TEST 1 - DATA

<u>Condition</u>	<u>T_R (°K)</u>
Wet Asphalt	150
Wet Slush (Melting)	186
1" Slush (25.4 mm)	231
Icy Slush	250
Wet Snow:	
2 inches (50 mm)	247*
5 inches (127 mm)	244
6 inches (152 mm)	251
4.75 inches (121 mm)	248
3.1 inches (79 mm)	243
2 inches (50 mm)	241

*This extremely warm T_R is probably caused by a warm asphalt surface temperature. This occurred because the snow layers indicated were built up on a warm asphalt surface.

4.2.2.3 Field Test - Trip 2

Since results from Trip 1 did not meet the objectives of field testing, Trip 2 was taken with the advance knowledge that a storm of Arctic origin was approaching the field test area. The data obtained during two nights of testing at the Boreal Ridge test area during this storm was completely satisfactory in meeting the objective of obtaining data for ice and snow on asphalt. Data for ice on concrete at the Floriston bridge test site was not obtained due to the warmer temperatures encountered at lower elevation.

A breadboard detection and alarm circuit was added to the configuration for this field trip. Although this unit had only been bench tested just prior to the trip, and one portion of the circuit was not working properly (the T_A input would not track the surface temperature sensor), the overall operation of the unit was satisfactory. A further discussion of this unit is provided in Section 4.3.

The ice on asphalt test was performed in the same manner as the simulator tests. A dry spot on the surface was found and the equipment set up to monitor the T_R of this spot. Water was then added so that ice layers could be built up. Figure 40 shows an overall time plot of this 2 hour test, with 4 layers of black ice being formed. Thickness of the first thin layer formed (less than 0.1 cm) was not measured, but proved to be detectable with sufficient quality to trigger the ice indicator of the alarm circuit. The first measured ice thickness of 0.11 cm shows a T_R difference of + 20K. Power to the test equipment was interrupted at this point (generator ran out of gas), but the T_R of this ice layer remained the same when power was restored. Two more ice layers were formed up to the thickness

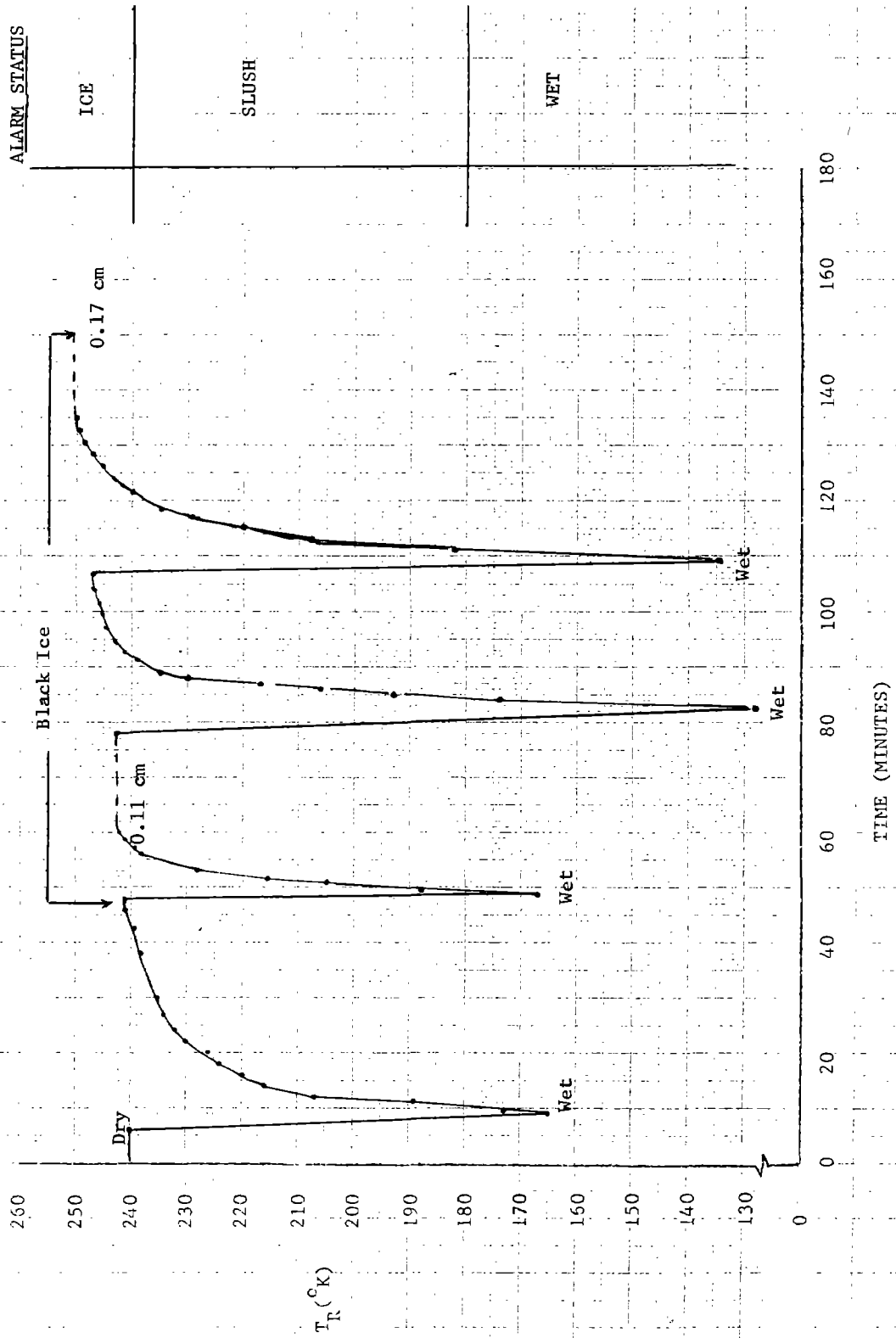


FIGURE 40. FIELD TEST 2 - ICE LAYERS ON ASPHALT SURFACE

of 0.17 cm at which time the test was stopped. Data for the two measured ice layers is plotted in Figure 41. It is apparent from this test that ice layers on an asphalt surface at an actual test site will affect T_R in the same manner as in the simulator laboratory tests.

The snow on asphalt data also shown in Figure 41 was obtained on the following night. A very fine, dry powder snow was falling when we arrived at the Boreal Ridge test area. After the equipment was set up and allowed to stabilize, the snow was cleared from the radiometer field of view. During the following 2 hour period, a snowfall of almost 3.5 cm was monitored. The data from this test (corrected for scale factor drift due to receiver temperature change) shows an oscillatory behavior with increase in snow depth similar to that noted previously (Section 4.1.4.3) for ice layers. From this data curve, a depth of approximately 0.7 cm was sufficient to trigger the hazard alarm ice indicator. Data obtained on this test indicates that snow depths of less than 1 cm are detectable and provide sufficient T_R to T_A change to trigger a hazard alarm.

An attempt was made to obtain field data for ice on a concrete surface, but the temperature was not cold enough to form ice in a timely manner.

4.3 ALARM LOGIC AND CIRCUIT DEVELOPMENT

4.3.1 Logic Rationale

Data obtained during the simulator tests was sufficient to generate the basic concept for a simple alarm circuit. This concept is based on the following conclusions drawn from the simulator test program:

- a) Radiometric temperature changes occur in direct proportion to the thermometric temperature and the emissivity of a dry surface. The approximate relationship is:

$$T_R \cong T_A \epsilon$$

where

T_R = radiometric temperature ($^{\circ}K$)

T_A = thermometric temperature ($^{\circ}K$)

ϵ = emissivity value

- b) A surface which is sufficiently wet to cause a hazard during freezing weather has a T_R which is much colder than the same surface when dry. Usually this value is below $190^{\circ}K$ dependent upon surface wetness.

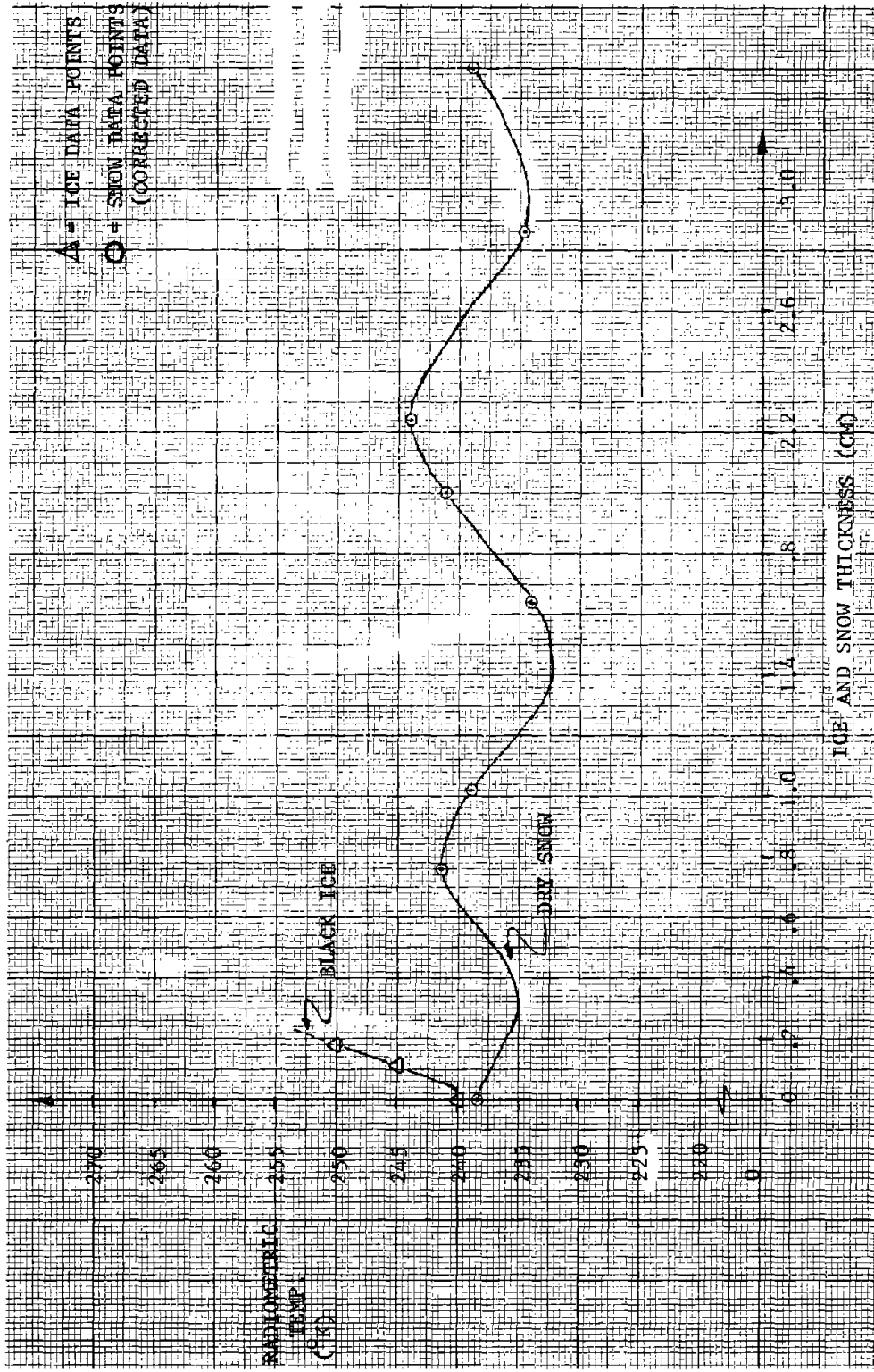


FIGURE 41. FIELD TEST 2 - ICE AND SNOW ON ASPHALT

- c) Formation of a thin ice layer causes T_R to rise above the value it would have if the ice layer were not present. Progressively thick ice layers cause T_R to oscillate in a periodic manner as ice thickness increases. T_R increases immediately upon formation of thin ice.
- d) Formation of frost does not change T_R in an amount significant enough to be detectable.
- e) A surface layer of slush has T_R limits between that of ice and water. By proper definition of this hazard, the limits may be set to trigger an alarm circuit.
- f) Salt, when added to a surface of ice, causes melting which produces the same characteristics as slush or water.
- g) Sand, when added to ice, does not effectively alter T_R at the time of application. Wet sand has the same characteristics as slush.

The primary physical conditions which could cause a hazardous bridge surface are:

- 1) Surface Temperature
- 2) Dew Point
- 3) Precipitation

These conditions and their effects on bridge surface condition are shown in Table 10.

TABLE 10 . PHYSICAL PARAMETERS AFFECTING SURFACE CONDITION

SURFACE TEMPERATURE	DEWPOINT	PRECIPITATION	BRIDGE CONDITION
ABOVE FREEZING $T_A > 273^\circ\text{K}$	\geq Bridge Temperature	No	Wet
	$<$ Bridge Temperature	Yes	Wet
	$<$ Bridge Temperature	No	Dry
BELOW FREEZING $T_A < 273^\circ\text{K}$	$<$ Bridge Temperature	No	Dry
	$<$ Bridge Temperature	No	Slush*
	$<$ Bridge Temperature	Yes	Ice
	$<$ Bridge Temperature	Yes	Snow
	$>$ Bridge Temperature	No	Frost

*Slush is a special case of hazards not defined by physical parameters. The bridge temperature would only be slightly above freezing level when slush is present. Slush would occur only after a snow or ice hazard.

As noted in the table, conditions which are considered a hazard all occur when the bridge surface temperature is below freezing.* This implies that any device used to alarm a bridge hazard would necessarily require an input corresponding to bridge thermometric temperature (T_A).

It is also necessary to know bridge surface temperature (T_A) in the radiometric approach to the problem because of the fact that $T_R \cong T_A \epsilon$. It is conceivable that the bridge temperature will fall below the freezing level and remain dry, which is considered a safe condition. In this case, T_R will change in proportion to T_A which may trigger a false alarm unless the actual T_R - T_A value is taken into consideration. This point is described in Section 4.3.2, below.

Dewpoint, as shown in the table, only causes the single hazardous condition of frost. Since frost is not deemed detectable by a radiometric approach, no provision can be made to provide a hazard alarm when frost forms on the bridge surface. Other methods of providing a frost hazard alarm utilizing bridge surface temperature and dewpoint information are discussed in Section 8.5.

Precipitation, when accumulating on a freezing bridge surface, will cause a hazardous condition in the form of ice, snow, or slush. A simple approach to detecting these conditions is described in the following discussion.

4.3.1.1 Alarm Logic

Based on simulator test data, the logic table of Table 11 was developed. A thermometric sensor is required to determine road temperature input, T_A , and must be scaled to match equivalent changes in T_R . The lower T_A limit of 4.85 volts (SAFE) corresponds to a temperature of 35°F (275°K). The upper T_A limit of 4.82 volts (HAZARD) corresponds to a temperature of 32°F (273°K). T_R represents the radiometric temperature output with a scale factor of 20 mv/°K.

To illustrate the derivation of these voltage levels, shown in Table 11, a smooth asphalt surface is assumed with a relative dielectric constant of:

$$\epsilon_R = 4.3 + j 0.1 \cong 4.3^{(1)}$$

*A wet surface when the bridge is not freezing may also present a hazard in some cases. This case is dependent upon surface roughness and run off capability. These instances can be detected and alarmed very easily using only the radiometric temperature.

(1) Ref.: "The Response of Terrestrial Surfaces at Microwave Frequencies", W. H. Peak and T. L. Oliver, Ohio State University, for AF Avionics Lab, May 1971, p. 101 (AD 884106).

The voltage/current reflection coefficient at normal incidence is:

$$b_o = \frac{1/\sqrt{\epsilon_R - 1}}{1/\sqrt{\epsilon_R + 1}}$$

$$\text{Reflectance } \rho = |b_o|^2 = 1 - \epsilon \text{ (power reflection coefficient)}$$

where ϵ = emissivity of the road surface

$$\text{Then } T_R = (1 - \epsilon) T_s + \epsilon T_g \text{ (for smooth surfaces)}$$

where T_s = sky temperature $\cong 10^\circ\text{K}$

T_g = ground (surface) temperature, e.g., $294^\circ\text{K} = 21^\circ\text{C} = 70^\circ\text{F}$

Using the value of ϵ_R , above:

$$b_o = 0.349$$

$$|b_o|^2 = 0.122$$

and $\epsilon = 0.878$

Thus, for a surface temperature of 32°F (273°K), we have:

$$T_R = (0.122)(10) + (0.878)(273) = 240.9^\circ\text{K}$$

At $20 \text{ mv}/^\circ\text{K}$, this T_R value therefore corresponds to a radiometer output of 4.82 volts, the upper T_A HAZARD limit described above (i.e., ice may form at this temperature, or below).

A similar calculation at a road surface temperature of 35°K will result in the lower T_A SAFE limit of 4.85 volts (i.e., ice can never form at this temperature or above).

The singular property of an ice layer over a road surface, as compared to a water layer, which offers the most promise for reliable detection is that radiometric temperatures appear to be higher than a dry, cold surface. A water layer, on the other hand, will always produce a lower radiometric temperature than a dry, cold surface. Thus, the detector scheme can be selected to exclude the potential "false alarm" condition represented by a water layer on a road surface at a thermometric temperature above freezing.

To illustrate this point, consider the emissivities of various materials in the microwave region.⁽²⁾ Nominal values are (unclassified data):

<u>Material</u>	<u>Emissivity (ϵ)</u>
Grass	1
Dry Soil	0.93
Moist Soil	0.63
Concrete	0.85
Water	0.45
Metal	0

Taking $\epsilon = 0.45$ for water, we have:

$$T_R = (1 - 0.45) 10 + (0.45)(273) = 128.4^{\circ}\text{K}$$

This calculation applies for a water layer thicker than about three skin depths, where skin depth $\sigma = 0.11$ cm at 10 GHz.⁽³⁾ (Skin depth σ is defined as the point at which an incident electric field has been attenuated to 36.8% of its initial value. At 3σ , the electric field value is 5.0%.) At these thicknesses, the effect of an underlying road surface (asphalt or concrete) is negligible. At water layers approaching a thickness of one skin depth and below, the two-layer theoretical analysis would apply, as in the case of ice over concrete (see Figure 32) and a cyclic temperature function would be expected with varying water thickness. Other factors would come into play with water penetration of the surface which would change the road's relative dielectric constant; the case of ice over water over road would pose a still more complex analytical exercise. In any event, a wet road reading for the conditions stated would certainly fall between 240.9°K and 128.4°K, both of which lie below a road covered with ice at any thickness.

Table 11 indicates the selected level limits for T_A and T_R along with the expected combinations of conditions and desired displays.

(2) Ref.: "Passive Millimeter-Wave Radiometry and Some Possible Applications", L. C. Mundie, Rand Corp., DARPA Report R-1175, April 1973 (Confidential), AD 528057

(3) Based on dielectric constant of water at 17°C: $\epsilon_R = 61.4 + j 33.5$. Note that with decreasing temperature the real part of ϵ_R decreases. Ref.: "Electromagnetic Properties of Water, at Frequencies Below 1,000 GHz, as Met in Its Various Forms Found at the Surface of the Earth", P. M. Halley, Advisory Group for Aerospace Research & Development (AGARD) Conference Proceedings No. 208 (NATO), October 1976.

TABLE 11 . HAZARD LOGIC TABLE

COMPARATOR LEVEL		CONDITION	DISPLAY	NOTES
$T_A > 4.85$ VDC		SAFE	DRY	INHIBIT HAZARD ; TURN OFF ICE DISPLAY
	(190° K) $T_R < 3.80$ VDC	SAFE	WET	
$T_A < 4.82$ VDC	$T_R = T_A \in$	SAFE	DRY	ENABLE HAZARD
	(5°K) $T_R - T_A > +0.10$ VDC	HAZARD	ICE OR SNOW	STAYS ON UNTIL $T_A > 4.85$ VDC
	(190°K) $T_R < 3.80$ VDC	HAZARD	WET	
	$0 > T_R - T_A > -0.8$ VDC (0 to -40°K)	HAZARD	SLUSH	

4.3.2 Development of Breadboard Alarm Unit

4.3.2.1 Block Diagram

From the data obtained during the simulator tests, a breadboard alarm circuit was developed. Figure 42 is a block diagram of this unit.

A simplified approach using the information presented in Section 4.3.1, above, was used to develop this unit and was implemented using readily available integrated circuits. Ample adjustments were provided to set comparator detection levels and T_A scaling.

4.3.2.2 Description of Operation

In operation, the alarm unit receives thermometric temperature data (T) from a surface temperature sensor and radiometric temperature input (T_R) from the radiometer processor unit. The thermometric temperature is scaled to match the scale factor of T_R . Gain and offset adjustments are provided for this purpose. The scaled signal is then buffered and provides an analog recorder output. The T_A signal is also fed into the hazard logic and differential amplifier.

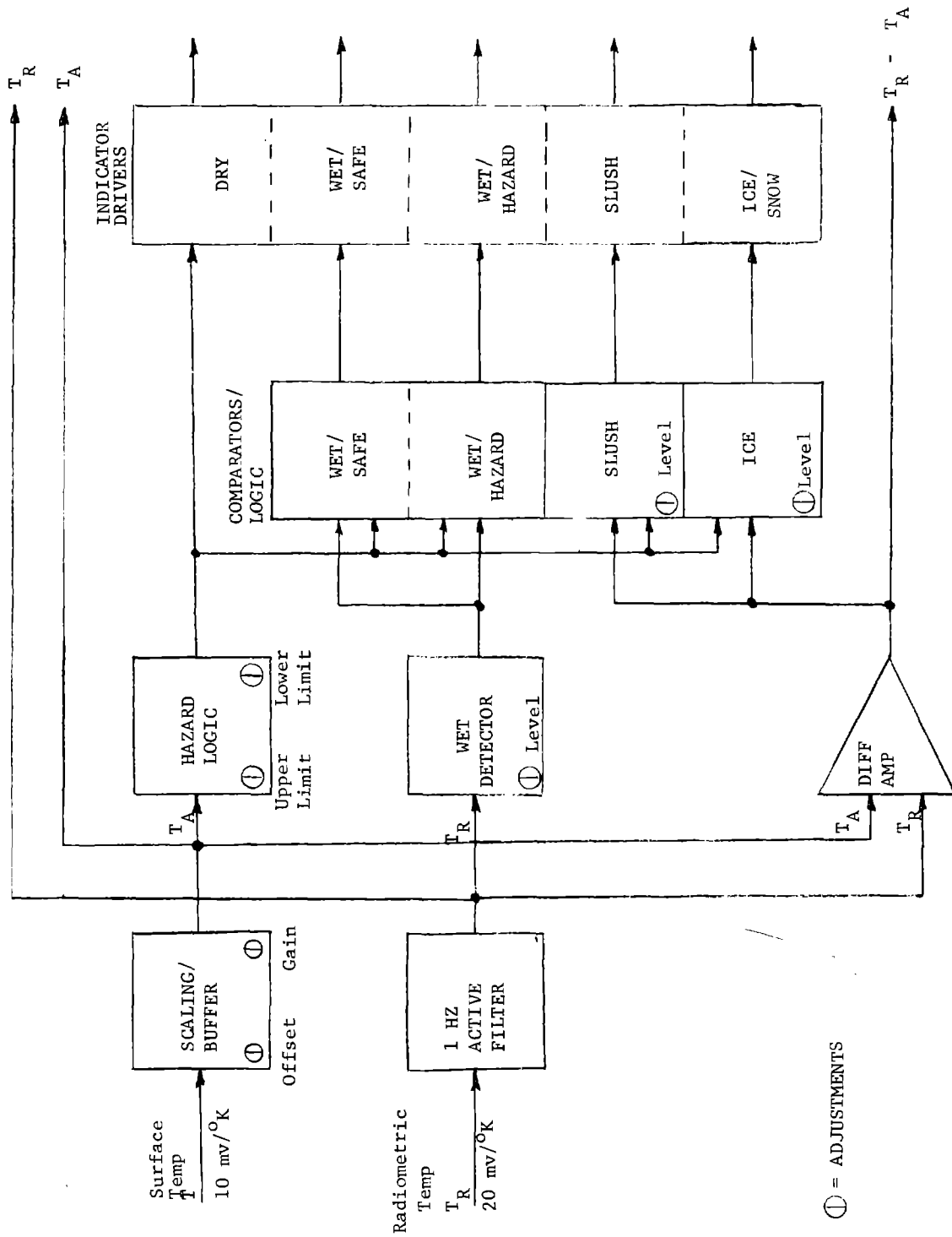


FIGURE 42. BREADBOARD ALARM CIRCUIT - BLOCK DIAGRAM

Radiometric temperature signal (T_R) is smoothed and filtered in the 1 Hz active filter used to eliminate transients. It is provided as an analog signal output for recording purposes and is also fed to the wet detector and the differential amplifier.

The differential amplifier output is the difference temperature, $T_R - T_A$. This signal is also provided as an analog output for recording purposes. The $T_R - T_A$ signal is the basis for detecting an icy surface. If the $T_R - T_A$ value is $> + 0.10$ VDC (representing 5°K), the ice logic comparator provides an output to LED indicators if the T_A signal is below a value equivalent to a freezing surface.

The hazard logic circuit has a provision for setting the upper and lower freeze levels and generates the signal necessary to determine whether a hazard exists or not. If the hazard logic level is above 4.85 VDC (274.6°K), the surface is assumed to be safe and the dry indicator is activated. If the signal is below 4.82 VDC (273°K), the surface is freezing and the hazard circuits are enabled.

The wet detection circuit is a comparator which is set to the level desired for a wet surface, normally at 3.80 VDC (190°K). This wet surface may be safe or hazardous depending upon the hazard logic level. Both of these indications (wet/safe and wet/hazard) are available.

The slush logic is enabled by the hazard logic and also has a level adjustment capability. This level is normally set to give an output when $0 > T_R - T_A > -0.8$ VDC and hazard logic indicates a freezing surface.

All driver outputs are connected to LED indicators and provide logic level outputs for recording purposes. The alarm unit operates from the +15, -15 and +5 VDC power provided by the processor and contains a +10 VDC reference source for the comparator level adjustments. The unit is presently contained in a 5 x 7 x 2 inch box. A photograph of this unit is shown in Figure 43.

4.3.3 Test Results

Fabrication of the alarm circuit was not completed until after completion of the simulator tests and just prior to field testing.

After de-bugging the unit, a bench test was performed. Variable voltages representing the T_A and T_R input signals were applied to the unit and the scaling and level adjustments were set as follows:

T_A Gain	= 1.76
T_A Offset	= 0.0 VDC
Hazard Upper Limit	= 4.85 VDC

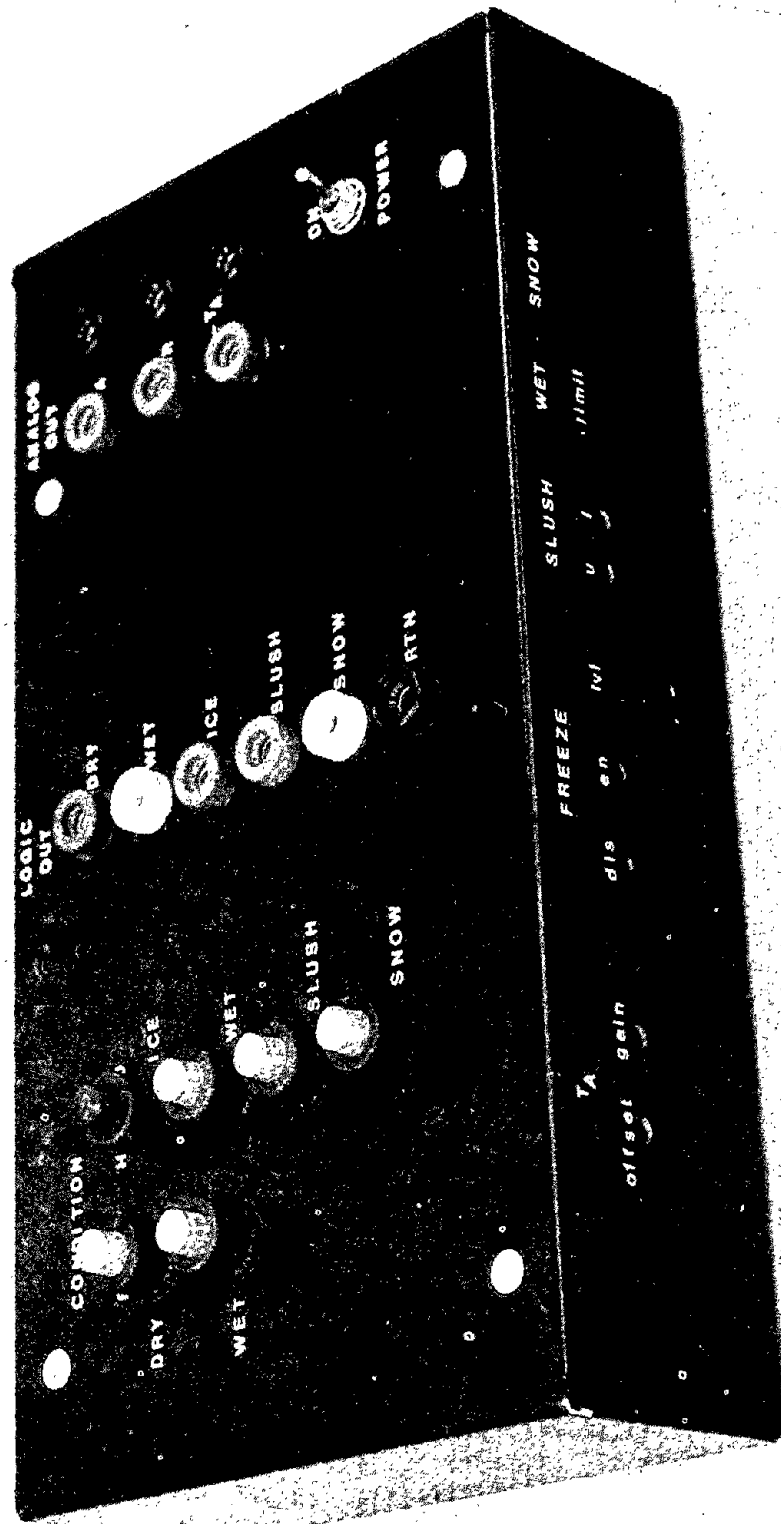


FIGURE 43. BREADBOARD ALARM UNIT (PHOTO)

Hazard Lower Limit	= 4.82 VDC
Wet Limit	= 3.80 VDC
Slush Limits	= $0 > T_R - T_A > -0.80$ VDC
Ice Limit	= $T_R - T_A > + 0.10$ VDC

The unit then performed as expected during the bench tests.

The alarm unit was available during the Field Test 1 trip, but was not used due to lack of hazardous conditions for testing. However, the alarm circuits were in operation during the ice and snow tests on the Field Test 2 trip.

One problem was encountered during these tests: the T_A input from the surface temperature sensor would not operate properly because the alarm circuit input was referenced to power return. It was later found that the surface sensor requires a differential (floating) input and this provision was added after completion of the field tests.

Since the required circuit modification was not feasible during the field tests, the alarm unit was tested using a fixed T_A input corresponding to the surface temperature sensor output. The unit indicated the alarm status outputs shown in Figure 40 (3 ice and 4 each wet and slush indications), during the ice tests. During the snow tests of the following night, the ice level was readjusted to $T_R - T_A > + 0.04$ VDC (2°K) and an ice hazard was indicated after 0.8 cm of snow had accumulated. This indication remained on for the remainder of the test.

Stability of the unit appears good enough to lower the $T_R - T_A$ deadband from 5°K to 2°K, thereby generating an alarm with very thin ice layers, but no testing had been accomplished to substantiate this change.

After field tests, the modification to the T_A input was accomplished, and a brief test of this circuit proved satisfactory. No further testing of the alarm breadboard unit has been performed, due to constraints of schedule and budget.

4.4 RECOMMENDED MODIFICATIONS

Modifications recommended for incorporation in the Phase III prototype radiometer system are noted in the following three subsections. These modifications are proposed in order to provide more rugged and more weatherproof unit packages and to ensure stable receiver performance with ambient temperature. Other changes are proposed in the interest of shorter parts procurement spans and better utilization of common dc power supplies.

4.4.1 Antenna and Receiver

The antenna and receiver modifications will consist of repackaging to provide environmental and weather protection in the form of a housing. Also, the power supply and L.O. driving circuit will be incorporated as part of the processor.

Other modifications are the direct substitution of equivalent components as listed below:

<u>Component</u>	<u>Breadboard Part</u>	<u>Phase III Part</u>
IF Amplifier	7132US/Amplica	MHT-250/Aydin Vector
Directional Coupler	WX2A/Bendix Microwave	4015C-20/Narda Microwave
Mixer	CX-1/Spacekom	7H0118/Anaren

These substitutions were made to circumvent a longer lead procurement span required by the breadboard equivalent parts. However, the mixer change was also made to provide improved stability of the radiometer over the operating temperature range. Provisions will be made to accommodate the inclusion of heaters to obtain an extended operational temperature range. A receiver temperature sensor unit will be added for heater control and temperature monitoring. Threaded mounting holes will be provided in the receiver base plate to accommodate any mounting brackets selected by the FHWA during future use of this system.

4.4.2 Processor and Alarm Circuit

- o Processor - The modifications to the processor will include the following items:
 - a) Removal of the second radiometer channel which eliminates two cards: Module 2B and Module 3B.
 - b) Consolidation of the +15 VDC power supply to power the processor and the receiver.
 - c) Addition of the local oscillator driving circuit.
 - d) Change of digital display from LED to LCD for better visibility in an outdoor environment.
 - e) Change of interconnect connector (DFC 9S-Cannon) to a weather-proof type connector.
 - f) Repackaging into a more ruggedized unit with provision to include alarm circuitry.
 - g) Provision for better accessibility for calibration controls.

- o Alarm Circuit - Modifications to the alarm circuit will include the following:
 - a) Repackage electronics on two Douglas type p.c. cards for inclusion in processor unit.
 - b) Add an inhibit function to all hazard circuits so that they cannot operate when $T_A > 4.85$ VDC.
 - c) Use incandescent indicators for better visibility (will require more power).
 - d) Reconfigure outputs to provide either a Safe or Hazard warning only, for exclusive use of auxiliary equipment; however, maintain ice, wet and slush indicators as in breadboard unit.
 - e) Provide suitable access to all adjustment controls of the alarm circuit.

4.4.3 Interconnection Cables and Connectors

- o Interconnection Cables - Provide weather-proof cables and connectors for the Receiver-to-Processor cables and the Processor-to-power line cable. Also provide a weather-proof cable running from the Processor to the road surface temperature sensor.
- o Connectors - Mating cable connectors will also be weather-proof. An additional connector will be provided in the Processor unit to provide hazard warning data to any interfacing, auxiliary equipment.

Section 5.0

DESCRIPTION OF PHASE III EFFORT

5.1 PROTOTYPE DESIGN AND TEST DETAILS

The breadboard receiver and processor units which were used during Phase II tests were developed for an earlier test program. These units were neither designed nor packaged for application as a snow and ice detection system. They did, however, serve the required objectives of the feasibility study.

The design philosophy for the prototype system was to utilize the breadboard design as far as possible with the following exceptions:

- o Modify the receiver to correct the temperature instability discussed in Section 4.1.3.2.
- o Repackage the receiver and processor units with consideration for the operating environment.
- o Add alarm circuitry to the processor unit.

Discussion details following this design approach are provided below.

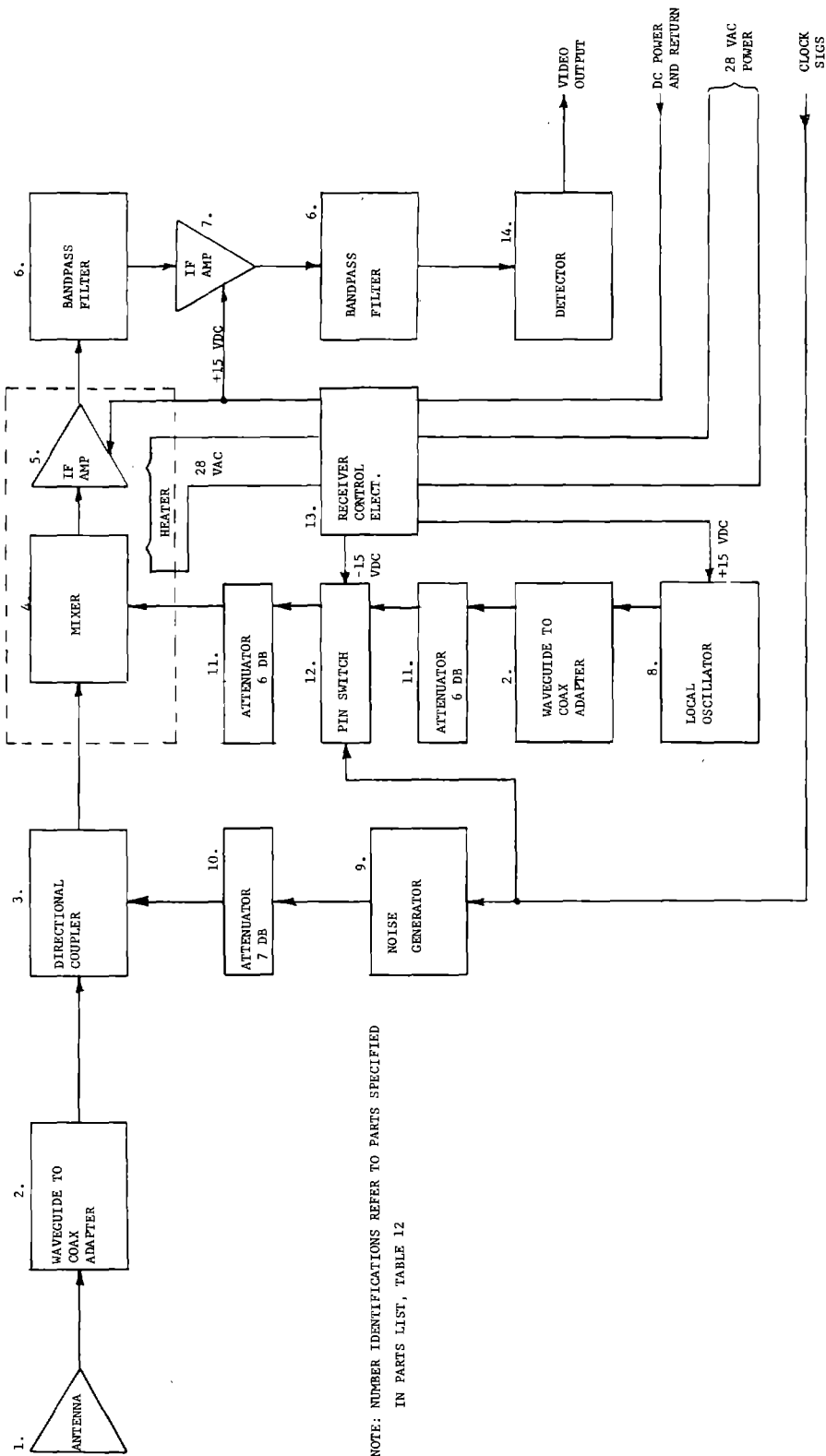
5.1.1 Receiver Functional Modifications

A detailed block diagram of the prototype receiver unit is shown in Figure 44. An accompanying parts list is given in Table 12. Several modifications from the breadboard design are incorporated to compensate for the temperature drift of various components.

The mixer and IF amplifier component manufacturers were changed to take advantage of parts with better temperature characteristics. In addition, the mixer and first IF stage are mounted on a thermally-isolated 2 x 5 x 0.2 inch (5.1 x 12.7 x 0.5 cm) aluminum plate with heater sensor units to obtain further temperature stability improvement.

A Receiver Control Electronics circuit board is added for D.C. power distribution and heater control.

Instead of switching the local oscillator on and off, as in the breadboard unit, the local oscillator is continuously on and the switching function is performed by the added Pin Switch. This change should eliminate errors introduced by extended local oscillator start-up time at low temperatures.



NOTE: NUMBER IDENTIFICATIONS REFER TO PARTS SPECIFIED
IN PARTS LIST, TABLE 12

FIGURE 44. PHASE III PROTOTYPE RECEIVER BLOCK DIAGRAM

TABLE 12. PHASE III PROTOTYPE RECEIVER PARTS LIST

<u>PART NUMBER</u>	<u>NOMENCLATURE</u>	<u>VENDOR</u>	<u>QTY.</u>
1. SA 12-8.2	ANTENNA	SCIENTIFIC-ATLANTA	1
2. 2000-6254	COAX/WG ADAPTER	OMNI SPECTRA	2
3. 4015C-20	DIRECTIONAL COUPLER	NARDA	1
4. 7H0118	MIXER	ANAREN	1
5. MHT-250	IF AMPLIFIER	AYDIN VECTOR	2
TC-2	CASE	AVANTEK	1
TB-2	P.C. BOARD	AVANTEK	1
6. ----	BANDPASS FILTER	LMSC	2
7. MHT-250	IF AMPLIFIER	AYDIN VECTOR	3
TC-4	CASE	AVANTEK	1
TB-3	P.C. BOARD	AVANTEK	1
8. C2070L	LOCAL OSCILLATOR	GENERAL ELECTRIC	1
9. MC5812	NOISE GENERATOR	MICROWAVE SEMI-CONDUCTOR CORP.	1
10. M291-7	ATTENUATOR	MIDWEST MICROWAVE	1
11. M291-6	ATTENUATOR	MIDWEST MICROWAVE	2
12. 33104A	MICROWAVE SWITCH	HEWLETT PACKARD	1
13. ----	RECEIVER CONTROL ELECTRONICS	LMSC	1
14. 215HJ	DETECTOR	MICROPHASE	1

With these changes incorporated in the prototype receiver unit, the objective temperature stability of $\pm 2^{\circ}\text{K}$ over the range of -20 to $+100^{\circ}\text{F}$ (-29 to $+38^{\circ}\text{C}$) should be achieved.

5.1.2 Receiver and Processor Packaging

The receiver was repackaged so that it would be weatherproof. Environment resistant connectors are used in both the receiver and its associated connecting cable and a weather resistant aluminum cover is used as a housing around the entire receiver. The horn antenna is covered and sealed with a low loss microwave material (radome) as used throughout the Phase II test effort. A calibration hood for this antenna will be provided as an accessory.

The processor unit is repackaged into a 9 x 9 x 13 inch (22.8 x 22.8 x 33 cm) weather resistant aluminum carrying case. This unit is not intended to be exposed to the same environment as the receiver unit, but will be considerably more rugged than the breadboard unit.

The receiver and processor are interconnected by 100 ft (30 meter) cable assemblies, one to carry all power and signals between the two units and the other carrying the receiver video signal.

The roadway surface temperature sensor will be on a separate 100 ft (30 meter) cable to the processor unit.

5.1.3 Alarm Circuit Addition

The alarm circuitry which was developed during Phase II (ref.: Section 4.3.2) is repackaged onto two 4.5 x 4.5 inch (11.4 x 11.4 cm), general purpose circuit cards. These cards are designated as:

Card 9 - Alarm Circuit Input Board

Card 10 - Alarm Circuit Logic and Driver Board

The same circuitry as used in the breadboard unit (ref.: Block Diagram, Figure 42) is incorporated into the prototype processor card rack with the addition of an inhibit signal which is fed to each hazard alarm output. The inhibit signal is generated when surface temperature T_A is greater than freezing. When the inhibit signal is present, the hazard outputs of ice, slush, and wet (hazard) cannot operate. Figure 45 shows the alarm circuit block diagram with the inhibit circuit addition. This figure also indicates the makeup of alarm circuit cards 9 and 10.

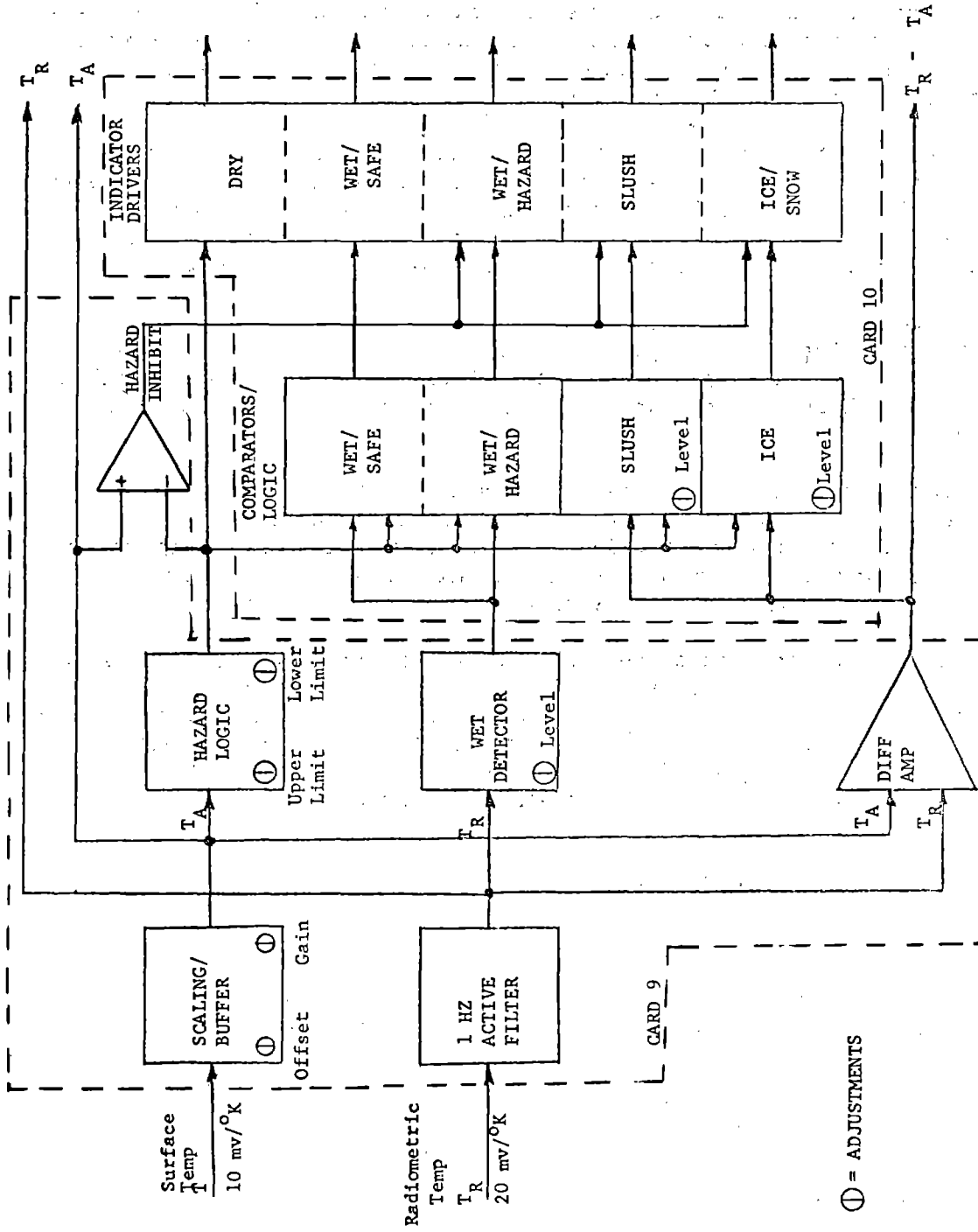


FIGURE 45. PROTOTYPE ALARM CIRCUIT - BLOCK DIAGRAM (HAZARD INHIBIT ADDED)

5.1.4 Test Results

Subsystem and system adjustments, calibration and functional tests were conducted on the prototype system model. These tests were equivalent to the bench tests conducted on the breadboard radiometer in Phase II, as described in Section 4.1.1.

Test results were satisfactory in meeting anticipated performance requirements. Although tests on actual ice-covered road surfaces were not run during Phase III, the alarm circuits were adjusted using simulated inputs as necessary to verify proper circuit operation. Alarm circuit set-up procedures are described in Section 6.3.3.

A typical functional test was measurement of receiver gain. Referring to the block diagram of Figure 44, the gain from the input of the directional coupler to the output of the second bandpass filter was 68 db. This is 5 db over a nominal minimum acceptable gain value of 63 db.

Another critical measurement was receiver noise figure, F. A reading of $F = 6$ db was obtained at the input of the directional coupler of the prototype receiver. This represents a 2 db improvement over the nominal 8 db value used in calculations of radiometer resolution, ΔT min. (see Section 6.1).

With the added controlled heater scheme in the receiver, the system temperature stability tests resulted in an output radiometric temperature (T_R) variation of $\pm 1.5^\circ\text{K}$ over a Receiver Unit case temperature ranging from $+14$ to $+77^\circ\text{F}$ (-10 to $+25^\circ\text{C}$). This T_R variation is within the desired zone of $\pm 2^\circ\text{K}$. The heater control circuitry has been set to hold the mixer-1st IF amplifier mounting plate to $85 \pm 1^\circ\text{F}$ ($29.4 \pm 0.6^\circ\text{C}$).

5.2 PROTOTYPE DESIGN DOCUMENTATION

5.2.1 Requirements

This contract required preparation and delivery with the final prototype system of a reproducible copy of applicable drawings and specifications. The standard invoked as a guideline for this documentation was the American National Standards Institute series of publications constituting the ANSI Drafting Manual Y14. The following types of drawings were included:

- a) Commercial-type electrical schematics.
- b) Wire lists.

- c) Printed circuit board layouts.
- d) Fabrication and/or assembly drawings including critical detail dimensions or adjustments.

5.2.2 Drawings

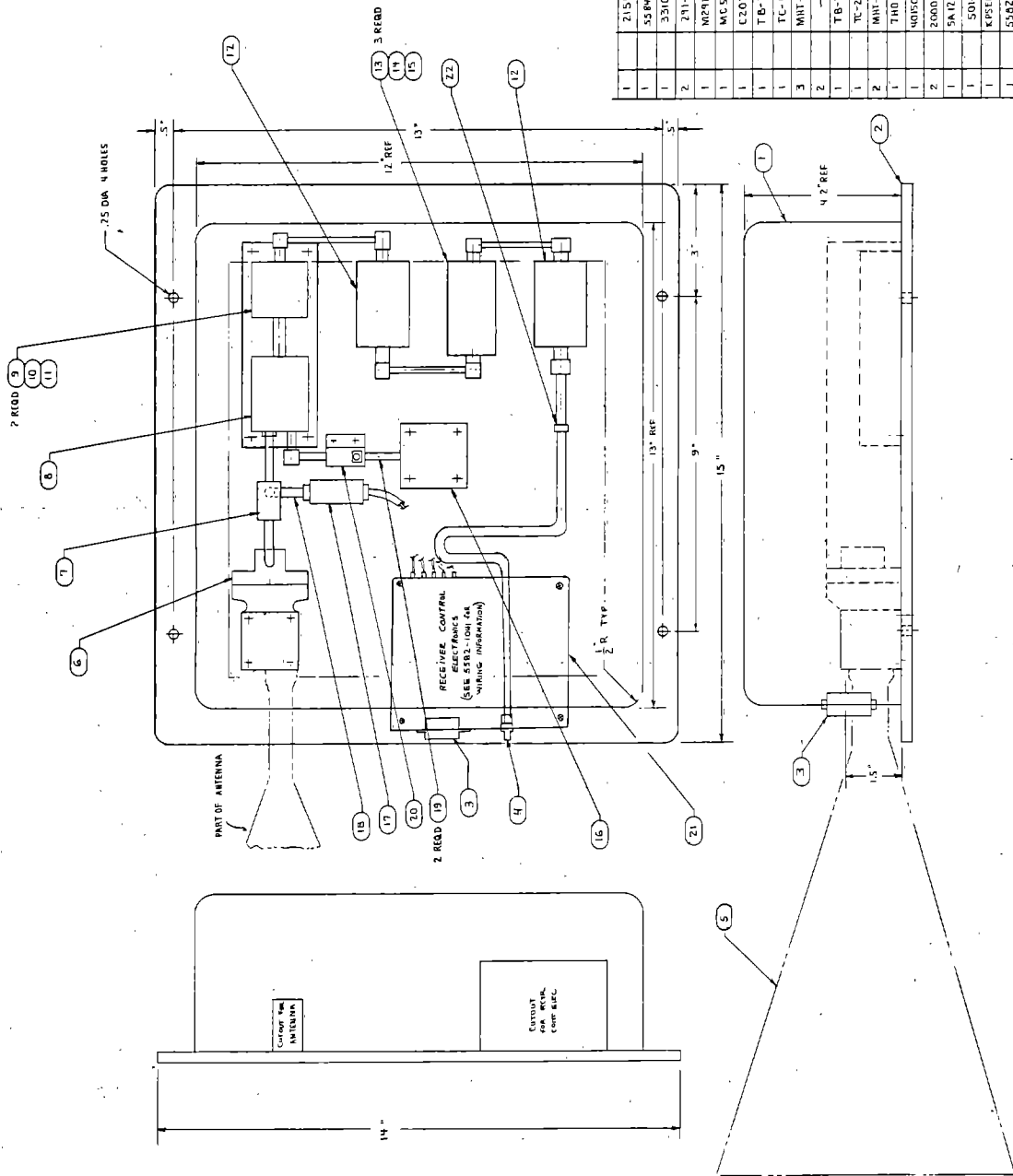
The required reproducible drawings were submitted under separate cover. For convenience and cross-reference purposes, a drawing list is provided in Table 13. Note that the processor unit contains nine modules with number 8 purposely omitted.

Top assembly drawings for the receiver and the processor are included herein as Figures 46 and 47, respectively.

TABLE 13. PROTOTYPE RADIOMETER DRAWING LIST

<u>DRAWING TITLE</u>	<u>DRAWING NUMBER</u>
PROCESSOR TOP ASSEMBLY	5582-1001
PROCESSOR WIRING DIAGRAM	5584-1002
MODULE 1 ASSEMBLY	5584-1005
SCHEMATIC	5584-1006
MODULE 2 ASSEMBLY	5584-1009
SCHEMATIC	5584-1010
MODULE 3 ASSEMBLY	5584-1013
SCHEMATIC	5584-1014
MODULE 4 ASSEMBLY	5584-1017
SCHEMATIC	5584-1018
MODULE 5 ASSEMBLY	5582-1021
SCHEMATIC	5582-1022
MODULE 6 ASSEMBLY	5584-1025
SCHEMATIC	5582-1026
MODULE 7 ASSEMBLY	* { 5584-1025
SCHEMATIC	5582-1026
MODULE 9 ASSEMBLY	5582-1029
SCHEMATIC	5582-1030
MODULE 10 ASSEMBLY	5582-1033
SCHEMATIC	5582-1034
RECEIVER TOP ASSEMBLY	5582-1040
RECEIVER WIRING DIAGRAM	5582-1041
CABLES TOP ASSEMBLY	5582-1045

*Same as Module 6.

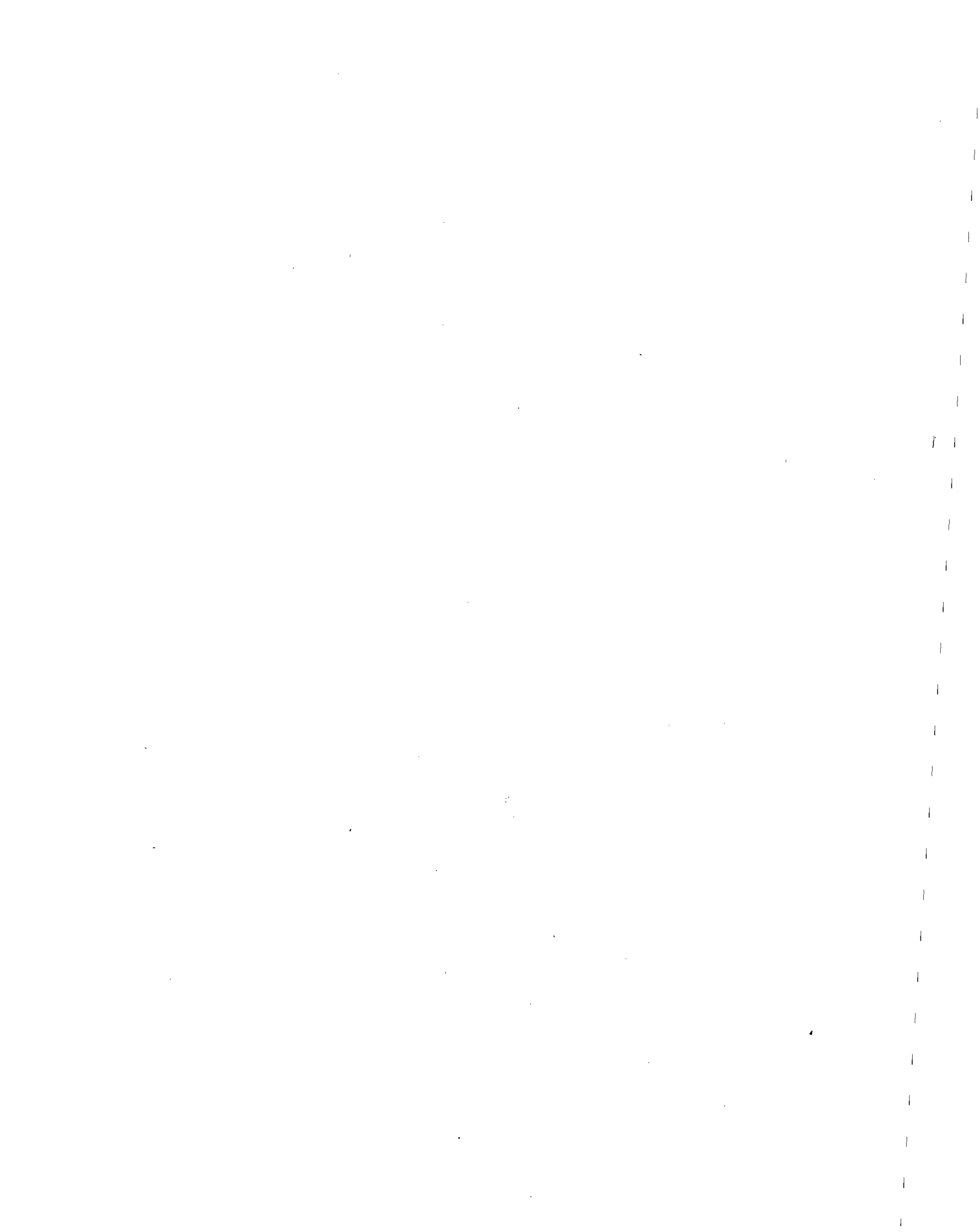


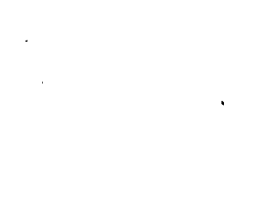
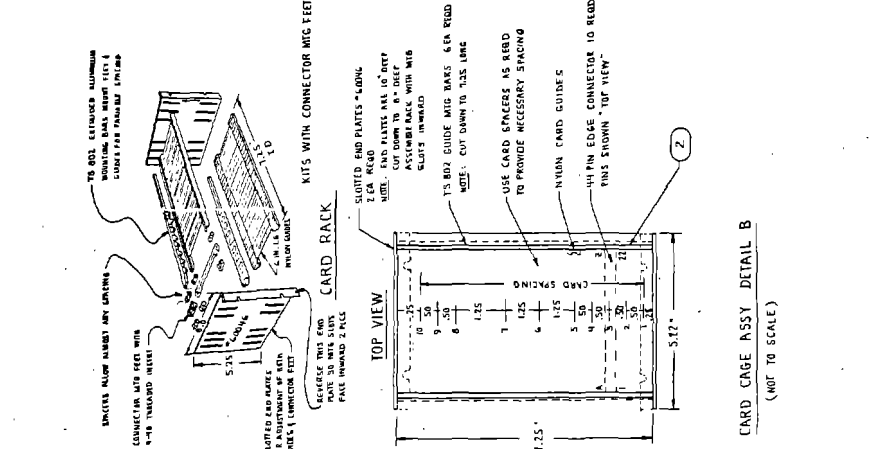
NOTE:
 1. ACTUAL LOCATION AND MOUNTING OF COMPONENTS ARE OPTIONAL.
 2. WIRE UNIT PER 5582-10H

QTY.	CODE IDENT.	PART OR IDENTIFYING NO.	MATERIAL DESCRIPTION OR FUNCTION OF NOTE	PARTS LIST	ITEM NO.
1	215R J	DETECTOR		MICROPHASE	22
1	5584-104	RECEIVER		LM SC	21
1	3304A	REVERSE		HEWLETT	
1	3304A	MICROWAVE SWITCH		PALMAD	20
2	291-6	ATTENUATOR		MILWAUKEE	19
1	M291-7	ATTENUATOR		MILWAUKEE	18
1	MC581Z	NOISE		MILWAUKEE	17
1	CE201L	SELECTOR		MILWAUKEE	16
1	TB-3	OSCILLATOR		EL-ELECTRIC	15
1	TE-4	P.C. BOARD		AVANTEK	14
1	TE-4	CASE		AVANTEK	13
3	MNT-250	IF AMPLIFIER		AVON VECTOR	12
2	—	IF AMPLIFIER		LM SC	11
1	TB-2	BANDPASS FILTER		AVANTEK	10
1	TC-2	P.C. BOARD		AVANTEK	9
2	MNT-250	IF AMPLIFIER		AVON VECTOR	8
1	TMD 11B	MIXER		ANAREN	7
1	4015C-20	DIRECTIONAL		NARDA	6
2	2000-6754	CORR/MICROAMPLIFIER		OMNI SPECTRA	5
1	5A12-8.2	ANTENNA		SCIENTIFIC	4
1	501-3	CONNECTOR		AVON	3
1	4PSEDET48P	CONNECTOR		CANNON	2
1	5582-1040-1	BASE PLATE	SEE DETAIL		1
1	2.152-708A	COVER		2 E.R.O.	1
1	—	MANUFACTURE OR MATERIAL SPECIFICATION OF NOTE			

NOT TO SCALE

FIGURE 46. RECEIVER, TOP ASSEMBLY



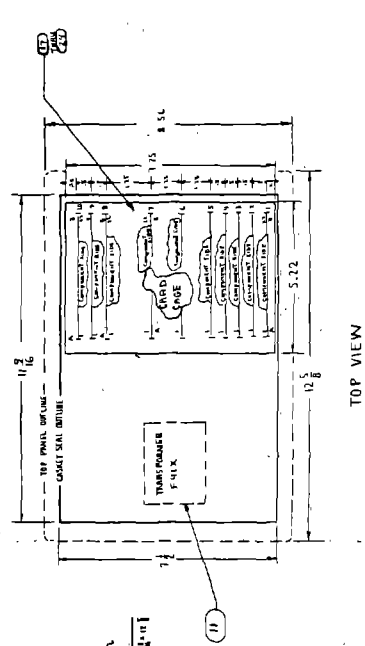


ITEM NO.	QTY.	DESCRIPTION	PART OR IDENTIFICATION NO.	NOMENCLATURE OR DESCRIPTION OF MATERIAL ON NOTE	MATERIAL SPECIFICATION	TONE FROM NO.
1	1	5582-1033	MODULE 10			24
2	1	5582-1029	9			23
3	1	5584-1025	6 1/7			22
4	1	5584-1021	5			21
5	1	5584-1017	4			20
6	1	5584-1013	3			19
7	1	5584-1009	2			18
8	1	5584-1005	MODULE 1			17
9	6	507-4757	LED CARTRIDGE DATALIGHT	LED1-5		16
10	6	508-7538	LED SOCKET DATALIGHT	LED1-5		15
11	1	DM2100X	DISPLAY	DMEL	DE1	14
12	1	44D30-02-1-HAM	SWITCH	GRAYHILL	S2	13
13	1	5C2-CK-1922-96	SWITCH	CUTLER/HAMMILL	S1	12
14	1	F41-X	TRANSFORMER	TRIAD	T1	11
15	1	M63102A-1P5-L	CONNECTOR	Amphenol		10
16	1	Z1Z-BZ21	CONNECTOR	OSM	DPJ7	9
17	1	J102-RE-20-2-P	CONNECTOR		DP J4	8
18	1	KP56074-1P25	CONNECTOR	CONNOR	DPJ5	7
19	16	1508-102	BANANA JACKS	TP S		6
20	1	BK625/10	BNC CONNECTOR	DPJ6		5
21	1	160-41	CONNECTOR	AMPHENOL	DPJ2	4
22	1	160-5	CONNECTOR	AMPHENOL	DPJ1	3
23	1	DETAIL B	CARD CAGE	SCANBE		2
24	1	Z1C 613	SUITS CASE	ZERO		1

NOTES:

- INTERNAL WIRING PER DWG. 5584-1002.
- EXACT MOUNTING LOCATION OF CARD RACK AND TRANSFORMER (11) OPTIONAL, TO BE DETERMINED AT ASSEMBLY.

FIGURE 47. PROCESSOR, TOP ASSEMBLY (SHEET 1 OF 2)
111/112



TOP VIEW

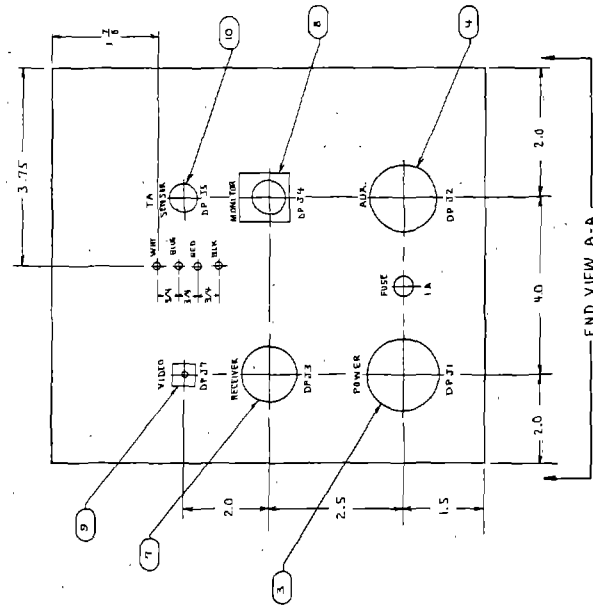
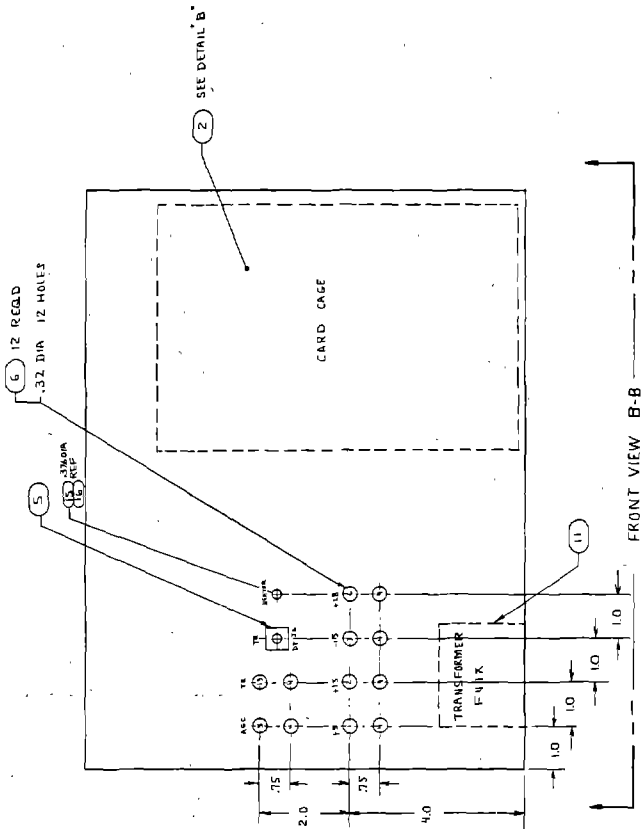
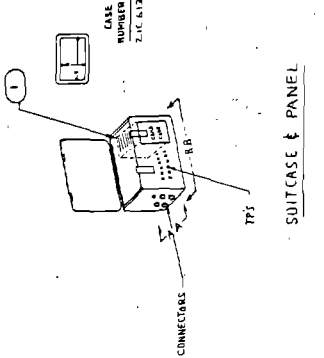


FIGURE 47. PROCESSOR, TOP ASSEMBLY (SHEET 2 OF 2) 113/114

Section 6.0
EQUIPMENT DESCRIPTION

6.1 PERFORMANCE SPECIFICATIONS

6.1.1 Radiometer Specifications

The specifications of the Phase III radiometer sensor are as follows:

Antenna Half Power Beamwidth	13°
Antenna Type	Horn
Receiver Noise Figure (F)	6.3 (8 db)
Frequency of Operation	10 GHz
IF Frequency Bandwidth (B)	400 MHz
Video Bandwidth ($B_v = \frac{1}{\tau}$)	10 Hz
Resolution (ΔT_{\min})	0.28°K
Accuracy (T_{ϵ})	2°K
Measurement Range	0 to 500°K
Output Scale Factor	20 mv/°K
Operating Environment	-20° to +65°C
Input Power	115 V AC @ 0.5 amp

6.1.2 Measurement Error Discussion

As noted in the system tradeoff discussion of Section 3.2.3, the two components of interest in a radiometer detection system are: (1) accuracy (T_{ϵ}); and (2) resolution (ΔT_{\min}). The accuracy parameter is obtained empirically and is a function of the long term and environmental stability of the radiometer. The resolution, ΔT_{\min} , is the noise component uncertainty in the radiometer measurement. This factor is related to the other parameters of the radiometer by the following equation:

$$\Delta T_{\min} = \frac{T_F + T_R}{(2B\tau)^{\frac{1}{2}}} \left[\left[1 + \left\{ \frac{T_F + T_R + T_G}{(T_F + T_R)} \right\}^2 \right] \left(\frac{T_R}{T_G} \right)^2 \left(\frac{\tau}{\tau_{\text{agc}}} \right) + \left[1 + \left\{ \frac{T_F}{T_F + T_R} \right\}^2 \right] \right]^{\frac{1}{2}}$$

where

- T_F = noise temperature of the receiver
 = 290 [F-1] = 1537°K
 T_R = radiometric temperature being measured
 (e.g., 273°K)
 T_G = noise temperature of the calibrating noise source
 during clock signal 2 = 300°K
 B = IF bandwidth = 400 MHz
 τ = video output time constant = $\frac{1}{B_V} = 0.1$ sec
 τ_{agc} = AGC time constant = 1 sec

This equation was derived for and pertains specifically to the Lockheed (Hong) radiometer configuration used on this program. The factor in brackets, []², corresponds to the "K" term in the conventional ΔT_{min} equation; the system loss factor (L_s) is assumed to be 0 db (see Section 3.2.3).

Inserting the values noted above, we obtain:

$$\begin{aligned}
 \Delta T_{min} &= \frac{1810}{(2 \times 400 \times 10^6 \times 0.1)^{\frac{1}{2}}} \left[\left[1 + \left(\frac{2110}{1810} \right)^2 \right] (0.91)^2 (0.1) + \left[1 + \left(\frac{1537}{1810} \right)^2 \right] \right]^{\frac{1}{2}} \\
 &= 0.202 \left[(1 + 1.360)(0.828)(0.1) + 1 + 0.721 \right]^{\frac{1}{2}} \\
 &= 0.202 \left[0.195 + 1.721 \right]^{\frac{1}{2}} = 0.202 \left[1.916 \right]^{\frac{1}{2}} \\
 &= 0.202 (1.384) = 0.280
 \end{aligned}$$

This ΔT_{min} value is that given in the specifications listing in Section 6.1.1. Note that the "K" value for this radiometer configuration is 1.384.

6.2 SIZE, WEIGHT, POWER AND ENVIRONMENTAL RESTRICTIONS

The prototype radiometric hazard detection system consists of two units, interconnected by a 100 ft (30 m) cable assembly. These units are the receiver unit with attached horn antenna, and a processor unit with built-in alarm circuitry. Additionally, a surface temperature sensing unit is provided with a 100 ft (30 m) cable for connection to the processor unit. Figures 48, 49 and 50 are photographs of these units.

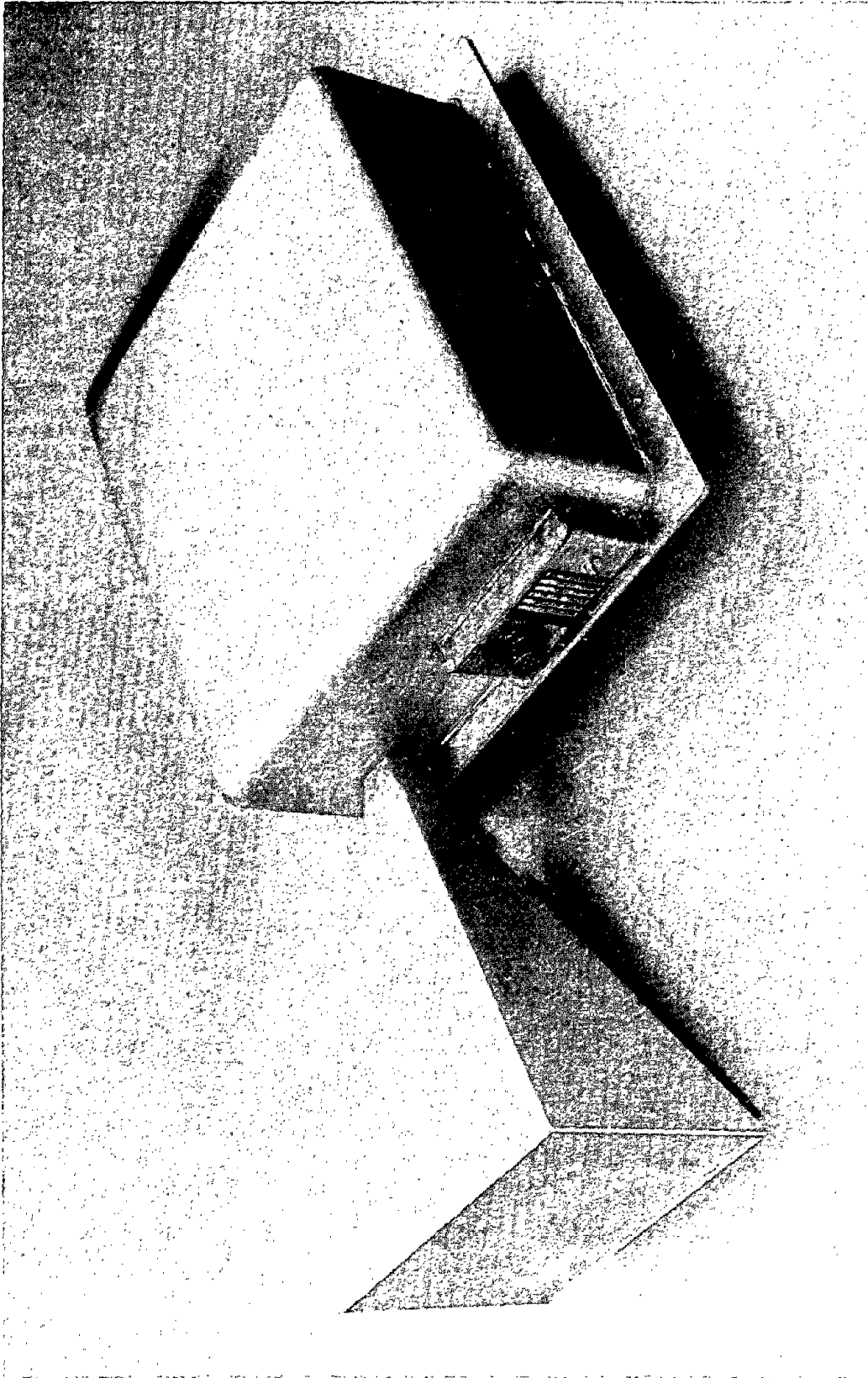


FIGURE 48. RECEIVER UNIT, OBLIQUE VIEW (PHOTO)

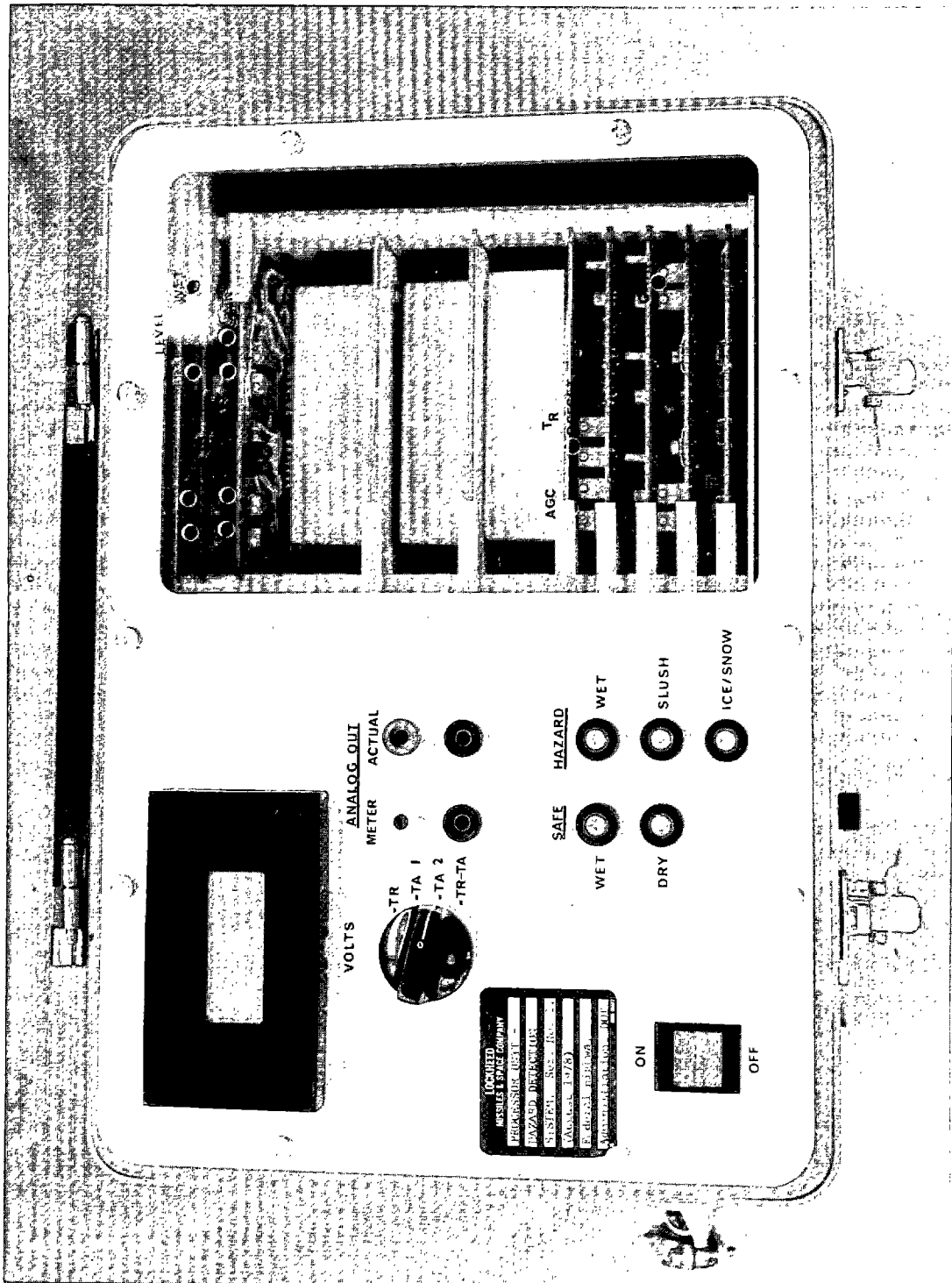


FIGURE 49. PROCESSOR UNIT, TOP VIEW (PHOTO)

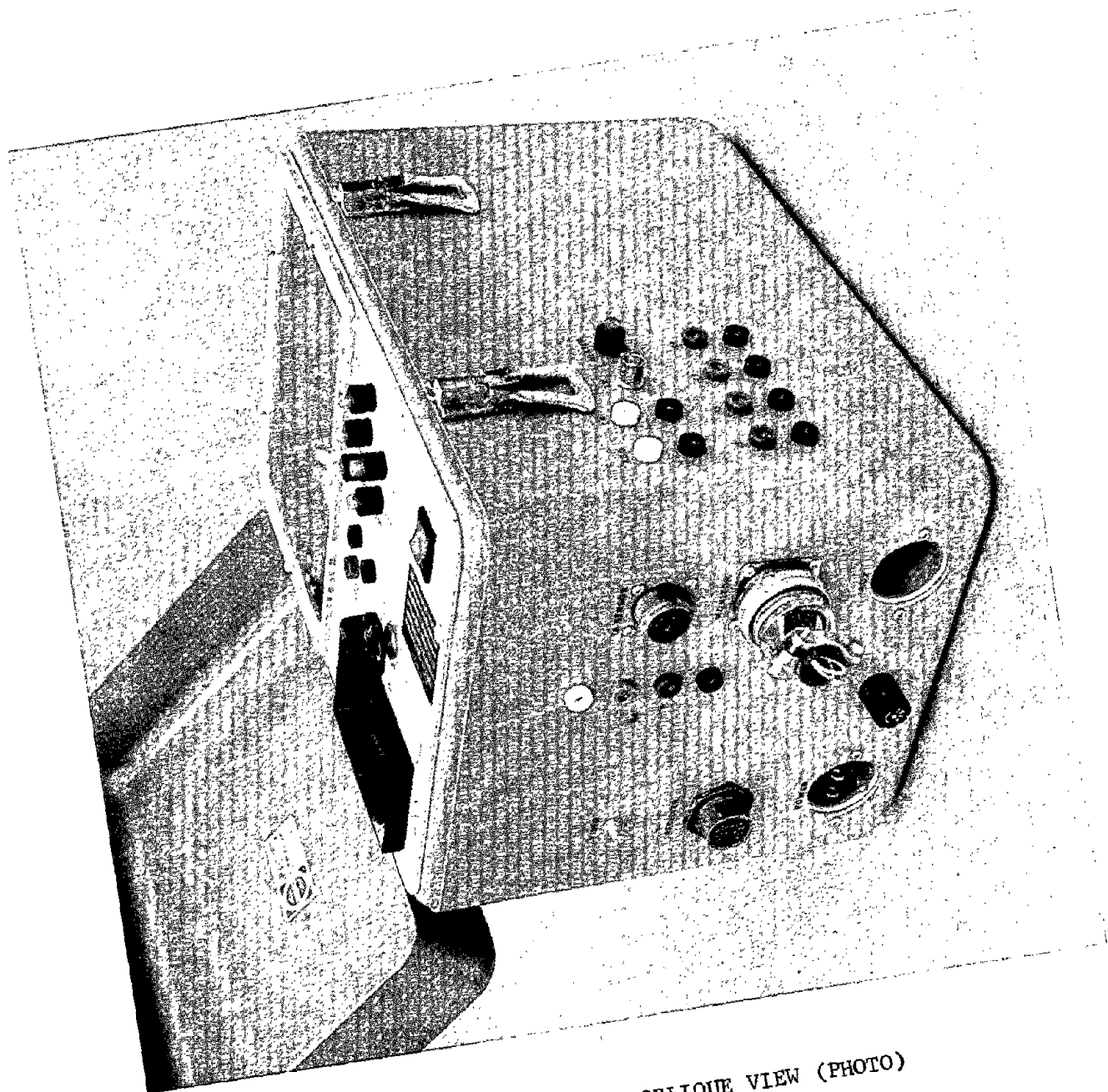


FIGURE 50. PROCESSOR UNIT, OBLIQUE VIEW (PHOTO)

6.2.1 Receiver and Horn Antenna

- o Size - Receiver electronic components are housed in a 12 x 13 x 4.5 inch (30 x 33 x 11.4 cm) aluminum box, with the horn antenna protruding from one end approximately 10 inches (25.4 cm). Maximum aperture dimensions of the horn antenna are 6 x 8 inches (15.2 x 20.3 cm). Overall minimum clearance requirement for the combined receiver/horn antenna unit is 23 x 12 x 8 inches (58 x 30 x 20 cm).
- o Weight - Weight of the combined receiver/antenna unit is 11.25 lbs (5.1 Kg).
- o Power - The receiver unit requires +15 VDC, -15 VDC and 24 VAC power for proper operation. These voltages are supplied by the processor unit through the interconnect cable. Total power requirement of the system, as noted in Section 6.1, is 115 VAC @ 0.5 amp.
- o Environmental Restrictions - The receiver/antenna unit is designed to be weather-proof to the extent that operation in an outdoor environment during a Winter season is feasible without any additional protection when the unit is mounted in its normal operating position (antenna pointing down, $\pm 30^{\circ}$ from normal incidence). The unit was not designed with any provision for shock and vibration resistance, although normal handling or shipping of the unit should not damage it in any way as long as reasonable care is observed. The unit is not waterproof to the extent that immersion is possible without causing damage to the unit. Power and signal interconnection is provided through a single, environmentally resistant connector.

6.2.2 Processor Electronics

- o Size - The combined processor and alarm circuitry is contained in an aluminum carrying case which measures 9 x 13 x 11 inches (23 x 33 x 28 cm) and has a hinged cover. All operating controls are mounted on a panel which is accessible when this cover is open.
- o Weight - Weight of the processor unit is 17.40 lbs (7.9 Kg).
- o Power - The processor electronics unit requires 115 VAC power input @ 0.5 amp. All D.C. power supplies required by the receiver and processor circuits are contained within the processor unit.

- o Environmental Restrictions - Although the carrying case cover is gasket sealed, no provision for weather proofing is provided. The unit should be protected from severe environments during all periods of operation.

6.2.3 Surface Temperature Sensing Unit

- o Size - The temperature sensing unit is mounted on a small aluminum heat sink and encapsulated in epoxy with high thermal transfer characteristics. Total size of the unit is approximately 1 cubic inch (16.4 cubic cm). A 100 ft (30 m) cable is attached to the unit with the cable termination embedded within the epoxy.
- o Weight - Weight of the sensing element is estimated at less than 100 grams.
- o Power - The temperature sensor is powered by +15 VDC which is supplied through a current limiting resistor from the processor unit. Total power required by the unit is approximately 10 ma.
- o Environmental Restrictions - The temperature sensor is intended to be embedded in a roadway surface. No temperature or weather restrictions are imposed, but reasonable handling precautions are recommended to preclude the possibility of cracking the epoxy material.

6.3 OPERATING INSTRUCTIONS

The radiometric hazard detection system is designed for hands-off, continuous operation. To this extent, operation of the system is controlled by the single On-Off switch located at the processor electronics unit. To insure proper operation of the unit after turn-on, the following calibration and alarm circuit set-up procedures should be followed.

6.3.1 System Turn-On

- 1) Set system power On-Off switch to ON.

NOTE: Allow approximately 15 minutes warmup time.

- 2) Using a Digital Voltmeter, verify proper operation by measuring the following test points to assure that voltages are within the limits indicated.

<u>Test Point</u>	<u>Minimum</u>	<u>Maximum</u>
+5 VDC	+4.8 VDC	+5.2 VDC
+15 VDC	+14.8 VDC	+15.2 VDC
-15 VDC	-14.8 VDC	-15.2 VDC
+28 VDC	+27.5 VDC	+28.5 VDC
28 VAC (Jacks)	27.0 VAC	29.0 VAC
A.G.C.	0.0 VDC	-0.6 VDC
T_R	0.0 VDC	+6.0 VDC
T	+2.55 VDC	+3.02 VDC

All D.C. measurements are with respect to D.C. power return.

NOTE: (a) T_R maximum value can range up to +6.5 VDC (varies with ambient; e.g., +6.5 VDC = 325°K = 52°C = 126°F).

(b) T values shown are for 0 to 85°F (-18 to 29°C; 255 to 302°K) representing temperature sensor output of 10 mv/°K.

6.3.2 System Calibration

The following system calibration procedure was developed during breadboard testing and has proven to be adequate for the prototype system.

- 1) Direct radiometer horn antenna toward the sky at zenith. Adjust "Offset Adjust", for an output of 10°K (0.200 VDC), as indicated at processor T_R output jack.
- 2) Measure temperature of microwave absorber material and convert to °K (e.g., absorber temperature = 68°F; 68°F = 20°C + 273° = 293°K). Adjust "Gain Adjust", for the calculated absorber temperature (293°K or 5.860 VDC).

NOTE: During steps 1) and 2), verify that the A.G.C. voltage reads between -0.1 and -0.2 VDC (only applicable for ambient temperatures between 60 and 85°F [16 and 29°C]). Use "A.G.C. Adjust" control to set voltage within this range.

- 3) The gain and offset adjustments interact with each other, so that Steps 1) and 2) need to be repeated until no further adjustments are required; three sets of adjustments will generally provide this condition.

Periodic calibration checks will probably be required at an interval which will be determined during evaluation testing.

6.3.3 Alarm Circuit Adjustments

The alarm circuit will require the following preliminary adjustments:

- 1) Perform system turn-on and calibration procedures.
- 2) T_A Scaling - Set T_A Gain Adjust so that T_A and T_R outputs are equal within ± 0.01 VDC.

NOTE: It is preferable to make this adjustment while roadway surface temperature is approximately 32^oF (0^oC).

- 3) Emissivity Calculation - Measure roadway surface temperature directly in ^oK at T_A input jacks (Blue Jack (-) and Red Jack (+) on connector side of processor). Measure T_R at T_R output jack and convert to ^oK by dividing T_R value by 0.02. Compute approximate emissivity (ϵ) by solving the following equation:

$$\epsilon = \frac{T_R}{T_A}$$

- 4) Freeze Disable Adjust - Set Meter Switch to position T_A1. Set T_A Gain Adjust for a T_A output of 5.50 $\epsilon \pm 0.01$ VDC where ϵ is as obtained in Step 3. Adjust Freeze Disable until LED indicator D2 changes state.
- 5) Freeze Enable Adjust - Set T_A Gain Adjust for a T_A output of 5.48 $\epsilon \pm 0.01$ VDC. Adjust Freeze Enable until LED indicator D1 changes state.
- 6) Set T_A Gain Adjust for a T_A output of 5.40 $\epsilon \pm 0.01$ VDC.
- 7) Remove Shorting Plug from Monitor Connector. Connect a variable 0 to 5 VDC source to T_R jacks on front of processor.
- 8) Freeze Level Adjust - Set Meter Switch to T_R-T_A position. Set T_R input voltage for a T_R-T_A output of +0.04 ± 0.01 VDC. Adjust Freeze Level until Ice indicator changes state.
- 9) Reduce T_R input until T_R-T_A output is 0 ± 0.01 VDC.
- 10) Slush Upper Limit Adjust - Adjust Slush Upper Limit until slush indicator changes state.
- 11) Reduce T_R input until T_R-T_A output is -1.00 ± 0.05 VDC.

- 12) Slush Lower Limit Adjust - Adjust Slush Lower Limit until slush indicator changes state.
- 13) Adjust T_R input until T_R output equals 3.80 ± 0.05 VDC.
- 14) Wet Limit Adjust - Adjust Wet Limit until Wet (HAZARD) indicator changes state.
- 15) Remove variable voltage source and reconnect Shorting Plug to Monitor Connector.
- 16) Reset T_A Gain Adjust as in Step 2).

A comparison with the Hazard Logic Table (Table 11, described in Section 4.3.1.1) indicates that the T_R-T_A setting for ice or snow hazard was +0.10 rather than +0.04 VDC as in Step 8) above. This new setting tightens the dead band between ice and slush. Similarly, the Table 11 T_R-T_A setting for slush hazard was -0.80 rather than -1.00 VDC as in Step 11) above. This setting eliminates any dead band between wet and slush. The net result of these revised settings is to assure that an alarm display indicator will always be activated.

6.4 SUGGESTIONS FOR LOCATION AND TEST/EVALUATION PROCEDURES

6.4.1 Location

Evaluation of the prototype radiometer equipment will necessarily require that it be located in an area which experiences a high percentage of winter days with temperatures below freezing. Until such a time as a more sophisticated roadway surface simulator is available (see Section 8.3), evaluation testing will then be limited to approximately a 3 or 4 month period each year. Many areas of the Continental United States meet these required conditions each year, but are not necessarily suitable because they are not near enough to the evaluation team.

For an evaluation effort based in the San Francisco Bay Area, the most logical choice for an evaluation site would be the Sierra Nevada Mountain area near Truckee, California. The minimum daily temperature average for the five month period of November through March is less than 20°F (-7°C). There are many potential sites available with relatively good winter access. A major Interstate Highway (I-80) goes through the area, providing an easy four hour drive from the Bay Area.

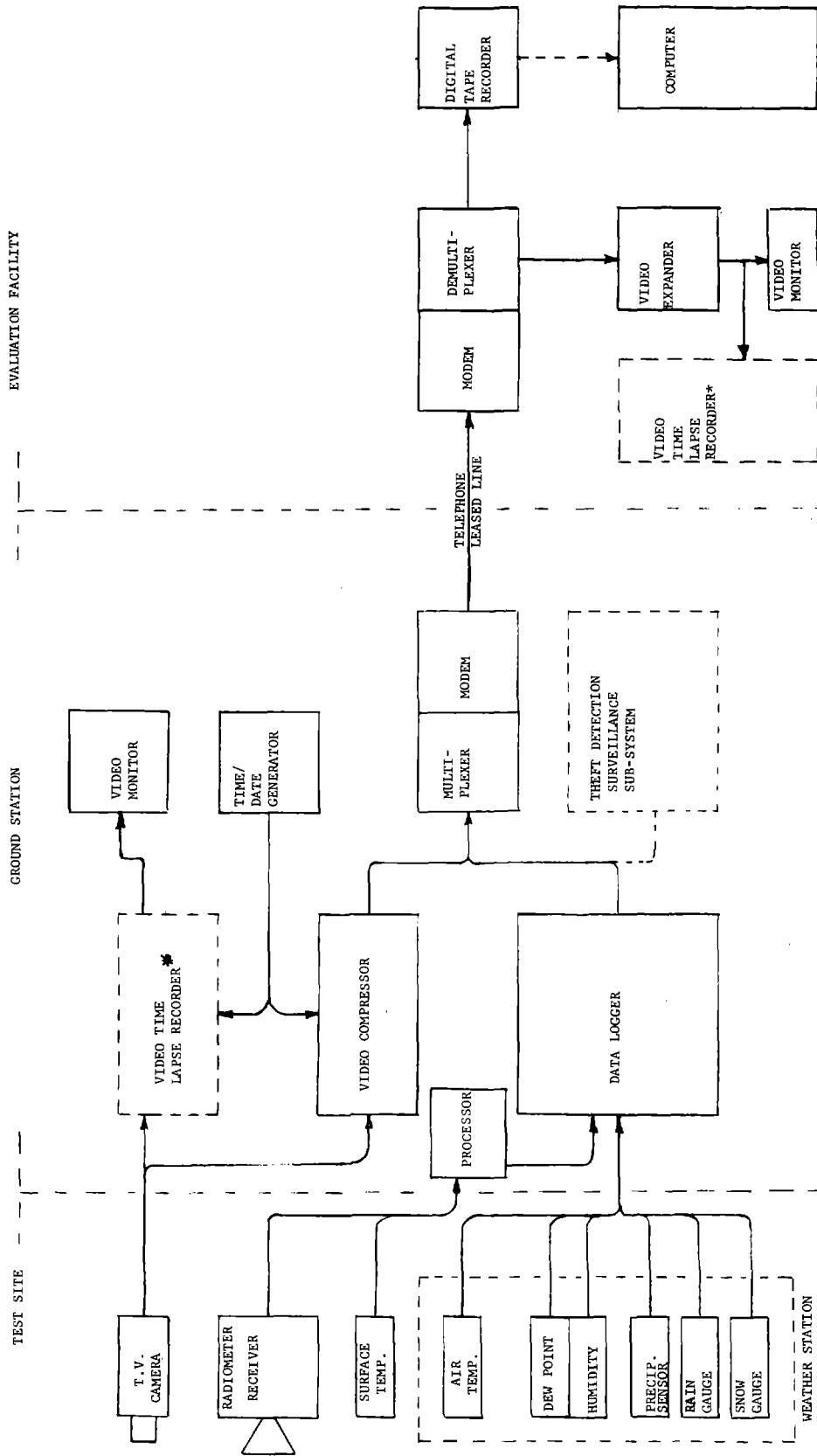
The California Department of Transportation (CALTRANS) maintains a vigorous snow removal program along the route. Many secondary roads are available within close proximity to the City of Truckee.

6.4.2 Test/Evaluation Procedures

The radiometer receiver unit is the only equipment which needs to be mounted above the road surface. The mounting height is not critical, but some thought must be given to desired minimum detection area. A mounting height of 20 ft (6 meters) was used in earlier analytical calculations and this is probably a good mounting height for test and evaluation purposes. These analyses indicate that a 20 ft (6 m) height and a 70% beamfill condition ($\theta = 8^\circ$) would correspond to a detection area of about 25 ft² (7.6 m²). The radiometer receiver does not have to be mounted over the road surface but may be mounted to one side of the roadway and look into the area at an angle of up to 20° off vertical, thus eliminating the need for clearance by larger vehicles.

Power and control signals to the Receiver Unit are delivered via a 100 ft (30 m) cable. The maximum voltage at the receiver is 28 VDC. This cable also carries 28 VAC heater voltage to the receiver. Received video is carried over a 100 ft (30 m) coaxial cable from the receiver to the processor. Surface temperature data will also be on a 100 ft (30 m) cable which connects to the Processor Unit. The processor will then have to be located within the 100 ft distance from the Receiver Unit. A small rental trailer is recommended as a housing for the processor and data collection equipment.

Data monitoring and collection equipment may be configured in many ways. One recommended approach is to use the ground station method discussed under Advanced Surface Simulator, Section 8.3. In essence, the incoming data (including television monitoring of the road surface) would be digitized, multiplexed and transmitted via telephone leased line to the evaluation facility. Evaluation data could then be processed on a daily basis with the use of computers which are located at the facility thus eliminating the time lag involved in collecting data and returning to the facility. This would eliminate the need for trips to the test site for data collection and, at the same time, provide a 24 hour a day monitoring capability. Figure 49 illustrates this concept.



*NOTE: VIDEO TIME LAPSE RECORDER MAY BE USED IN GROUND STATION OR EVALUATION FACILITY.

FIGURE 51. TEST DATA COLLECTION BLOCK DIAGRAM

Section 7.0

CONCLUSIONS

7.1 EVALUATION OF EQUIPMENT PERFORMANCE

7.1.1 Breadboard Radiometer Performance

The breadboard unit, as noted in Section 4.1, exhibited a drift of T_R output with ambient temperature change. The effect of this drift was minimized by allowing a warm-up time permitting the internal receiver to stabilize. Where this warm-up was not feasible, a known correction factor was applied to the raw measurement data.

The breadboard radiometer receiver and processor unit performed very well throughout the entire test program. The single failure which occurred was caused by water entering the electrical connector on the receiver during a snow storm on Field Trip 1. No provision had been made on the breadboard to prevent this from happening, so the unit was waterproofed prior to Field Trip 2 by adding plastic sheeting around the receiver. The system was operated for a total of about 200 hours during the 3-month test program, a contract Phase II activity.

At one time the receiver unit was inadvertently dropped from a height of 5 feet, landing on the attached horn antenna. The receiver was reinstalled on its mounting post and the test was continued with no required adjustments or other corrective action. The processor unit, which has no thermal insulation, was operated at a temperature of -5°C during Field Trip 2 with no degradation of performance. Considering that the test unit was only a breadboard and was not packaged with any particular environment in mind, results were excellent.

7.1.2 Prototype Radiometer Performance

Appropriate breadboard design modifications were made for the fabrication of the prototype system. These changes were detailed in Section 5.1 and relate primarily to obtaining the required receiver thermal stability and to providing more rugged and more weatherproof antenna/receiver and processor/alarm circuit packages.

From a thermal stability standpoint, the test results on the prototype, as described in Section 5.1.4, indicate that receiver parameter changes will not result in radiometric temperature output variations exceeding $\pm 2^{\circ}\text{K}$ over a Receiver Unit ambient temperature range of 0 to 85°F (-18 to 29°C), or greater.

The packaging techniques applied to both the Receiver Unit and the Processor Unit, illustrated in the photographs of Figures 48, 49 and 50, resulted in a weather-resistant, rugged prototype system far superior to the environmental capability of the breadboard system.

7.2 COMPARISON WITH DEVELOPMENT OBJECTIVES

The breadboard radiometer, in combination with the alarm unit described in Section 4.3, met the proposed road hazard detection objectives for dry or wet snow, freezing rain (0.1 cm thin ice layer), thicker ice layers, and slush. No opportunity was presented for measurement of hail. The radiometer detector system did not respond to a frost condition; however, the addition of a dew point sensor may also provide a frost alarm capability. A technique and approach to a frost alarm circuit are described in Section 8.5, Advanced Alarm Logic.

Although no specific vehicle traffic tests were run on this program, the hazard alarm circuit of the delivered model will be affected by passing vehicles within the antenna field of view. (See Sections 3.1.2, Detection Performance, and 3.3.2, Description of Analytical Reports). Addition of more sophisticated alarm logic (e.g., based on time delays or rates of change of temperature) would minimize vehicle effects.

Most of the other stated specific requirements noted in Section 2.1 have been met. However the road surface temperature sensor used for successful operation of the hazard alarm circuits may be harmed by snowplowing operations, chains, or heavy trucks if not suitably embedded in the road deck. No harmful effects on the system are anticipated through the use of de-icing chemicals. The system, being passive, will not create any hazard to drivers or pedestrians through radiation or use of distracting visible light beams. Based on reliability analysis and design improvements incorporated in the prototype system, the latter equipment is expected to provide 24 hours per day operation over the 9 coldest months of the year independent of seasonal or diurnal sun effects.

Although the prototype radiometer was not tested on actual ice-covered simulator or road surfaces, the alarm circuit portion of the Processor Unit was checked using simulated inputs to verify proper operation. In these tests, all display indicators corresponding to the various Safe and Hazard conditions (i.e., dry; wet; ice or snow; slush) functioned as anticipated. Dead bands between respective conditions were adjusted to assure that each detected condition corresponded to activation of a unique indicator.

Section 8.0

RECOMMENDATIONS

This concluding section of the Final Report presents a number of additional development and study tasks recommended for consideration by the Office of Research of the Federal Highway Administration. Based on the experience and findings to date on the Area Detectors for Snow and Ice contract, these proposed projects are believed to be logical and potentially fruitful extensions of work accomplished to date. The sections below are not presented in any particular order of preference; however, as indicated within the brief descriptions noted, some proposed projects are dependent upon others.

8.1 EVALUATION OF PROTOTYPE RADIOMETER SYSTEM

8.1.1 Objectives

An evaluation of the prototype system should address the following primary objectives:

- o Radiometer Performance Reliability - Evaluate radiometer operating performance over a long, continuous period to insure acceptable reliability of the entire system. It would be desirable to perform some long term "burn-in" prior to actual field installation. This would overcome the inherent infant mortality rate of the commercial components used in the prototype system. The operational "burn-in" period should include a temperature cycling period of approximately 2 weeks to reduce possible failures due to temperature shock during test site operation. Further long term performance would be evaluated during longer term test site operation.
- o False Alarm/Missed Alarm Rates - Perform a long duration field site test in a severe environment. A four month, continuous test should be adequate to provide a preliminary data base for determination of false alarm/missed alarm rates. This test should be conducted on a 24-hour per day basis so that all hazard events occurring within the radiometer field of view will be covered. Visual verification of road surface conditions will be necessary on a 24-hour basis and may best be implemented through the use of slow-scan and time lapse video recording techniques. It would also be desirable to have a minimum time lag of 24 hours between data collections. This would allow a relatively continuous update of radiometric and environmental data from the test site and reduce the time to detect any failure which may occur.

As a secondary objective of the evaluation program, driver response to a hazard warning sign could be evaluated. This, however, would be instituted after a reasonable determination of false alarm/missed alarm rates has been established. Since some previous effort has been expended toward this goal by another contractor, this objective is secondary in nature in the evaluation of a radiometric approach to snow and ice detection. Previous results show that drivers respond favorably to a hazard warning sign, although the statistical data base for this determination was limited. Some extra cost would be incurred to achieve this goal, which should be traded off against value received from implementation of this test.

8.1.2 Approach

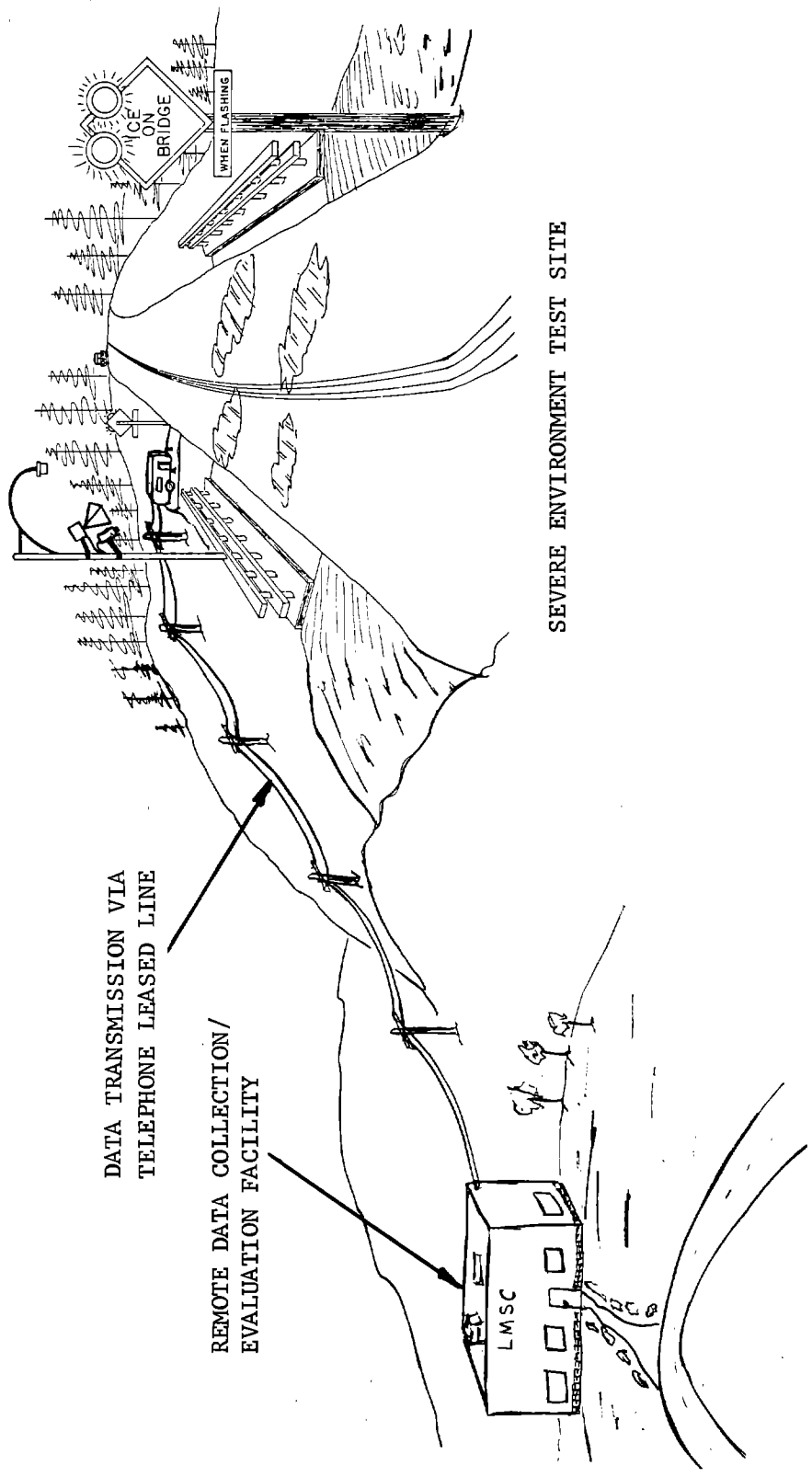
The Lockheed approach to the prototype evaluation program is illustrated in Figure 50. Environmental, radiometric, and video data would be collected and digitized at the test site. The data would then be multiplexed and transmitted via telephone leased line to the evaluation facility on a 24-hour continuous basis. The evaluation facility would have the necessary, demultiplexing, digital and video recording, and computer data reduction equipment available to perform a continuously updated evaluation program. The need for an on-site observer would be eliminated and only periodic visits to the test site by an evaluation team member would be necessary. A further discussion of this approach is included under the ground station description in Section 8.3.2, part of the recommended Advanced Surface Simulator.

8.2 SINGLE AXIS AND 2-AXIS SCANNING ANTENNAS

8.2.1 General Comments

Radiometric techniques for detecting hazardous roadway conditions represent a quantum jump over the previous detection methods in terms of area of coverage. Previous detection methods could only evaluate conditions present at one small spot (on the order of 2 inches (5.1 cm) or less diameter), and were inherently unreliable for various reasons. The radiometric approach to hazardous condition detection expands the area of coverage to a spot size of 4 or more feet (1.2 m) diameter, dependent upon the tradeoffs of mounting height and antenna aperture size. The reliability problem is also overcome by above surface mounting of the sensor unit, with the exception of the surface temperature sensing element which may be embedded sufficiently deep to not be affected by chains, snow plowing, etc.

A further increase in area of coverage would be realized by implementation of either single or 2-axis scanning techniques. As an example, a radiometer with antenna aperture of 12° , mounted at a height of 20 ft (6 meters) in a stationary configuration with normal



SEVERE ENVIRONMENT TEST SITE

DATA TRANSMISSION VIA
TELEPHONE LEASED LINE

REMOTE DATA COLLECTION/
EVALUATION FACILITY

FIGURE 52. PROTOTYPE EVALUATION CONTINUOUS MONITOR APPROACH

incidence angle would have a field of view of 14 ft^2 (4.27 m^2). By adding a single axis scanning mechanization scanning $\pm 30^\circ$, the area of coverage would be increased approximately 7 times, to approximately 100 ft^2 (30 m^2). Two-axis scanning of $\pm 30^\circ$ each axis would increase the total area of coverage to 38 times the stationary mounting or an area of coverage of 530 ft^2 (161 m^2). Mounting at heights greater than 20 ft (6 m) would provide proportionately larger coverage areas. A simplified case of rectangular scan coverage was used in the above example, as shown in Figure 51.

8.2.2 Proposed Tasks

Mechanization of a single axis scanning system appears relatively easy, requiring a single pivot axis, with a corresponding antenna position pick off (either a digital encoder or analog potentiometer might be used, depending upon alarm circuit interface requirements). This development should be combined with the Advanced Alarm Logic development of Section 8.5, because of a probable requirement for memory capability.

A 2-axis system is not much more complex than the single axis system. However, any increase in area of coverage by this method will necessitate some advanced methods of detection and alarm logic. An approach to development of this logic is given in Section 8.6, which describes the application of map-matching techniques.

It is recommended that both the single axis and the 2-axis scanners be developed if the map-matching study effort is implemented. If this effort (described in Section 8.6) is not initiated, it is recommended that only a single axis scanner be developed.

8.3 ADVANCED SURFACE SIMULATOR

The simulators which were constructed during Phase II of the Area Detectors for Snow and Ice program proved adequate for testing the feasibility of using a radiometric approach to detection of hazard conditions. These low cost, simple simulators would not be satisfactory for more advanced testing and evaluation of radiometric sensors and alarm circuits. Details on a recommended alternate are provided below.

8.3.1 Capability

A new roadway surface simulator facility could be constructed to provide the following capabilities:

- o Long Term Testing - The present simulators provide a short term test capability: up to 4 hours test duration. The new simulator should have the capability of performing continuous

Area of Coverage

Single Axis $A = 2D \times 2r$
 $= 2 (h \tan \phi) \times 2 \left(\sin \alpha \frac{h}{\cos \alpha} \right)$

2-AXIS $A = (2D)^2$
 $= [2 (h \tan \phi)]^2$

- h = Radiometer Mounting Height
- ϕ = Scan Angle = 30°
- $\alpha = 6^\circ$ ($\frac{1}{2}$ ant. beamwidth)
- r = Radius of F.O.V. = $\sin \alpha \left(\frac{h}{\cos \alpha} \right)$
- $D = \frac{1}{2}$ Scan Distance = $h \tan \phi$

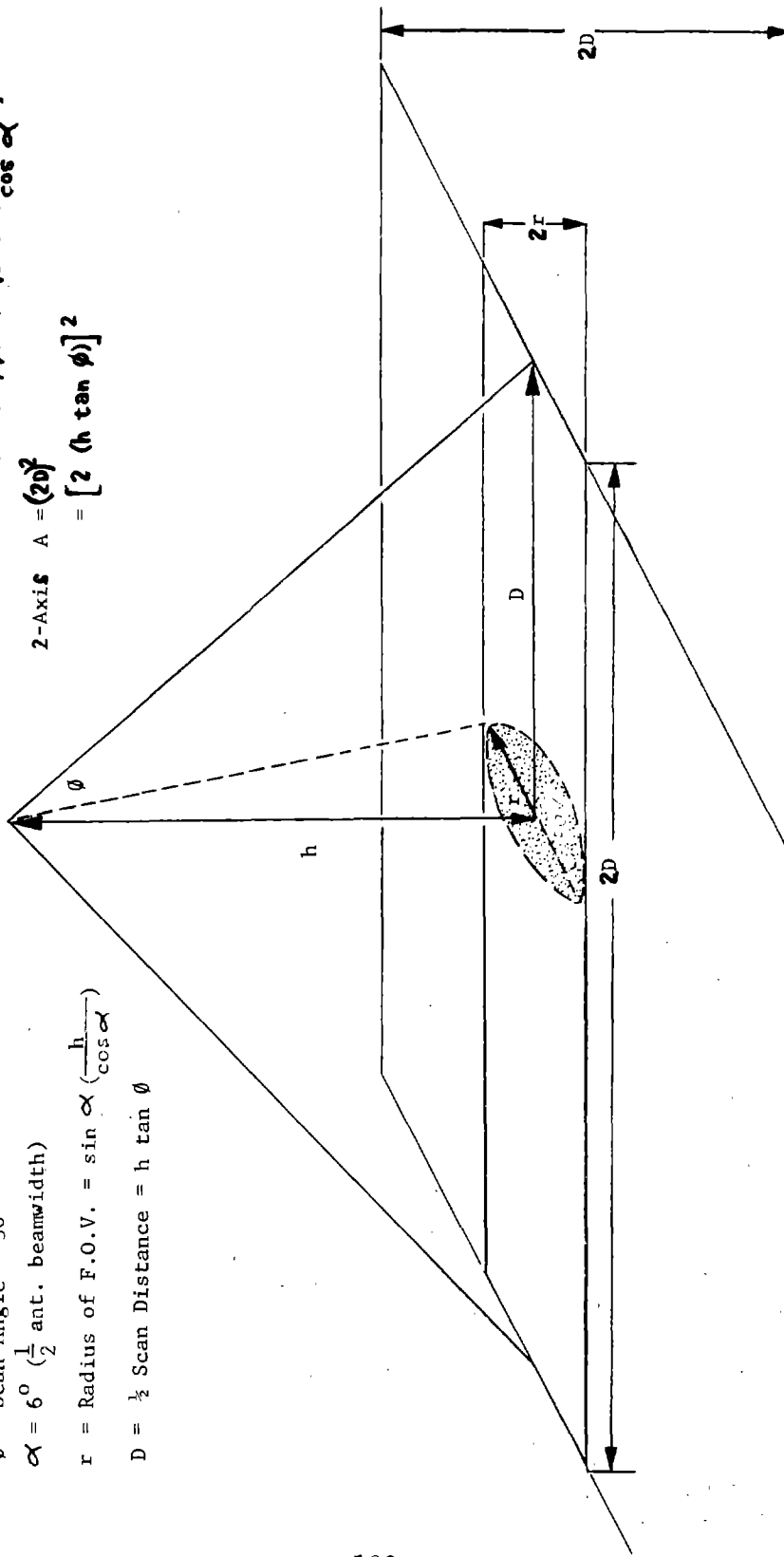


FIGURE 53. SAMPLE SCAN COVERAGE PATTERN

testing for up to one week or greater duration. Detailed evaluation of equipment stability (including ambient temperature and diurnal sun position) could then be performed under laboratory-controlled conditions.

- o Multi-Seasonal Use - Evaluation and testing during actual environmental conditions is now limited to the 3 or 4 month winter season each year. A new simulator facility would allow testing on a year-round basis, thus permitting continuous collection of data over a longer term evaluation period.
- o Automated Environmental Control - Roadway surface and ambient temperature conditions should be automated to the extent that simulated conditions will reflect actual cold season diurnal conditions.
- o Simulator Sizing - The simulator should be large enough to represent one lane of a bridge surface at an appropriate radiometer receiver mounting height and accommodate a future antenna scanning system of $\pm 30^\circ$ along the simulated lane.
- o Automatic Data Acquisition - The data collection system should be automated and formatted such that a computer can be used for data reduction and comparison. Time lapse video tape techniques should be incorporated to provide a visual record of surface conditions throughout any long term testing.

8.3.2 Approach

A roadway surface of appropriate size, e.g. 8 x 20 ft. (2.4 x 6.1 m), would be enclosed in a microwave transparent structure 25 ft. (7.6 m) in height. The roadway surface would be constructed of material similar to that used in actual road surfaces (e.g., asphalt or concrete). A wood frame enclosure covered with a microwave transparent material (polystyrene foam) would enclose the simulator surface and act as an environmental chamber allowing simulated ambient temperatures of -10°C to be reached. The simulator and enclosure temperatures would be individually controlled by two separate commercial refrigeration units with time vs. temperature programming controls. An automated, time-controlled sprinkler system would provide the necessary precipitation to create icy surface conditions. Frost conditions would be simulated by lowering the roadway surface temperature to some point below the dewpoint (also below freezing) within the enclosure.

The enclosure would be instrumented with the following:

- Various Temperature Sensors
- Dewpoint Sensor
- Humidity Sensor
- T.V. Camera

A ground station for data acquisition would contain the necessary equipment for recording the environmental and visual (T.V.) data. This equipment would be:

- Data Logger (with RS 232C interface)
- Digital Recorder
- Time Lapse Video Recorder
- Video Monitor
- Video Time/Date Generator

The ground station would be a self-contained unit capable of being moved to remote locations during the winter season.

Data reduction would be accomplished by playing the digitized data cassette into a computer which would provide time vs. data plots for comparison to the time lapse video recorder information reflecting actual roadway surface conditions. Computer comparisons could be accomplished to develop statistical data pertaining to false alarm/missed alarm rates for varying hazard conditions.

A slow-scan video transmission system would allow data transmission from remote site locations to the data reduction terminal during winter season operations.

8.4 SELF-TEST TECHNIQUES

8.4.1 Proposed Self-Test Modifications

For a 100% confidence test, a two-step test is proposed: (1) a reference radiometric source is measured by the system; and (2) a simulated alarm condition is injected into the processor circuitry. The first step tests the radiometer sensor, and the second step tests the alarm circuitry. The sequence of events that would occur is as follows:

- a) A timer initiates the self-test sequence at a predetermined interval based on performance reliability experience.
- b) A motor drive points the sensor system towards the zenith providing the sky temperature as a reference source.*

*This reading should obviate the need for an additional ambient temperature measurement since a shift in the latter is expected to equal the shift in sky temperature. If experience indicates that an ambient reading is required, the sensor could also be pointed at the (unobstructed) horizon for this purpose.

- c) The monitor circuits compare the radiometer sensor reading against a preset reference value on a go-no go basis. Alternatively, through the use of microprocessor logic (see 8.5), readings out of tolerance limits could be automatically corrected.
- d) Next, a simulated alarm condition is injected at the input of the alarm circuitry.
- e) Monitor circuits then verify alarm activation.

The simulated alarm test will be of short duration, approximately one second, in order to differentiate an actual alarm from this simulated test. Two additional monitors which are to function continuously will monitor: (1) the AGC voltage; and (2) the +28, +15, -15 and +5 VDC power supplies. When a failure condition is sensed by any of the monitoring circuits, a failure alarm is generated. This failure alarm would be in the form of a 0 VDC output (ground) permitting the monitoring of all anticipated failure modes including line power failures.

The failure alarm circuitry as described here will identify a system failure. Further fault isolation will be performed manually via a test connector with test points at the signal processor in order to isolate the failure to the following areas: (1) receiver failure; (2) power supply failure; (3) alarm circuit failure; and (4) sensor processor failure. It is recommended that these modifications be incorporated in the Phase III radiometer system.

8.4.2 Alternate Self-Test Methods

An alternative self-test method, providing a 90% confidence test, would inject the reference radiometric temperature through a microwave switch installed between the antenna and the directional coupler, leaving the alarm test and continuous monitor circuits the same as previously described. The advantage of this method is the elimination of the motorized drive system, which would increase reliability and decrease maintenance requirements. This method does not test the antenna radome system; this is a small risk area since antenna radomes are passive components with very few failure modes.

A minimal self-test method, providing for an 80% confidence level, is by the use of the two continuously monitoring circuits of the AGC and power supply lines and an additional radiometric temperature limits monitor.

8.5 ADVANCED ALARM LOGIC

8.5.1 Microprocessor Implementation

The present alarm logic discussed in Section 4.3 is based on analog signal comparisons. Any additions or changes to the basic alarm circuits will necessitate an actual hardware configuration change. By employing a single chip microprocessor and associated digital circuitry, as shown in Figure 52, the need for hardware changes and/or adjustments will be eliminated. The alarm circuit may be simply reprogrammed through the digital tape interface. A further advantage would be realized from such a system in that the microprocessor approach would:

- o Have memory capability for past events (e.g., temperatures are dropping or rising).
- o Perform data linearization and comparisons.
- o Handle more data from different sources and perform averaging operations.
- o Operate with algorithms and perform math functions.
- o Calculate second and third order derivatives (useful for determining the rate of change of T_R as water changes state from liquid to solid or as a vehicle crosses monitor area).

Development of such a unit would necessitate large quantities of statistical data from the evaluation tests so that the most accurate decisions could be made, virtually eliminating false alarms and missed alarms. Hazard/Safe decisions could be based on the additional knowledge of time of day, air temperature rising/falling, surface temperature rising/falling, dewpoint rising/falling, slope and rate of change of T_R , as well as the basic real time environmental inputs.

After initial development, during which many program changes will probably be made, the digital tape interface would be replaced with a ROM (Read Only Memory) for programming purposes. Any future changes would then be handled by simply changing the program ROM.

The Advanced Alarm Logic circuit would be packaged on a single 4.5 x 4.5 inch (11.4 x 11.4 cm) card and would cut the parts count by a factor of 20. The microprocessor chip costs are in the \$50 price range today with future prices sure to decrease, thereby allowing cheaper production costs.

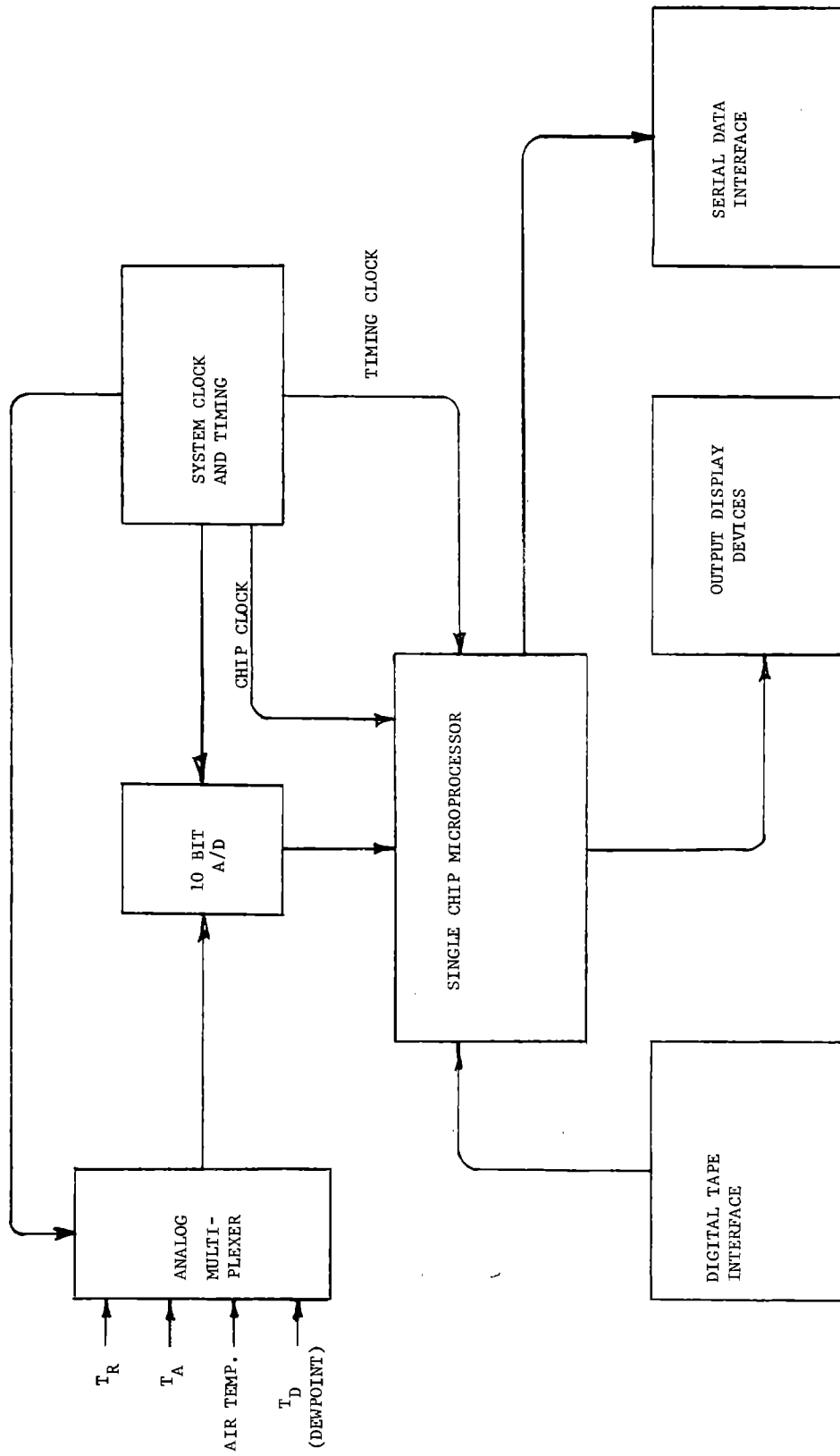


FIGURE 54. ADVANCED ALARM LOGIC BLOCK DIAGRAM

8.5.2 Frost Alarm Circuit

As previously discussed in Section 4.1, the radiometer and associated alarm circuitry does not have adequate sensitivity for the reliable detection of frost. However, the formation of frost on a bridge deck surface will occur when a very specific set of environmental conditions exists. These conditions are:

- o Dewpoint temperature higher than the bridge deck surface temperature.
- o Bridge deck surface temperature less than freezing (0°C).

Since bridge deck surface temperature is presently available in the prototype alarm circuit, the simple addition of dewpoint data is the only additional information required to produce an alarm for a frost hazard. Such a dewpoint sensor is presently marketed by Weather Measure Corporation of Sacramento, California for approximately \$300.

In addition to a dewpoint sensor, the prototype alarm circuit will need some modification and additions to condition the dewpoint signal and to detect the difference between dewpoint and surface temperature. Figure 53 is a block diagram of the additional required circuitry.

8.6 "MAP MATCHING" TECHNIQUES FOR DETECTION/DISCRIMINATION OF HAZARDS

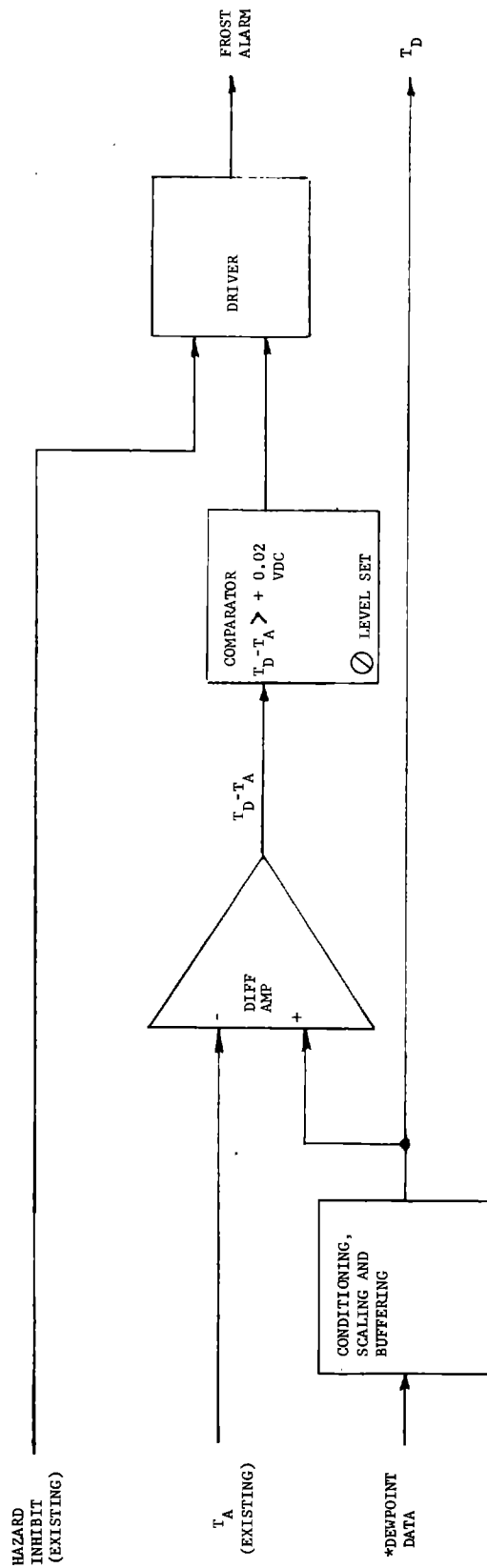
8.6.1 Background

During the period 1969 to the present time, Lockheed has performed tasks on a series of Air Force (AF) contracts in the area of microwave radiometric area correlation guidance. These contracts were for the Avionics Laboratory at Wright-Patterson Air Force Base and, most recently, the Armament Development Test Center at Eglin Air Force Base. Effort involved study, analysis, hardware development, and captive flight test phases.

Key activities during several of these programs were derivation of a probabilistic correlation model and analysis of the experimentally derived relationship between references and both real and simulated sensed maps with various scene characteristics affecting the correlation process. Computer simulation techniques were developed and refined to optimize algorithms used in related tradeoff studies.

8.6.2 Approach

It is proposed that the extensive experience gained on the contracts noted above be applied to the hazard detection problem utilizing a passive microwave radiometric sensor. In this case, map differences for sample hazardous conditions will be established with reference to



*FROM DEWPOINT SENSOR MOD. H361-DPYA
 WEATHER MEASURE CORP.
 SACRAMENTO, CALIFORNIA

FIGURE 55. DEWPOINT ALARM BLOCK DIAGRAM

maps of known non-hazardous conditions; this is in contrast to the map matching objectives in the area correlation guidance scheme. It is expected that similar correlation and processing methods can be applied.

A typical study and preliminary design program would comprise the sequence of tasks as described below. Use of an available 2-axis scanning antenna system is assumed, developed per the recommended program described in Section 8.2 (Single Axis and 2-Axis Scanning Antennas).

- o Data Collection - Hazardous and non-hazardous radiometric measurements will be collected under field conditions or using the advanced laboratory simulator (see Section 8.3) with the resultant data recorded on magnetic tape in a form suitable for digital formatting into 2-dimensional maps. These maps represent the antenna scanning both across and along a roadway lane. The recorded data will consist of a time history of the radiometer analog output and a corresponding time history of the antenna pointing coordinates. Ground truth information of environmental conditions will be documented.
- o Data Reduction - The recorded data will be reduced and formatted into two-dimensional digital array maps of the scanned area. Existing computer programs can be utilized for this purpose with only minor modifications incorporated to reflect specific needs.
- o Map Experimentation - In this task, difference array signatures would be generated by normalizing (removing map mean) both hazard and non-hazard maps and computing a point-by-point difference between the normalized maps. Data printouts and plots will be generated to aid in the analysis of the difference arrays. Map characteristics would be identified in terms of providing best success in a digital hazard detector.
- o Alarm Logic - Based on the findings of the Map Experimentation task, one or more logic concepts will be developed and tested through computer simulation experiments to determine their suitability for hazard detection. The most promising approach will be selected and refined.
- o Application - Finally, the selected logic concept will be applied to the collected map data, including variations of interest, to derive data from which resultant false alarm and missed alarm probabilities and rates can be determined.

No hardware is anticipated; final program output is the description of a map-making scheme and preliminary design of a hazard detection circuit for use with the prototype radiometer modified to include a 2-axis antenna scanner.

8.7 ANALYSIS OF MULTILAYER ROUGH SURFACES

8.7.1 General Comments

In the study of surface radiometric temperatures, multilayer smooth surfaces are relatively simple to analyze. Maxwell's equations plus the matching of boundary conditions between the layers generally are sufficient. When one or more of the layers are rough, the problem becomes more complex. Statistical techniques, in addition to Maxwell's equations, are then required. Depending upon the degree of roughness, various models have been suggested, one of which has been used in the analysis of "slightly rough" surfaces presented in Appendix B5 (submitted under separate cover) to aid in understanding some of the measurement data.

8.7.2 Proposed Study

A systematic rough surface multilayer study is proposed since many road surfaces are rough, particularly at the smaller millimeter wavelengths (e.g., 8.6 mm/35 GHz). In fact, some road surfaces are rough even at 10 GHz. This study is also significant since a scanning radiometer system is being proposed (see Section 8.2). As we depart from a normal incidence case, surface roughness can play a dominant role in achievable results. Unlike smooth surfaces, scattering phenomena are not too well understood as the angle of incidence is varied.

8.8 DESIGN STUDY FOR LOW-COST 10 GHZ RADIOMETER

8.8.1 General Comments

For the radiometer sensor hazard detector to be a viable candidate for widespread usage, the cost of such a system will become one of the major consideration factors. Two areas where major cost improvements immediately come to mind are: (1) the integration of the receiver utilizing microstrip techniques (this is the microwave equivalent of the conventional printed wiring board); and (2) microcomputer mechanization of the processor including both receiver-related and alarm functions.

Area (2), above, will probably provide the highest potential for cost reduction. The accuracy requirement is the major cost driver in the overall radiometer. With a microcomputer implementation of the processor, self-calibration and non-linear, repeatable errors can

easily be corrected by the computer, thus increasing and maintaining the radiometer accuracy. This, in turn, can relax some of the high accuracy requirements for components in the receiver. An additional advantage derives from the flexibility of changing the microprogramming which permits simple adaptation of the radiometric sensor for optimum use with various geographic conditions.

8.8.2 Proposed Study

It is proposed that the following tasks be performed:

- a) Analysis of the cost reduction targets in the Phase III prototype radiometer design.
- b) Study of receiver integration techniques.
- c) Study of microcomputer implementation of the processor.
- d) Breadboard of a microcomputer processor.
- e) Design of processor software.
- f) System tradeoffs, selection and design of a low-cost radiometer configuration.
- g) Production cost analysis of the final configuration.
- h) Documentation of the receiver and processor design and cost studies.

The study will use the Phase III prototype as the initial baseline. The frequency of the radiometer will be 10 GHz. Since the receiver integration process is a normal progression of design maturity, only a paper study will be performed under task b). This will provide a 90% confidence that the resulting cost could be achieved.

In the microcomputer area [tasks c), d), and e)], the projection of success from paper studies is not as straightforward. Therefore, a breadboard processor would be implemented using a microcomputer along with software. The microcomputer will be a general purpose type functionally simulating the resulting low-cost processor. The microcomputer processor would be bench tested with Lockheed's breadboard 10 GHz radiometer which would be directly interchangeable with the Phase III prototype receiver.

In task f), functional and cost tradeoffs will be performed based on results of all the earlier tasks; a radiometer configuration will be selected; and a design will be generated. This design will be subjected to a production cost analysis in task g); production quantity will be taken as 1,000 systems. It is expected that the final, low-cost radiometer system will also include additional features like self-calibration, self-test and data correction, at no significant added hardware cost.

End items of this study will be: (1) a breadboard microcomputer processor compatible with the Phase III prototype receiver (processor restricted to laboratory environment use); and (2) documentation of the low-cost receiver model, the low-cost processor model, processor software, and a production cost analysis with associated backup data.